Aus dem Institut für Physiologische Genomik der Ludwig-Maximilians-Universität München, aus dem Institut für Stammzellforschung des Helmholtz Zentrums München
Direktor: Prof. Dr. rer. nat. Magdalena Götz

Aus der Abteilung für Proteinanalytik des Helmholtz Zentrums München
Leitung: Dr. rer. nat. Stefanie Hauck

DISSERTATION ZUM ERWERB DES

DOKTORGRADES DER NATURWISSENSCHAFTEN

AN DER MEDIZINISCHEN FAKULTÄT DER LUDWIG-MAXIMILIANS-UNIVERSITÄT MÜNCHEN

Galectins and modulation of glycomic fingerprints of retinal pigment epithelial cells as a novel therapeutic approach for proliferative vitreoretinopathy

von

Jara Kristina Obermann

aus

Karlsruhe

2017

Gedruckt mit Genehmigung der Medizinischen Fakultät der Ludwig-Maximilians-Universität München

Betreuerin: Prof. Dr. rer. nat. Magdalena Götz

Zweitgutachterin: Prof. Dr. Antje Grosche

Dekan: Prof. Dr. med. dent. Reinhard Hickel

Tag der mündlichen Prüfung: 28.03.2018

1. Inhaltsverzeichnis

2. Eidesstattliche Versicherung

Ich, Jara Kristina Obermann, erkläre hiermit an Eides statt, dass ich die vorliegende Dissertation mit dem Thema

Galectins and modulation of glycomic fingerprints of retinal pigment epithelial cells as a novel therapeutic approach for proliferative vitreoretinopathy

selbständig verfasst, mich außer der angegebenen keiner weiteren Hilfsmittel bedient und alle Erkenntnisse, die aus dem Schrifttum ganz oder annähernd übernommen sind, als solche kenntlich gemacht und nach ihrer Herkunft unter Bezeichnung der Fundstelle einzeln nachgewiesen habe.

Ich erkläre des Weiteren, dass die hier vorgelegte Dissertation nicht in gleicher oder in ähnlicher Form bei einer anderen Stelle zur Erlangung eines akademischen Grades eingereicht wurde.

Mannheim, 18.04.2018	Jara Obermann
Ort, Datum	Unterschrift

3. Summary

Proliferative vitreoretinopathy (PVR) is the major cause of failure of retinal reattachment surgery and may lead to permanent loss of vision. It is characterized by the proliferation, migration and epithelial-to-mesenchymal transition (EMT) of retinal pigment epithelial cells (RPE) in the vitreous. Currently there is no pharmacological adjuvant for preventing or treating PVR. The aim of this PhD project was to get deeper insights in the complex cellular events - especially EMT processes - underlying PVR development and to investigate the carbohydrate-binding proteins galectin (Gal)-1 and Gal-3 as potential pharmacological agents to treat PVR. Our results showed that EMT of RPE cells *in vitro* is not only accompanied by a transition from an epithelial to a stable mesenchymal phenotype but also by a glycomic shift to complex-type N-glycans of RPE cell surface glycoproteins, conferring increased binding of Gal-1 and Gal-3 on mesenchymal RPE cells compared to epithelial ones. Phenotype transition of primary RPE cells was blocked *in vitro* by diverse inhibitors of the TGFβ pathway; change to a complex N-glycan-structure was inhibited by blocking Golgi glycosyltransferase activity of α-mannosidase. Yet blocking one of those processes had no influence on the other one. Exogenously added Gal-1 and Gal-3 inhibited carbohydrate-dependently migration of mesenchymal RPE cells in scratch-wound healing assays, but EMT processes were not influenced by galectin treatment. Whereas Gal-1 and Gal-3 were upregulated upon EMT in RPE cells, no changes in glycan structures or galectin-binding efficacy were detectable in galectin knockdown cells compared to wildtype cells. In a proteome-wide comprehensive Gal-1 and Gal-3 interactome screening approach we identified 131 Gal-3 interactors and 15 Gal-1 interactors, mainly localized on the RPE cell surface and involved in PVR-associated molecular functions. Furthermore, two of the identified interactors, namely low-density lipoprotein receptor LRP1 and beta-type platelet-derived growth factor receptor PDGFRB, could be validated as Gal-1 and Gal-3 interactors by galectin-induced cross-linking of LRP1, PDGFRB and the integrin ITGB1 on the RPE cell surface in a complex-type N-glycan-binding-dependent manner. Galectin binding also resulted in dynamin- and carbohydrate-dependent endocytosis of Gal-1 and Gal-3 and both ERK/MAPK and Akt signaling pathways were activated. In conclusion, analyzing changes of phenotype, proteome and cell surface glycan structures of RPE cells undergoing EMT *in vitro* and

identifying specific galectin interactors helped to get an increasing understanding in the pathogenesis of PVR and to unravel functional effects of galectins. The glycomic shift of RPE cell surface glycoproteins upon EMT may provide a basis for diagnostic glycophenotyping of cells isolated from the vitreous of patients suffering from early PVR and galectins may contribute to the development of a glycan-based therapy for PVR.

4. Zusammenfassung

Die Proliferative Vitreoretinopathie (PVR) ist eine häufige Komplikation, die bei Netzhautablösungen sowie vitreoretinalen chirurgischen Eingriffen auftreten kann und schließlich zur Erblindung der Patienten führt. Proliferation, Migration und die epithelial-mesenchymale Transition (EMT) von retinalen Pigmentepithelzellen (RPE) kennzeichnen das Krankheitsbild der PVR. Einen pharmakologischen Wirkstoff um die Entstehung der PVR zu verhindern oder zu behandeln gibt es momentan noch nicht. Das Ziel dieser Doktorarbeit war zum einen die zellulären Prozesse (insbesondere die EMT), die der PVR zugrunde liegen, zu untersuchen und zum anderen die zuckerbindenden Proteine Galektin-1 (Gal-1) und Galektin-3 (Gal-3) als mögliche pharmakologische Wirkstoffe zu testen. Die Ergebnisse zeigten, dass EMT von RPE Zellen *in vitro* nicht nur zu einer kompletten Änderung des Phänotyps, sondern auch zu einer höheren Expression von komplexen N-Glykanstrukturen an der RPE Zelloberfläche führte, sodass Gal-1 und Gal-3 stärker an mesenchymale RPE Zellen binden. Während die Transition zu einem mensenchymalen Phänotyp *in vitro* durch Inhibitoren des TGFβ Signalweges verhindert werden konnte, wurde die Bildung von N-Glykanstrukturen durch Hemmung der Golgi-Glykosyltransferase α-Mannosidase unterbunden. Durch die Inhibierung einer dieser Prozesse wurde der andere jedoch nicht beeinflusst. Die exogene Behandlung von RPE Zellen mit Gal-1 oder Gal-3 verlangsamte deren Migration in Wundheilungs-Assays, EMT Prozesse wurden nicht beeinflusst. Gal-1 und Gal-3 sind in mesenchymalen RPE Zellen überexprimiert. Galektin-knockdown Zellen zeigten jedoch keine Unterschiede in ihren Oberflächen-Glykanstrukturen oder in der Bindungsaffinität von Galektinen im Vergleich zu Wildtyp-Zellen. In einer Proteom-weiten Gal-1 und Gal-3 Interaktom-Studie wurden 131 Gal-3 Interaktoren und 15 Gal-1 Interaktoren identifiziert. Diese Interaktoren waren überwiegend membranständige oder oberflächenassoziierte Glykoproteine und in vielen PVR-relevanten zellulären Prozessen involviert. Zwei der identifizierten Interaktoren – das Low Density Lipoprotein Receptor-related Protein 1 (LRP1) und der Beta-type platelet-derived growth factor receptor (PDGFRB) – konnten durch N-Glykan-abhängige Galektin-induzierte Cluster-Bildung unter Einbeziehung von Integrin ITGB1 an der RPE Zelloberfläche validiert werden. Es konnte ebenfalls gezeigt werden, dass Gal-1 und Gal-3 auf einem Dynamin- und N-Glykan-abhängigen Weg über Endozytose in RPE Zellen

aufgenommen werden und dabei ERK/MAPK und Akt Signalwege aktiviert werden. Zusammenfassend zeigen die Ergebnisse dieser Arbeit, dass die Analysen von Veränderungen im Phänotyp, im Proteom und in der Glykanstruktur von RPE Zellen und die Identifizierung spezifischer Galektin-Interaktoren essentiell sind um die Pathogenese der PVR molekular zu verstehen, aber auch um funktionelle Effekte von Galektinen zu untersuchen. Die Veränderung der Zuckerstrukturen von Oberflächenproteinen der RPE Zellen können ein Ansatz für die Entwicklung von Biomarkern sein um anhand von Glaskörperzellen, die aus dem Auge von PVR Patienten in frühem Stadium isoliert wurden, die PVR frühzeitig zu erkennen und mithilfe von Galektinen eine Glykan-basierte Therapie zu entwickeln.

5. Introduction

5.1. Proliferative vitreoretinopathy

Proliferative vitreoretinopathy (PVR) is a blinding disease occurring as a complication after rhegmatogenous retinal detachment surgery[1-4]. The Retina Society Terminology Committee introduced in 1983 the term proliferative vitreoretinopathy[4], which was formerly called "massive periretinal proliferation"[5]. PVR is not defined as specific clinical entity, but rather an end point of a number of intraocular diseases with various stimuli[6]. It is assumed that PVR is a reparative and scarring process primarily induced by retinal detachment, caused by a retinal break and accompanied by an excessive inflammatory reaction[3]. To classify different stages of PVR, it is divided into three grades: A, B and C with increasing severity of PVR[7]. Stage A describes the presence of retinal cells in the vitreous, stage B is associated with inner retinal surface wrinkling or formation of retinal tears, stage C is divided into posterior (CP) and anterior (CA) PVR and is reached by formation of retinal folds or subretinal strands CP or CA to equator[7].

Rhegmatogenous retinal detachment induces breakdown of the blood-retina barrier and triggers wound-healing processes, including cell migration and proliferation of distinct cell types: retinal pigment epithelial (RPE) and retinal Müller Glial (RMG) cells, fibrous astrocytes, fibroblasts, myofibroblasts, and macrophages (figure 1)[8, 9]. RPE cells as a main component of the PVR membranes are in focus of PVR research. Under physiological conditions RPE cells are mitotically quiescent and located in a monolayer between the neural retina and the choroid in the eye[10]. Early in disease development the integrity of the retina is broken and RPE cells dislodge from Bruch's membrane, migrate in the vitreous and/or periretinal area and epithelial-to-mesenchymal transition (EMT) takes place[2, 5, 11]. During EMT RPE cells convert from epithelial into mesenchymal cells, lose their epithelial characteristics and acquire migratory mesenchymal properties, accompanied by formation of an extracellular matrix structure containing collagen, fibronectin, thrombospondin, and other matrix proteins[8, 10, 12]. Migration, proliferation and dedifferentiation of retinal cells promotes development of sub- and epiretinal fibrocellular membranes, which contract and lead to repetitive tractional retinal detachment (figure 1)[2, 5, 6, 8, 13]. The retinal break causes release of growth factors and

cytokines in the vitreous which contributes to cell-growth regulation in PVR[8, 12, 14]. It is assumed that platelet-derived growth factor (PDGF), tumor growth factor-beta (TGF-β), epidermal growth factor (EGF), tumor necrosis factor-alpha (TNF-α), TNF-β and fibroblast growth factor (FGF) as well as cytokines like interleukin-1 (IL-1), IL-6, IL-8, IL-10, and interferon-gamma (INF-γ) may play a role in PVR development (figure 1)[8, 15-21]. Yet growth factors and cytokines are very multifunctional and involved in many different cellular processes. Increased understanding of the complex pathways and the interplay between growth factors and cytokines in PVR development remains a prerequisite for future prevention and treatment of PVR[22].

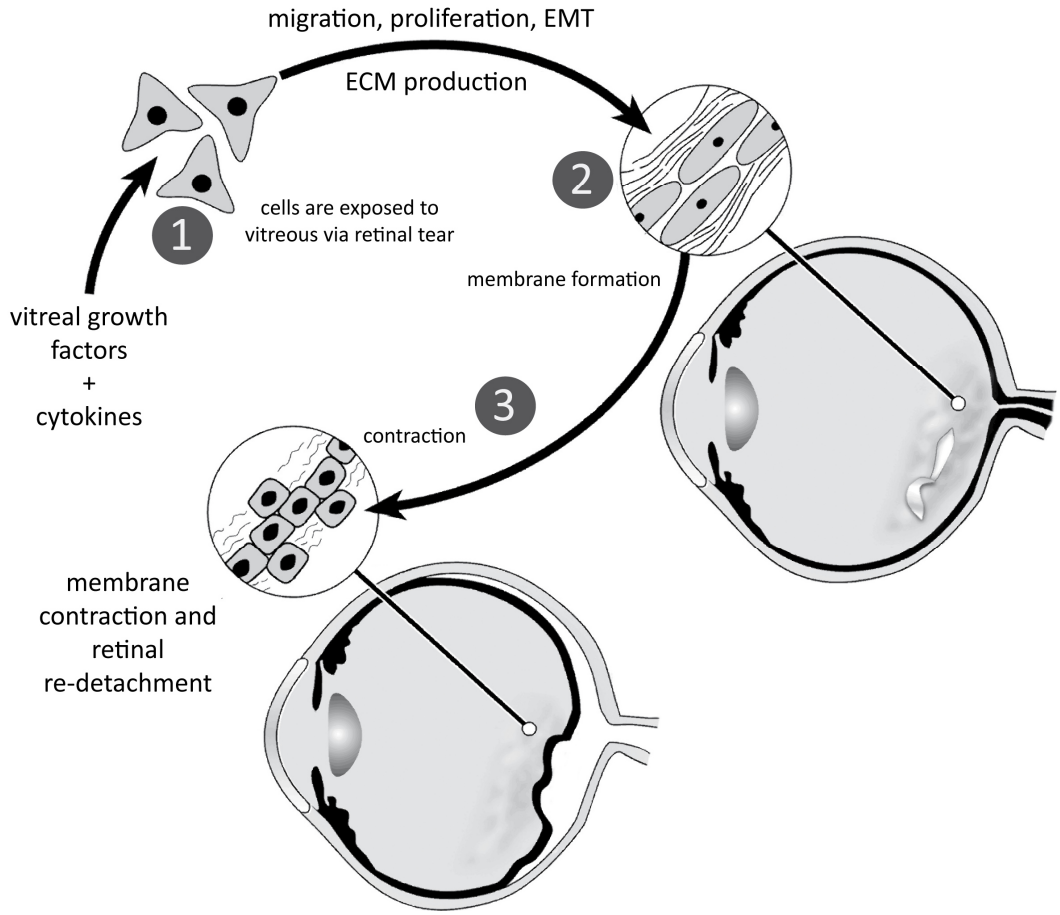

Figure 1: The growth factor/cytokine hypothesis for PVR development, published in Lei et al. [15]. By retinal tear formation and retinal detachment, retinal cells can be exposed to vitreal growth factors and cytokines, which promote cellular processes like migration, proliferation, epithelial-to-mesenchymal transition (EMT) and extracellular-matrix (ECM) production. Sub- and epiretinal membranes are built and cells within the membranes are stimulated by growth factors and cytokines in the vitreous to contract and the retina re-detaches.

Even though knowledge about pathophysiology of PVR is increasing, it still remains the primary barrier to successful retinal detachment surgery[23]. 5%-10% of all rhegmatogenous retinal detachment processes are accompanied with PVR and after re-attachment of the retina by surgical means, PVR occurs in 75% of all cases[3, 8]. The more advanced the PVR, the poorer is the outcome of the surgery and the lower the re-attachment rate of the retina[6]. Surgery may even stimulate PVR because it triggers inflammation processes inducing extensive proliferation of retinal cells[8, 23]. Nevertheless vitreous surgery is still the standard treatment method for PVR[6]. Identification of a pharmacological agent that is capable to prevent or interfere with cellular processes underlying PVR development is necessary to improve the final outcome. Most of the recent experimental therapeutic approaches attempted to control PVR development by anti-proliferative or anti-inflammatory compounds or by inhibition of single growth factors and their signaling pathways[24-31]. However, PVR is caused by an interplay between different cytokines and growth factors, matrix proteins and the various cell types, resulting in formation of tractional membranes[8]. Consequently, counteracting PVR requires a multimodal concept[6].

5.1.1. The retinal pigment epithelium

The retinal pigment epithelium (RPE) is a monolayer of highly pigmented cells found between Bruch's membrane and the photoreceptor layer of the neural retina (figure 2)[32]. RPE cells are strongly polarized, have a hexagonal shape and they fit together in a tight matrix[33, 34]. The RPE has a barrier function to prevent large molecules and particles from entering the vitreous from the bloodstream[35]. The function as blood-retina-barrier is to some extend similar to that of the blood-brain barrier, because the RPE separates neural and vascular tissue, which is critical for the correct function of the neuroretina[35]. On the apical side of the RPE, highly specialized photoreceptors are embedded in an interphotoreceptor matrix[35-37]. The light-sensitive outer segments of the photoreceptors are in close structural interaction with long apical microvilli of RPE cells[36]. On the basal side, an elastogenesis product of the RPE and choroid, called Bruch's membrane, is located, which separates the RPE from the endothelium of the choriocapillaris[35, 36].

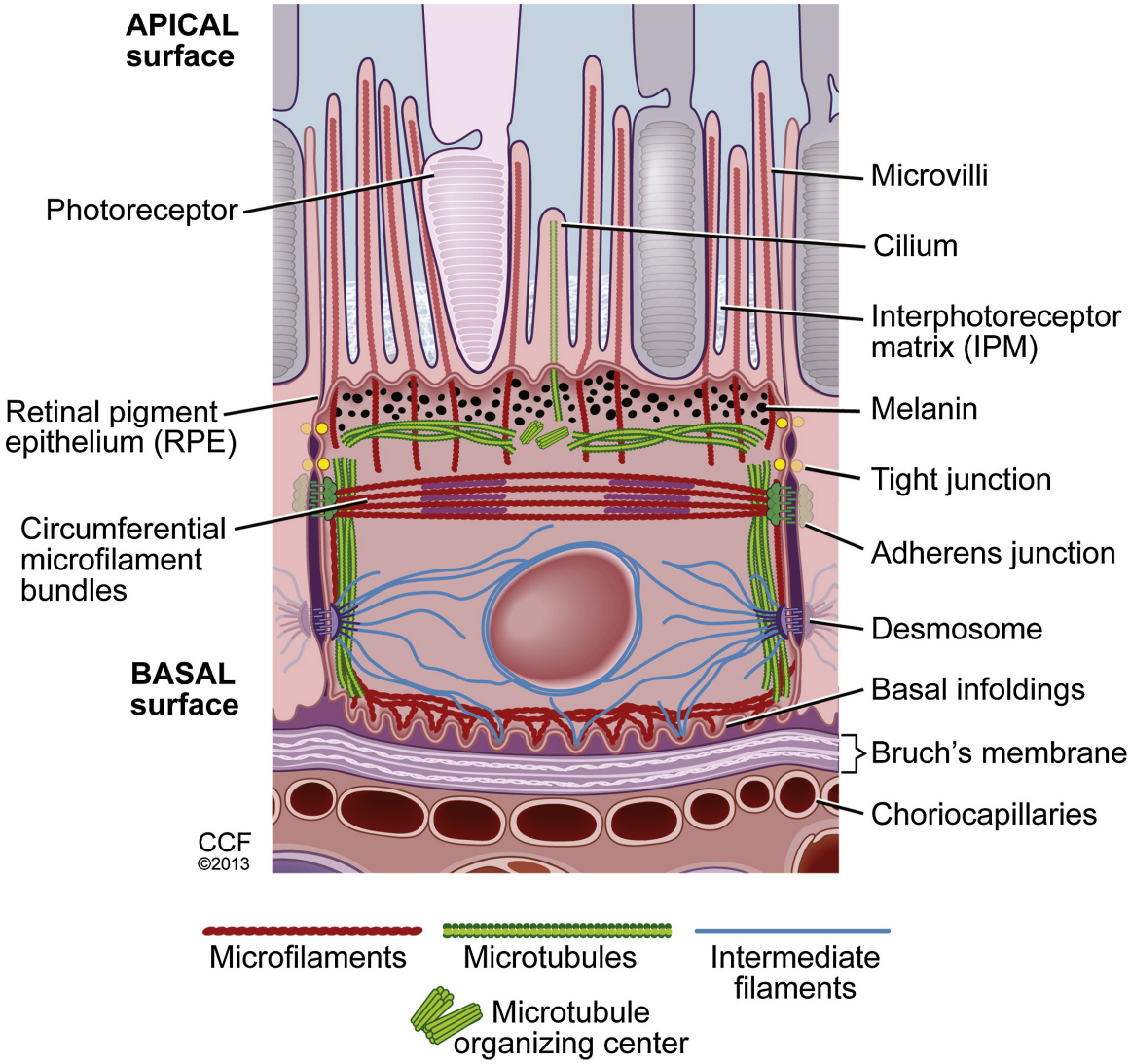

Figure 2: A schematic model of the RPE structure, as published in Bonilha [33]. RPE interacts at the apical surface with photoreceptor cells and on the basal side with the Bruch's membrane. The shape of individual RPE cells is maintained by their cytoskeleton components.

The RPE is involved in many complex processes in the visual cycle. It is involved in the uptake, processing – including re-isomerization of all-trans-retinal to 11-cis-retinal –, transport and release of retinal (vitamin A), in phagocytosis of shed photoreceptor outer segments and in rebuilding of light-sensitive outer segments from the base of photoreceptors[36, 38]. Physiologically, the RPE absorbs excess light entering the eye to reduce photo-oxidative stress[32]. It regulates the development of the retina and the supply with nutrients such as glucose, retinol, and fatty acids from the choroid to the photoreceptor cells as well as transportation of metabolites and fluids in the opposite direction[33, 36]. RPE are part of the innate immune system and thus involved in immune

responses of the eye; RPE also secretes growth factors like vascular endothelial growth factor (VEGF) and pigment epithelium-derived growth factor (PEDF)[35, 39, 40]. Because of its various functions in physiological processes, the RPE plays a role in many ocular disorders, including *Retinitis Pigmentosa*, diabetic retinopathy and macular degeneration[32].

5.1.2. Epithelial to mesenchymal transition

The epithelial-to-mesenchymal-transition (EMT) of RPE cells plays a key role in PVR development[11]. EMT is a cellular process naturally occurring during development and differentiation of distinct tissues and organs or as a physiological response to injury, but it is also associated with distinct pathological processes as tissue fibrosis, tumor invasiveness and metastasis[41, 42]. During EMT, epithelial cells lose their epithelial cell characteristics, change their morphology and phenotype and acquire mesenchymal-like properties[22, 42, 43]. Epithelial cells are characterized by their tight cell-cell contacts mediated by adherens junctions, desmosomes and tight junctions as well as by an apicobasal axis of polarity, which promotes the function of epithelia as barriers in absorption[41]. By EMT, cells increase their production of ECM components, their resistance to apoptosis and their migratory and invasive properties by losing their organized cell-cell structures and cell polarity[41, 42]. EMT is reversible and is accordingly called mesenchymal-to-epithelial-transition (MET). EMT and MET processes are characterized by change of the expression of specific cell-surface proteins, reorganization of cytoskeletal proteins or activation of distinct transcription factors (figure 3)[42]. Epithelial markers such as zonula occludens-1 (ZO-1) and E-cadherin are up- and downregulated in epithelial and mesenchymal cells respectively. Approved mesenchymal cell markers are α-smooth muscle actin (α-SMA), vimentin, and fibronectin[44]. Those factors are suitable biomarkers to define the state of a cell undergoing EMT or MET (figure 3).

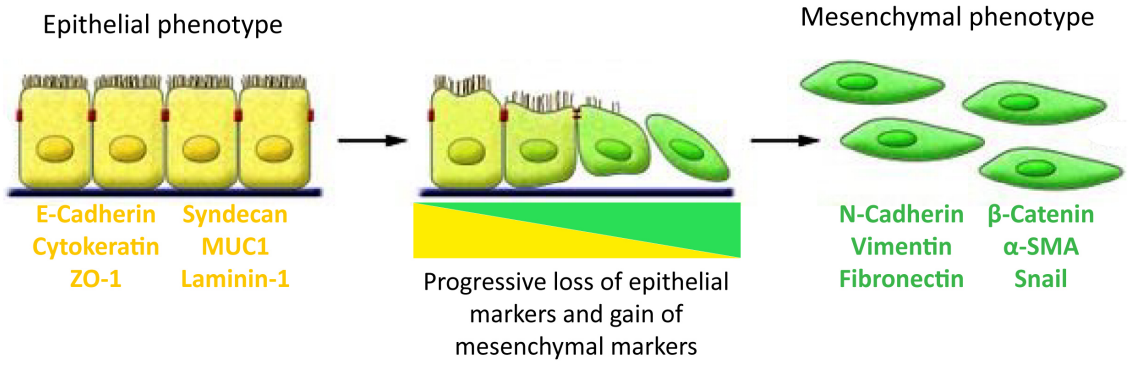

Figure 3: Epithelial to mesenchymal transition and the corresponding cell markers, published in Kalluri and Weinberg [42]. Polarized epithelial cells transform into mobile mesenchymal cells. ZO-1: zona occludens 1; MUC1: mucin 1; SMA: smooth muscle actin.

Three types of EMT can be distinguished. Type 1 EMT is characterized by the transition of epithelial cells into primary mesenchymal cells, which in turn undergo MET, form secondary epithelia or undergo apoptosis[42, 44]. In these processes the cells don't obtain an invasive phenotype and are not spread via circulation[42]. Type 2 EMT is associated with organ fibrosis, tissue regeneration and wound healing processes accompanied by inflammation[42]. Epithelial cells transform into fibroblasts as part of a repair-associated event, but if there is persistent inflammation over extended periods of time affected organs can be destroyed[42, 44]. Type 3 EMT is seen in metastatic processes. Epithelial cells can transform in epithelial tumor cells and undergo EMT, which enables migration and metastasis[42, 44]. The metastatic tumor cells reform as a secondary tumor nodule, generating the final, life-threatening manifestations of cancer progression[42, 44].

In context of PVR, RPE cells are exposed to many cytokines and growth factors in the vitreous by retinal break. Those factors stimulate EMT, migration and proliferation of RPE cells and lead to the formation of fibrotic tissue on the retina. Recent studies indicated that EMT in RPE cells contributes mainly to PVR and it is presumably caused by many different factors, such as changes in cell-cell adhesion profile, modified growth factor signaling or loss of ECM adhesion[10, 43]. *In vitro*, EMT occurs by cultivation of primary RPE cells on plastic in serum-containing media[45]. Cultured human RPE cells are a well-accepted *in vitro* model system for early PVR. Triggered by distinct growth factors contained in fetal bovine serum (FBS), RPE cells begin to dedifferentiate and to transform into a fibroblast-like phenotype[43, 45]. One of the key drivers of EMT is TGFβ[46].

TGFβ is a multifunctional cytokine that exists in three isoforms (TGFβ1, TGFβ2 and TGFβ3) and is involved in many biological processes like differentiation, apoptosis, migration, immune cell function and ECM synthesis and thus it plays a role in many distinct diseases[47]. TGFβ signaling pathways are divided in the canonical Smad signaling pathway[48] and non-canonical pathways, but the different types of pathways can interact with each other and contribute to EMT[22]. Non-canonical pathways include the mitogen-activated kinase (MAPK), the extracellular signal-regulated kinase 1/2(ERK1/2) and the phosphatidyl inositol 3-kinase (PI3-K)/Akt[22]. TGFβ2 is the most important isoform driving EMT and PVR processes and it is often used to induce EMT *in vitro*[30].

EMT processes are also very dependent on cell-cell contacts. Disruption of such contacts triggers EMT, whereas intact and close cell-cell contacts maintain the epithelial phenotype of cells[43, 45]. Tamiya et al. [43] showed that mainly loss of cell-cell contacts initiates EMT in RPE cells and that TGFβ2 treatment promotes EMT, but has no effect on RPE cells when cell-cell contacts are retained. Besides, transcription factors, intracellular signaling pathways and microRNAs are critical for EMT induction in PVR *in vitro* and *in vivo*[22, 49, 50]. Preventing EMT processes by inhibiting those distinct factors is one important therapeutic approach in PVR research[22].

5.2. Galectins

Galectins constitute a family of soluble animal lectins and are β-galactoside binding proteins, which share homology in a highly conserved 130 amino acid sequence of their carbohydrate recognition domain (CRD) [51-54]. Based on this conserved galectin CRD many galectins were identified in the last 40 years[55]. Galectins are expressed in many different organisms, for example in vertebrates (fish, birds), invertebrates (insects, worms) and even in fungi, sponges, plants, viruses and bacteria[54, 56]. In mammals, 15 proteins of this family are characterized so far, 12 of them in humans [55, 57]. The nomenclature for galectins in mammals was introduced in 1994 and the members of this protein family were numbered consecutively by order of their discovery[51].

5.2.1. Structure of galectins

Crystallography has been used to determine the three-dimensional structure of the CRDs of some mammalian galectins and all of them have in common, that they have a

globular fold of anti-parallel β-sheets with five to six strands respectively[58-62]. Four adjacent β-strands are involved in carbohydrate binding, either by formation of hydrogen bonds or van der Waals interactions with the sugar moiety[58].

Regarding their molecular structure, galectins are clustered in three groups: proto-, chimera- and tandem-repeat-type[54]. Prototype galectins (galectin-1, 2, 5, 7, 10, 11, 13, 14, (15)) consist of one CRD and usually form noncovalent dimers [52, 53, 57] (figure 4). Chimera type galectins, whose only member known so far is galectin-3, are characterized by two distinct domains, a C-terminal CRD and a N-terminal non-lectin proline-, tyrosine- and glycine-rich domain[63, 64] (figure 4). Tandem-repeat galectins (galectin-4, 8, 9, 12) contain two different CRDs connected by a short peptide [53, 57].

In general, galectins have a lot of features of cytosolic proteins. They are acetylated at their N-terminus, have no signal peptides or post-translational modifications (only Gal-3 can be phosphorylated) and are synthesized at cytosolic ribosomes[53]. As galectins are present in the extracellular matrix or on cell surfaces, but lack secretion signal sequences, it is assumed, that galectins are secreted by non-classical (non ER-Golgi) pathways, which is not fully understood yet [52, 65].

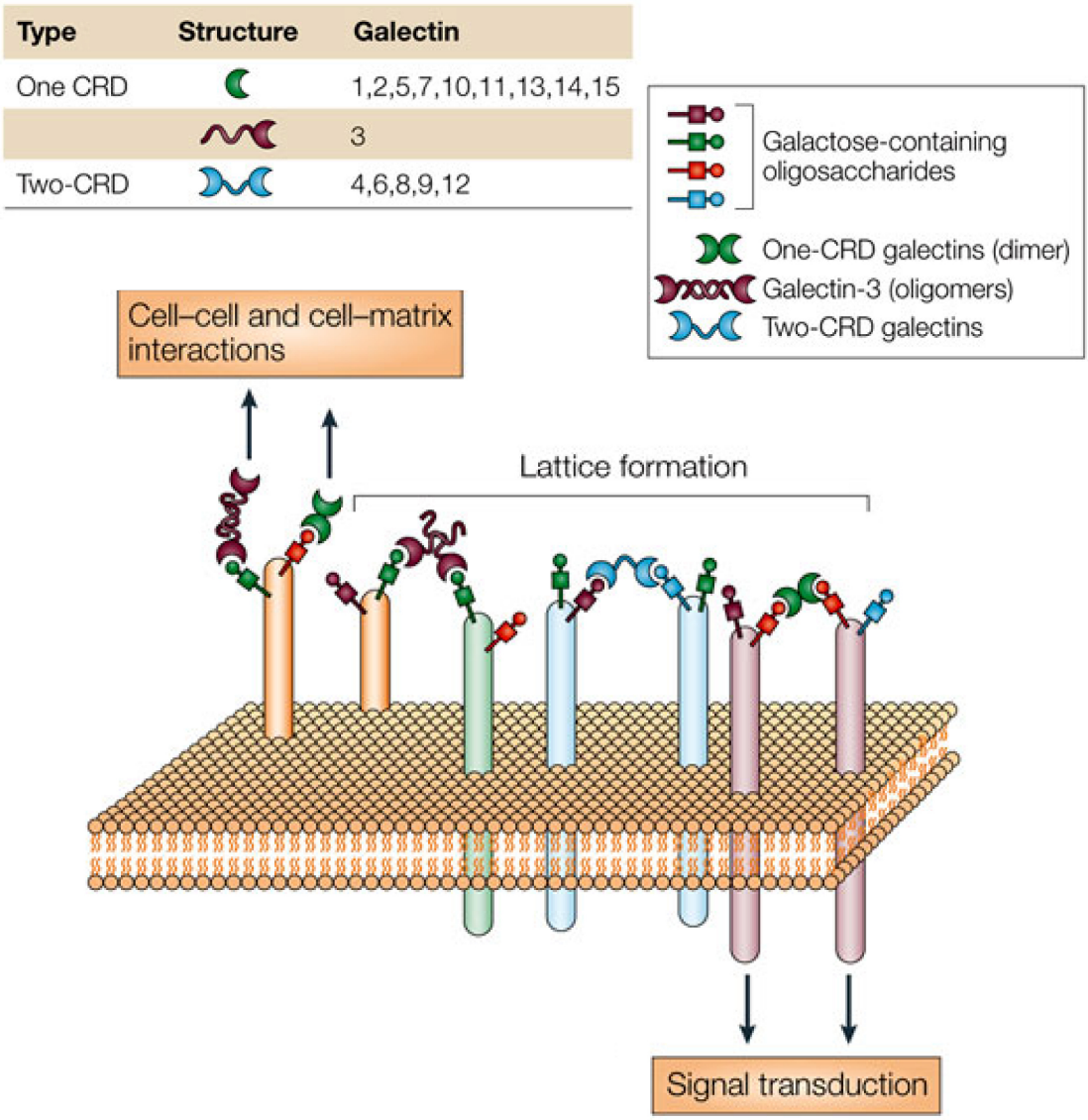

Figure 4: The Galectin family as published in Liu and Rabinovich [66]. The 15 mammalian galectins can be subdivided into three groups. Prototype galectins (galectin-1, 2, 5, 7, 10, 11, 13, 14, (15)) consist of one CRD. Gal-3, which consists of one CRD fused to an N-terminal non-lectin proline-, tyrosine- and glycine-rich domain, is assigned to chimera type galectins. Tandem-repeat galectins (galectin-4, 8, 9, 12) contain two different CRDs connected by a short peptide. Galectins can crosslink and interact with cell-surface glycoconjugates by forming dimers or oligomers and thus trigger a cascade of signaling events. Galectins can also influence cell-cell and cell-matrix interactions by bridging cells among each other or by bridging cells to extracellular matrix proteins.

5.2.2. Functions of galectins

Galectins are very multifunctional proteins involved in many cellular processes under both physiological and pathophysiological conditions. Some mammalian galectins are

distributed over many different tissues, others are more specifically expressed[66]. Both intra- and extracellular functions have been described: cell-cell and cell-extracellular matrix interactions, cell signaling and intracellular trafficking, apoptosis, organization and clustering of membrane proteins, regulation of cell cycle, cancer progression, immune response and many more[66]. An overall biological function of galectins has not emerged yet and a knockout of Gal-1 and Gal-3 (single and double knockout) in mice doesn't influence survival or fertilization of the animals. Still, some transient and very complex consequences of lacking galectins during development have been found[53, 67].

Whether the intra- and extracellular activities of galectins are connected or not, is not clarified yet[53]. Intracellularly, galectins interact through protein-protein interactions with cytoplasmic and nuclear proteins and thus may influence basic cellular processes like pre-mRNA splicing and cell-cycle progression[66, 68]. Yet, the exact mechanisms of these interactions are not known[66]. On the cell surface and ECM, galectins interact with their protein ligands by binding to β-galactoside containing moieties on the glycosylated peptide backbones (figure 4)[51, 58, 69]. Galectins can crosslink those glycoconjugates by forming dimers or oligomers, thus decipher the information stored in the glycan chains and trigger a cascade of signaling events and influence many cellular functions including attachment, spreading, migration and proliferation[64, 66, 70]. The assembly of these ordered arrays of lectins and saccharides on the cell surface is required for optimal transmission of signals into a cell and the galectin lattice regulates the diffusion, compartmentalization and endocytosis of plasma membrane glycoproteins and glycolipids[71, 72]. By their bivalent and multivalent properties galectins also influence cell-cell and cell-matrix interactions by bridging cells to other cells or by attaching cells to extracellular matrix proteins (figure 4)[66]. Because of lectin multivalency, galectins are able to recognize multiple binding partners simultaneously, allowing to play leading roles in many different biological but also pathophysiological processes[71].

How galectins influence cellular processes is different within distinct biological systems and is dependent on many factors like galectin expression, concentration and oligomerization as well as glycan structure of the interactors[58]. The affinity of transmembrane glycoproteins to the galectin lattice is proportional to the number and branching of their N-glycans and thus the glycosylation pattern of cell surface proteins is

important for the role of galectins as agonist or antagonist in cell adhesion[64, 72]. Even though all members of the galectin family bind to galactose-β1,4-N-acetylglucosamine, it is assumed that the structural differences in their CRD domains not only lead to different specificities for distinct glycoproteins, but also to distinct biological activities[73-75]. Whereas Gal-3 for example is associated with antiapoptotic effects, Gal-1 induces apoptosis in several cell types [76, 77]. On the other hand, binding to different interactors does not necessarily mean that different downstream mechanisms are influenced. In the literature it is shown that Gal-1 and Gal-3 can bind to distinct receptors but converge on similar downstream signaling in several analyses for induction of T cell death[73] or of neutrophil respiratory burst[78, 79].

With respect to cell adhesion processes galectin concentration relative to the receptor glycoproteins is critical. At high concentrations galectins interact unspecifically with many receptors on the cell surface and thereby block them and prevent interaction with each other which is a prerequisite for cross-linking and adhesion processes[58]. At lower concentrations galectins interact more specifically with the preferred interactors on the cell surface[58, 64]. Depending on receptor availability on the specific cell type galectins bridge cells to ECM proteins or to other cells (figure 4)[58, 70].

Expression levels of galectins are naturally modulated during development of organisms and tissues as well as during differentiation of cells[66]. But the expression of galectins is also changed under pathological conditions and galectins are for example often overexpressed in cancerous cells[66, 80]. Interestingly, mainly those cell types, that express low levels of galectins under normal physiological conditions, overexpress galectins in disease state[66, 68, 81]. In contrast, when cells normally express high levels of a specific galectin isoform, these galectins are downregulated when those cells become abnormal[66]. The influence of galectins in various diseases such as cancer, fibrosis and inflammation makes them useful targets in medical interventions[68, 81]. It is also assumed that altered galectin expression correlates with the aggressiveness of tumor cells and influences disease outcome[66]. Yet, most cell types co-express different galectin isoforms, which may results in overlapping or opposite effects and the influence of one specific galectin can hardly be determined[58, 66].

5.2.3. Galectin-1

Gal-1 (~14kDa) was the first protein discovered in this family and is assigned to the prototype galectins, consisting of one CRD[82]. The molecular structure of Gal-1 involves a β-sandwich with two anti-parallel β-sheets (figure 5)[83]. By hydrophobic interactions at the N-terminal amino acid residues, prototype galectins can self-associate their monomer subunits to form homodimers (~29kDa) (figure 5)[52, 61, 84]. In solution, Gal-1 is mainly present in dimeric form[84]. Only at low concentrations (K_d ~ 7 µM) Gal-1 dissociates and thus glycan binding affinity is reduced[84]. By dimerization Gal-1 crosslinks specific multivalent carbohydrates or glycoconjugates, which result in the formation of cross-linked lattices and the activation of several cellular pathways [52, 85-88]. Gal-1 binds preferentially to N-acetyllactosamine and binding avidity can be increased by arrangement of terminal lactosamine disaccharides in multi-antennary repeating chains (up to three branches, K_d ~ 4 µM)[75, 83, 89]. Furthermore, affinity of Gal-1 to glycan structures can be enhanced when they are immobilized by location at cell surfaces or in ECM[89]. Gal-1 homodimers bind also to α3-sialylated and α2-fucosylated terminal N-acetyllactosamine, but not α6-sialylated and α3-fucosylated terminal N-acetyllactosamine[83, 89].

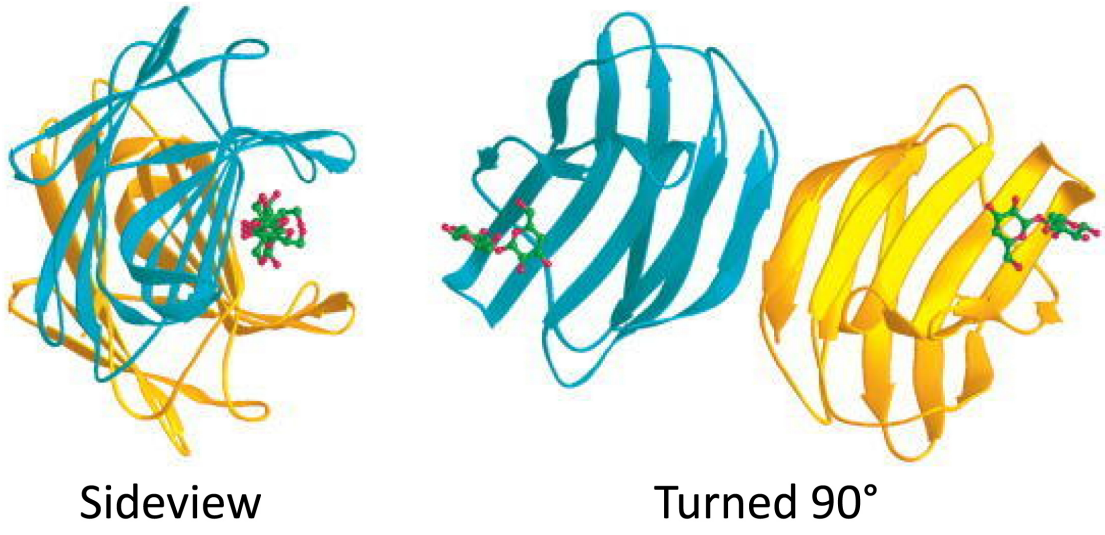

Figure 5: Ribbon diagram of the crystal structure of human galectin-1, based on X-ray crystallographic analyses of the protein complexed with lactose, as published in Cummings [90]. The homodimer is shown with each monomer colored differently and orthogonal views are presented. The subunit interface is based on interactions between the carboxy- and amino-terminal domains of each subunit.

As Gal-1 has six free cysteine-residues, activity of Gal-1 is dependent on reducing conditions. Nishi et al [91] showed, that a removal of the six cysteine residues increases stability of Gal-1 under both reducing and non-reducing conditions, while not influencing carbohydrate binding activity. As many other galectin isoforms, Gal-1 is present both intra- and extracellularly, but lacks a typical secretion signal sequence. Nickel [92] describes possible inside-out transportation mechanisms of Gal-1 similar to those of fibroblast growth factor-2 (FGF-2) and β-galactoside-containing surface molecules are used as export receptors for intracellular Gal-1[83, 92].

As most galectins, Gal-1 has also many distinct ambiguous biological functions. Gal-1 influences for example cell growth concentration-dependently. Low doses of Gal-1 (≤1 nM) promote cell growth carbohydrate-dependently, whereas high doses (≥1 µM) inhibit cell proliferation carbohydrate-independently[83, 93]. Via cross-linking of glycoproteins on the cell surface with ECM components, Gal-1 can influence cell adhesion of many distinct cell types, including heterotypical interactions of tumor and endothelial cells[94, 95]. Gal-1 also influences cytoskeleton organization and thus motility of cells, which can be again associated with higher aggressiveness of tumor cells[96], whereas Gal-1 enriched ECM structures decrease colon carcinoma cell motility[83, 97]. Gal-1 also plays a role in tissue development and differentiation[93, 98], as well as in neuronal[99, 100] and immune system[78].

5.2.4. Galectin-3

Gal-3, a ubiquitously expressed 34-kDa protein (in adult humans), is the only known chimera type galectin of the human lectin family[51, 53, 82]. It was previous known as epsilon BP for its IgE-binding activity and as Mac-2, a macrophage surface antigen, CBP35, CBP30, L-29, and L-34[63, 101]. Gal-3 consists of a C-terminal domain to bind specific carbohydrate branches, an N-terminal 12 amino acid leader sequence with two phosphorylation sites and a proline and glycine rich collagen like domain, which enables Gal-3 to multimerize (figure 6)[51, 58, 102]. The highly conserved N-terminal domain consists of 120 amino acids (in humans) and contains multiple homologous repeats[63]. The N-terminal 12 amino acid leader sequence is assumed to be involved in secretion of Gal-3 outside of cells and in Gal-3 anti-apoptotic signaling activity[103, 104]. In contrast to the C-

terminal domain the N-terminal domain has no carbohydrate-binding activity, but is essential for full biological activity of Gal-3[59, 63]. The C-terminal domain is composed of 130 amino acids, shows the typical galectin CRD folding structure and thus is responsible for lectin activity of Gal-3[63]. Whereas the C-terminal CRD is resistant to collagenase treatment, the N-terminal non-CRD region is susceptible[105].

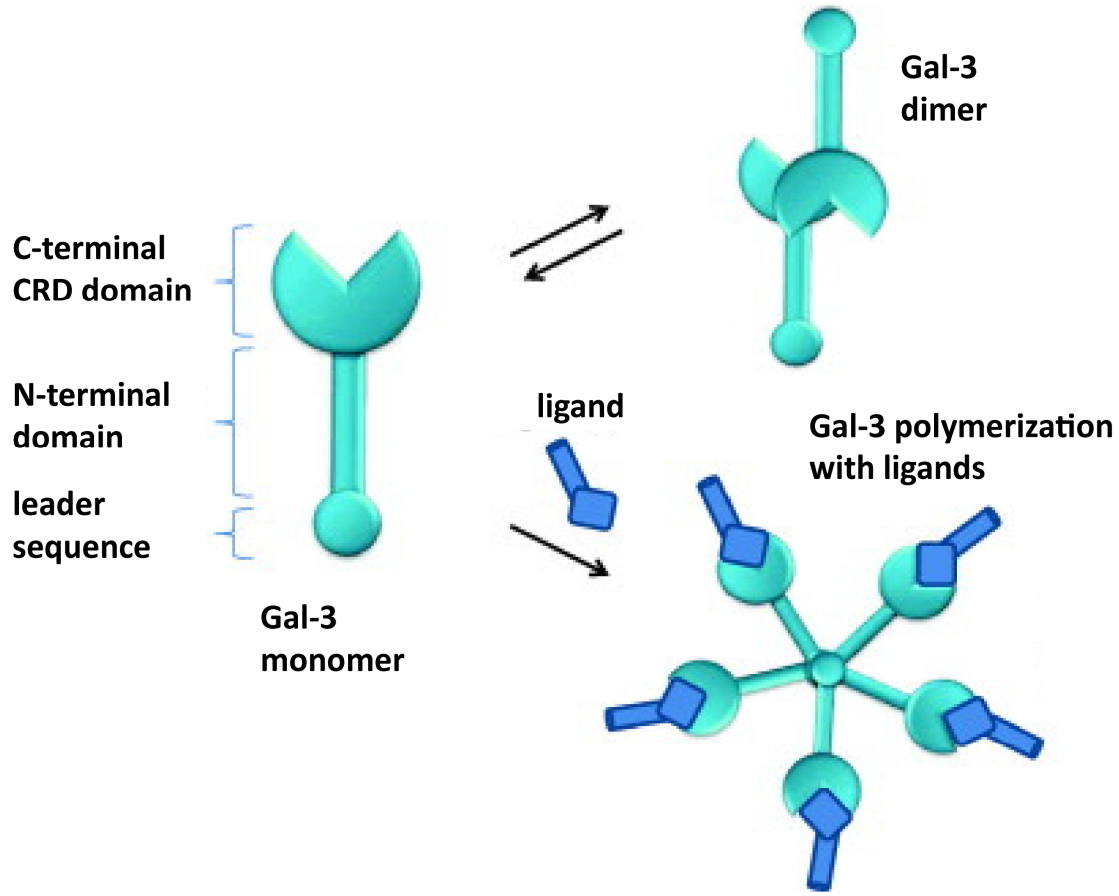

Figure 6: Schematic representations of the monomeric structure of galectin-3, galectin-3 dimerization through its C-terminal CRD domain in the absence of a binding ligand and galectin-3 polymerization through its N-terminus in the presence of carbohydrate binding ligands, as published in Newlaczyl and Yu [106]. CRD: carbohydrate recognition domain.

Gal-3 binding is specific for N-acetyllactosamine and N-acetylglucosamine containing glycoproteins as well as polylactosaminoglycans[105]. Phosphorylation at serine residues of Gal-3 is assumed to influence binding affinity and thus act as a regulatory modification of biological intracellular effects[107]. By interaction with carbohydrate ligands, Gal-3 and especially the CRD domain is conformationally changed[108]. Ligand binding occurs via the

CRD domain which precedes the N-terminal domain induced multimerization of galectins and formation of cross-linked lattices (figure 6)[102, 109].

Gal-3 is a multifunctional protein with both intra- and extracellular functions. The expression of Gal-3 on both protein and mRNA level can be associated with distinct physiological and pathophysiological effects and is influenced by different stimuli[63]. Intracellularly, Gal-3 is for instance involved in mRNA-splicing and apoptotic processes[77, 110]. Extracellularly, Gal-3 has the ability to bind cell surface and ECM glycans and thus affect many distinct physiologic and pathologic processes, including apoptosis, migration, angiogenesis, adhesion and inflammatory response[111]. Gal-3 is for example upregulated in proliferating fibroblasts compared to quiescent cells and its expression is also changed during differentiation of cells[101, 112].

5.2.5. Galectins in context of PVR

Current research approaches indicate that galectins as β-galactoside-binding and cross-linking lectins play important roles in diverse physiological and pathological processes[68]. Thus they may be suitable therapeutic targets but also therapeutic agents. In previous studies the capacity of Gal-1 and Gal-3 to inhibit early PVR-associated cellular events was explored. Gal-1 and Gal-3 were found to be upregulated in cultured mesenchymal RPE cells[113, 114] and Gal-1 is also present in the extracellular matrix of PVR membranes and may be derived from dedifferentiated RPE cells[115]. Furthermore, Gal-1 expression levels can be influenced by stimulation with hepatocyte growth factor (HGF) and are related to the migratory phenotype of RPE cells[115]. However, direct influence of modulated galectin expression and PVR pathology is not proven yet.

From a prognostic point of view we have recently identified that EMT of RPE cells leads to increased β-1,6-N-glycosylation on the cell surface and thus increased binding of Gal-3[116]. These results may provide a basis for diagnostic glycophenotyping of cells isolated from the vitreous of patients suffering from early PVR. Consequently this can contribute to the development of prognostic markers to define the individual risk for development of PVR.

From a therapeutic perspective, Gal-1 and Gal-3 bind to mesenchymal RPE cells in a dose- and carbohydrate-dependent manner and thus inhibit attachment and spreading

of these cells[114, 117]. Exogenous Gal-3 exerted its effect by interfering with adhesion-related ERK-dependent signaling[114]. Therefore Gal-1 and Gal-3 bear a high potential to counteract PVR-associated cellular events and these findings may aid in development of an individualized galectin-based therapy for PVR. Additionally, it was shown, that Gal-3 induces clustering of CD147 and integrin-β1 transmembrane glycoprotein receptors on the RPE cell surface [118]. However, the functional relevance of galectin-binding on these different receptors is not explicitly analyzed in context of PVR. Most of the cell surface proteins on RPE cells targeted by specific galectins are largely unknown. This in-depth knowledge is a prerequisite to unravel the possible influence of galectins on the signal transduction mechanisms associated with PVR processes.

5.2.6. Galectin interactors

Even though all galectins share homology in their highly conserved CRD regions, each galectin is characterized by a distinct set of ligands and thus molecular interactors. The interaction with galactose is common for all galectins, but very weak (dissociation constants ~10^{-4} M)[53, 71, 119]. Disaccharides that contain galactose bound to glucose by β-glyosidic bonds, N-acetyllactosamine (LacNAc) or N-acetylglucosamine (GlcNAc) interact with galectins with higher affinities[58, 105, 119]. Distinct galectin isoforms recognize different modifications of those saccharide ligands and thus certain galectins interact with specific ligands[75, 83]. Among the main binding partners of Gal-1 and Gal-3 are high-glycosylated N-glycans[120]. Galectin binding affinities to complex N-glycans are proportional to their LacNAc content and to their GlcNAc branching[71, 105].

In many cell types several interactors for Gal-1 or Gal-3 have been identified: these include among others lysosomal-membrane-associated glycoproteins (LAMPs)-1 and -2, neural cell adhesion molecule (NCAM), cell adhesion molecule L1, CD43, CD45, CD71, mucin-1 and receptors for distinct growth factors like the epidermal growth factor (EGF), transforming growth factor beta (TGF-β) or vascular endothelial growth factor (VEGF)[58, 63, 73, 118, 121-128]. Extracellular matrix (ECM) proteins like laminin, fibronectin or vitronectin as well as members of the β1 integrin family are also known Gal-1 and Gal-3 interactors[58, 63, 125, 129-131]. Integrins play a major role in cell-matrix-interactions. As transmembrane proteins they are able to bind to the ECM by their extracellular part and

induce several signal transduction cascades in the cell, e.g. remodeling of the cytoskeleton or proliferation[129, 132]. Priglinger et al. [118] showed that Gal-3 induces clustering of CD147 and integrin-β1 (ITGB1) transmembrane glycoprotein receptors on the RPE cell surface.

5.3. Glycosylation and Glycan structures

Glycosylation is a posttranslational modification that is universal in living organisms. Most secreted and membrane-anchored proteins are glycosylated and extracellular matrix (ECM) structures are rich in glycans and glycoconjugates[133]. Glycans are essential for the interaction between cells and the extracellular milieu and they are among the most diverse, complex and flexible molecules to react rapidly on intra- and extracellular changes[133]. Glycans are involved in biological processes such as cell signaling, embryogenesis, protein folding as well as proliferation of cells[134, 135]. Yet glycosylation also plays a role in pathogen recognition, immune responses and cancer[136-139]. Most of the naturally occurring glycan structures can be classified as N- or O- linked glycosides[140]. N-glycans are initiated by linkage of an N-acetylglucosamine (GlcNAc) to the amide side chain of an asparagine residue (figure 7)[139-141]. O-glycan synthesis is characterized by linking a saccharide (usually N-acetylgalactosamine, GalNAc) to the hydroxyl residue of serine, threonine or tyrosine (figure 7)[139, 140].

N-glycan biosynthesis starts in the ER by the transfer of a dolichol-linked glycan to an asparagine moiety of an Asn-Xaa-Ser/Thr sequon of a polypeptide[139, 142]. Quality control of the protein biosynthesis is done in the ER by Calnexin (CNX)[139, 143]. Properly folded proteins with a $Man_9GlcNAc_2$ structure are transported to the Golgi. In the stacks of the Golgi complex, various glycosyltransferases diversify the glycan structures of the glycoproteins, resulting in complex glycan structures (figure 7)[139, 141, 144].These complex-type N-linked glycoproteins are then transported to the cell surface or are secreted[139]. Complex glycan structures are characterized by glycans with multiple, extended branches, often containing N-acetyllactosamine units[145]. Crucial for galectin-binding and lattice formation are the number of glycoprotein ligands and the branching of their N-glycans[72]. In detail, the amount and the branching of N-acetyllactosamine (LacNAc) residues in the glycan pattern are decisive for affinity.

O-glycan synthesis begins in the Golgi by attaching a GalNAc residue to the hydroxyl of serine or threonine of the respective polypeptide, catalyzed by GalNAc transferase[139]. The resulting glycoprotein can be converted into various core structures that can be diversified by a range of glycosyltransferases (figure 7).

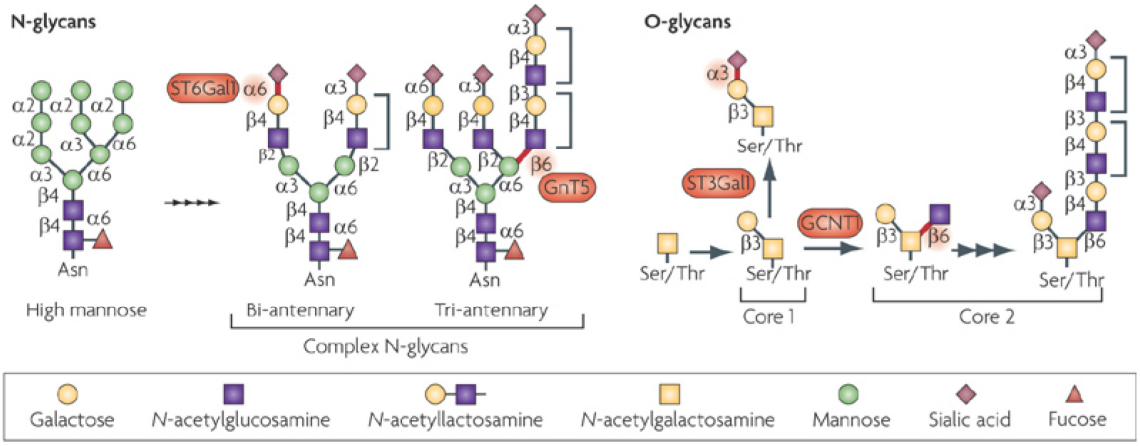

Figure 7: Schematic representation of N- and O-glycan biosynthesis, as published in Rabinovich and Toscano [146]. Glycosyltransferases like GCNT1, ST3Gal1, GnT5 and ST6Gal1 (illustrated in red) generate or mask common glycosylated ligands for galectins (such as N-acetyllactosamine (LacNAc) or poly-LacNAc residues in complex N-glycans or core 2 O-glycans). GCNT1: 2 N-acetylglucosaminyltransferase 1, GnT5: N-acetylglucosaminyltransferase 5, ST3Gal1: α2,3 sialyltransferase 1, ST6Gal1: α2,6 sialyltransferase 1.

Expression and activity of glycosyltransferases is essential for the availability of distinct glycan structures. N-glycans are substrates for N-acetylglucosaminyltransferases (Mgat genes). Among the most important glycosyltransferases with respect to galectin-glycan-interactions is the β-N-acetylglucosaminyltransferase 5 (Mgat5)[63]. Mgat5 induce addition of LacNAc on N-glycans and thus create preferred ligands of galectins (figure 7)[63]. Gal-3 for instance interacts with Mgat5-modified N-glycans on EGF and TGFβ receptors and induces cross-linking and thus prevents removal by constitutive endocytosis[124].

5.4. Proteomics

Many general and global biologic research fields and application areas are described by use of the "omics" ending – genomics, transcriptomics, proteomics, metabolomics, oncogenomics and many more. In 1995, the term "proteomics" was introduced as a "protein complement of the genome" and describes the analysis of a specific population of proteins at a given state and time-point within an experimental system[147-149]. Yet the proteome is more than the mere translation of the protein-coding regions of a genome[150]. Compared to the static genome, the proteome is very dynamic and can be influenced by any genetic and environmental changes[151]. One of the most popular examples is for instance the largely different proteome of a caterpillar and a butterfly, while the genome remains the same[151]. Due to splicing and editing processes at the RNA level as well as post-translational modifications and complex protein regulation processes the proteome is much more complex than the genome[149]. A crucial drawback of protein based techniques is that no amplification of proteins is possible before analysis and proteins highly distinguish in their physiochemical properties. Besides, protein abundances can span up to ten orders of magnitude (e.g. in human plasma) within a given proteome[152]. Identifying low abundant proteins in the presence of a large excess of many other proteins is always a challenge for all analytical methods[149]. Taken together, proteome based analysis is much more complex and difficult than genomics or transcriptomics, but it is also much closer to the functional level[149]. The smallest change of protein levels can lead to considerable biological consequences and by proteomic approaches it is possible to analyze these processes[151].

5.4.1. Proteomic workflow

The increasing complexity of biological samples in proteomic studies asks for fast and accurate analytical tools[153]. Conceptual breakthroughs and technical advances in separation techniques, protein chemistry, bioinformatics and sequencing techniques have contributed to the improvement of the science of proteomics[149]. Mass spectrometry (MS) has become the analytical instrumentation of choice for proteomic analyses because of its speed, wide dynamic signal range, quantitative capability and compatibility with chromatographic separation methods[153, 154]. Generally, mass spectrometry is an analytical technique that measures the mass-to-charge ratio (m/z

ratio) of ions in a mass spectrometer[155]. Biological samples are ionized by distinct procedures in the gas phase and separated according to their m/z ratios based on their motion in an electric or magnetic field[155]. Generally, it is distinguished between top-down and bottom-up proteomic approaches. In top-down strategies intact proteins are introduced into the gas phase, fragmented and identified. Yielding accurate mass measurements of the protein as well as of protein ion fragments, the complete primary structure of the protein can be generated[156]. The widely-used bottom-up protein analysis refers to the characterization of proteins by analysis of peptides released from the digestion of the protein[156, 157]. While a bottom-up approach is suitable for identifying a large number of proteins, it provides very limited molecular information about intact proteins[158]. Complete sequence coverage of proteins is rarely achieved and the identification of site-specific mutations and post-translational modifications is limited[157]. However, top-down proteomic approaches have significant limitations compared to bottom-up strategies. Protein fractionation, ionization and fragmentation in the gas phase, especially of large proteins, are very challenging[159]. In comparison, peptides are more easily fractionated, ionized and fragmented and thus bottom-up proteomic approaches can be more universally adopted for protein analysis and was also used in this study[159].

Basically, a bottom-up proteomic experiment is composed of the following main technical steps: sample preparation including protein digestion, peptide separation and ionization followed by identification and quantification of distinct proteins within a biological sample (figure 8)[160].

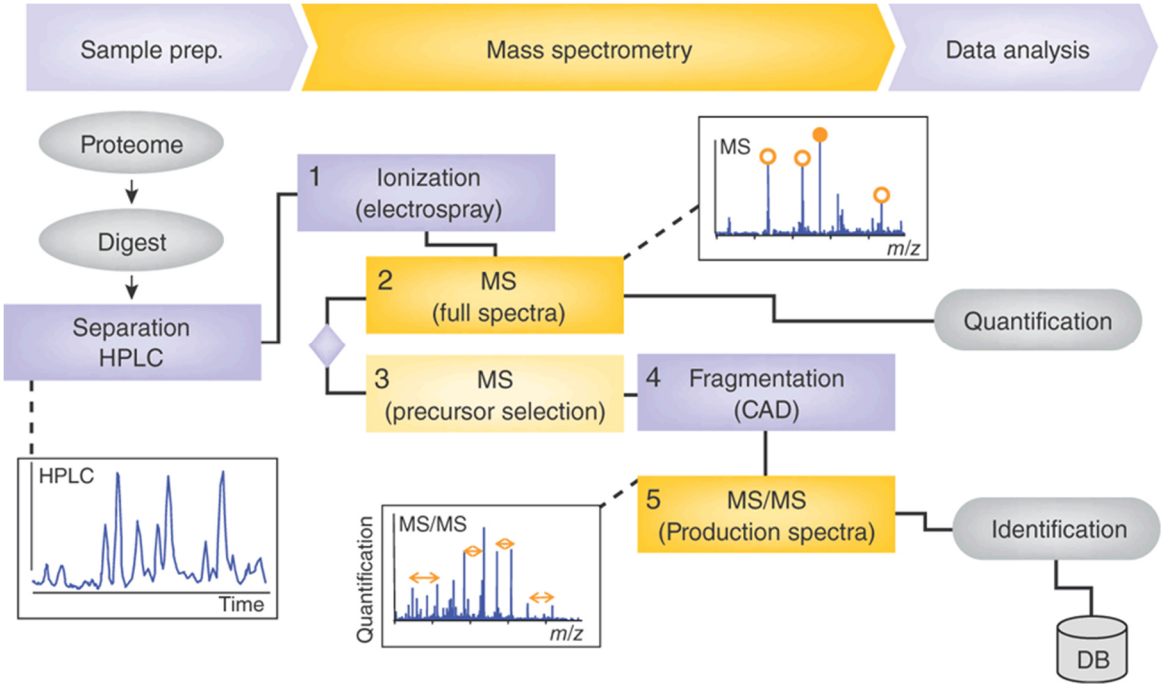

Figure 8: Proteomic workflow as published in Domon and Aebersold [150]. Protein samples are isolated from a biological source, prepared and digested. After protein digestion peptides are separated by HPLC with single or multiple dimensions. Peptides are then ionized by electrospray ionization (ESI) and analyzed in mass spectrometers. The acquisition of full MS spectra is followed by the selection of specific precursor ions to be fragmented, the collision induced fragmentation and the acquisition of MS/MS spectra. The data are processed to either quantify distinct proteins or the received MS/MS spectra are matched to peptide sequences in a database on the basis of the observed and expected fragment ions. MS: mass spectrometry; HPLC: high-performance liquid chromatography; CAD: collision-activated dissociation; DB: Database.

5.4.1.1. **Sample preparation**

A protein sample is isolated from a biological source (e.g. cell culture or organs) and needs to be prepared concerning both the sample characteristics (e.g. pH, temperature stability, hydrophobicity) and the biological question to be addressed (post-translational modification, membrane proteins, protein interaction)[161]. Sample preparation in MS-based workflows typically includes multiple steps such as sample desalting, concentration, sub-fractionation, and further separation and purification by gel electrophoresis or chromatography[161]. In "bottom-up" proteomic workflows proteins are proteolysed before separation. A high variety of endoproteases can be used for proteolysis. Most commonly used is trypsin which preferentially cleaves peptide bonds that are C-terminal to the basic amino acid residues arginine and lysine[161]. Peptides with

an average size of 800 to 2000 Da are generated and thus they are highly amenable to high sensitive MS/(MS) analysis[161]. Tryptic peptides are separated by high performance liquid chromatography (HPLC) – e.g. based on their hydrophobicity on a reverse phase (RP) C18 analytical column – and subsequently ionized by electrospray ionization (ESI) and introduced into the mass spectrometer[162].

5.4.1.2. **Mass spectrometry**

Originally in the so called "top-down" proteomic workflow, two-dimensional (2D) electrophoresis coupled with matrix-assisted laser desorption/ionization (MALDI) mass spectrometry was used for protein identification[155]. Yet, due to reproducibility problems and the limited identification rates, 2D-gel based approaches are nowadays mainly replaced by LC-MS/MS based processes[154]. Ionization of the peptides by ESI takes place in three steps which are nebulization of the sample into droplets, emission of ions from the droplets and transportation of ions from atmospheric pressure to vacuum (figure 9)[163].

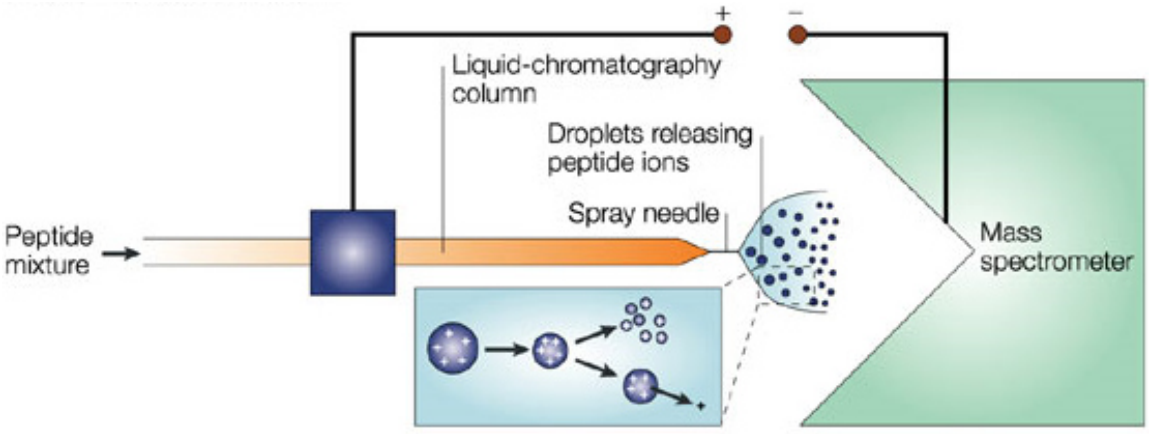

Figure 9: Electrospray ionization (ESI) in proteomics as published in Steen and Mann [160]. The solved analytes are eluted from a chromatography column and ionized by applying them to a narrow capillary tube and exposing to a high potential (1-2kV) relative to the inlet of the mass spectrometer. This generates highly positively charged droplets which explode into nanometer-sized droplets by Coulomb explosion and subsequently are transferred to mass analyzers.

The analytes are ionized out of solution by applying them to a narrow capillary tube and exposing them to a high potential (1-2kV) relative to the inlet of the mass spectrometer[154]. By the potential difference the liquid is extended to form a Taylor cone

from the capillary tip, from which a fine mist of charged droplets will emerge[155]. In the positive ion mode, which is usually applied in proteomics, positive ions are enriched at the surface of a droplet[161]. Due to increasing Coulombic repulsion between the positive charges on the surface and by exceeding the liquid surface tension (Raleigh limit) the droplets "explode" into nanometer-sized droplets (Coulomb explosion)[161]. The nebulization process continues until any ions become completely desolvated[155]. Whereas evaporation of the droplets reduces droplet size, the charge on the droplets remains constant, enabling the formation of multiply charged ions[155]. The analytes remain stable in the gas phase and thus ESI is considered as a soft ionization technique[161]. Besides, by producing multiply charged analyte molecules the mass range of analysis can be extended in proportion to the extent of the multiplicity of such charging[161].

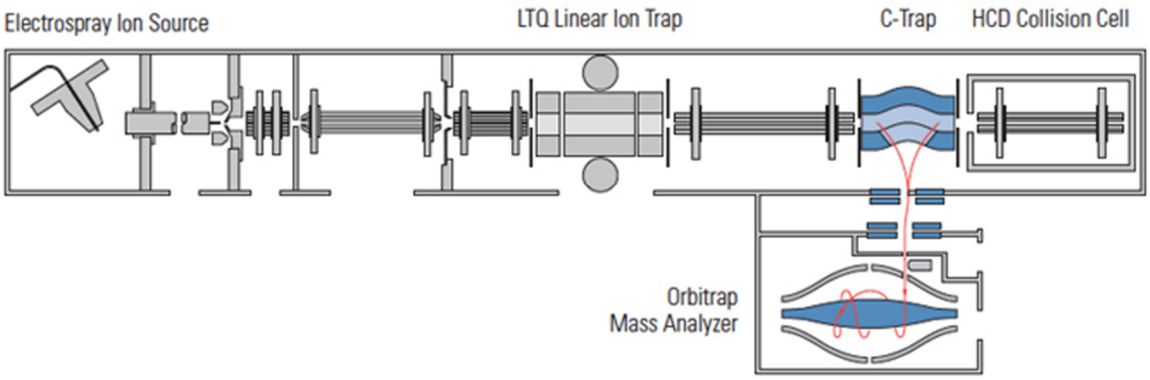

Figure 10: Scheme of a Thermo Scientific LTQ Orbitrap XL. Peptides are separated via a nano HPLC C18 column and ionized by electrospray ionization (ESI). The first part after the ion source is a LTQ linear ion trap. Ions are accumulated there and can be transferred into a C-Trap. In the orbitrap mass analyzer precursor ions are selected and MS spectra are recorded. Precursor ions are fragmented by collision induces dissociation and the corresponding MS/MS spectra are measured in the LTQ Linear Ion Trap (source of the scheme: Thermo Fisher Scientific, www.planetorbitrap.com).

After ionization peptides are transferred to mass analyzers to separate ions according to their mass-to-charge ratios. There are four basic types of mass analyzer used in proteomics research: ion trap, time-of-flight (TOF), quadrupole and Fourier transform ion cyclotron (FT-MS), which are mainly characterized by their sensitivity, resolution, mass accuracy and the ability to generate information-rich ion mass spectra from peptide fragments[154]. In mass spectrometers the mass analyzers can be used alone or

put together in tandem[154]. In this project the samples were measured either on a LTQ Orbitrap XL (Thermo Scientific, figure 10), combining the LTQ linear ion trap with the orbitrap technology, or on a Q Exactive™ HF (Thermo Scientific, figure 11) with hybrid quadrupole-Orbitrap features.

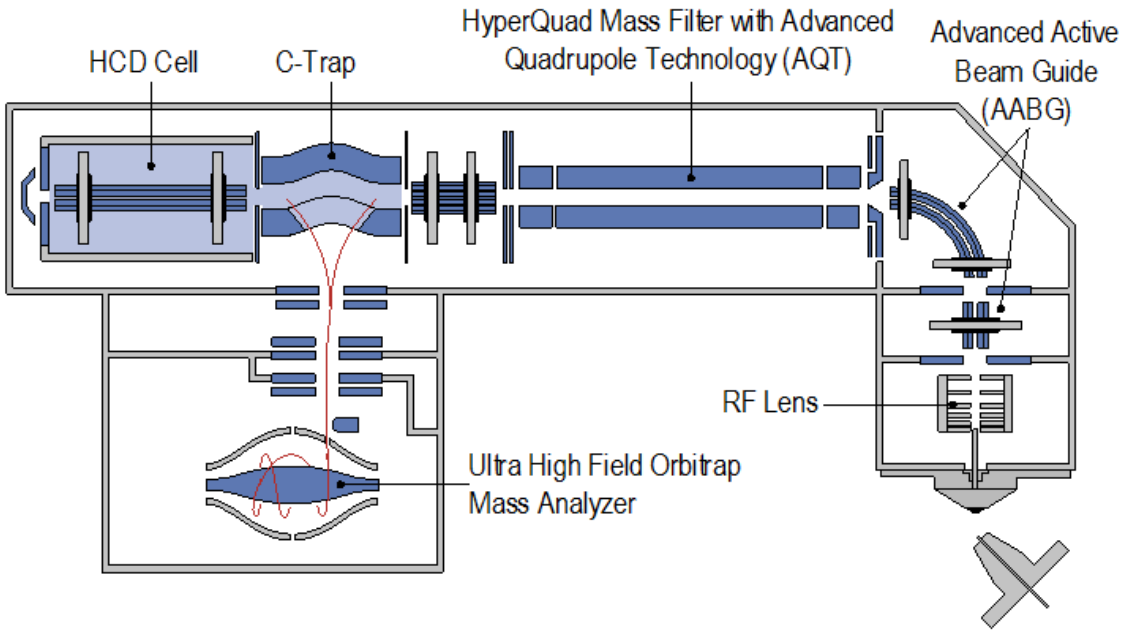

Figure 11: Scheme of a Thermo Fisher Q Exactive™ HF. Peptides are separated via a nano HPLC C18 column and ionized by electrospray ionization (ESI). The Q Exactive HF contains a mass selection pre-filter and a segmented quadrupole combined with a C-Trap and an ultra-high field orbitrap mass analyzer. Precursor ions are fragmented by collision induced dissociation in the HCD cell and the corresponding MS/MS spectra are analyzed in the Orbitrap, (source of the scheme: Thermo Fisher Scientific, www.planetorbitrap.com).

The Orbitrap analyzer radially traps ions in an electrostatic field about a central spindle electrode (figure 10)[164].The ions orbit around the central electrode and oscillate back and forth along the central electrode's long axis[165]. The oscillation frequencies are proportional to $(m/z)^{-1/2}$ and the accurate masses are extracted by Fourier Transformation[165]. Orbitrap analyzers are characterized by high resolution, high mass accuracy and increased dynamic range and high sensitivity[155]. Coupled with a linear ion trap both mass analyzers are capable to detect ions and record spectra. Thus the analyzers can be used independently or in conjunction as required[155]. In the linear ion trap ions are confined in a two-dimensional quadrupole field: radially by a two-dimensional radio frequency (RF) field and axially by stopping potentials applied to end

electrodes[166]. By adapting distinct potentials the linear ion trap can be used as a mass filter or as a trap[166]. Quadrupoles consists of four parallel metal rods and by time-varying electric fields only ions of a particular desired m/z ratio have a stable trajectory[154].

5.4.1.3. **Protein identification and quantification**

For protein identification two different approaches can be used: peptide mass fingerprinting (PMF) and tandem mass spectrometry (MS/MS)[155]. PMF is based on the measurement of m/z ratios and the calculated masses are indicative of the composition of the measured analytes[155]. In MS/MS analysis ions of a particular m/z value are selected and fragmented within the mass spectrometer[160]. First, the masses of intact tryptic peptides are determined and afterwards the peptide ions are fragmented in the gas phase to produce information on their sequence and modifications[156]. Typically, fragmentation is done by collision induced dissociation (CID/HCD) (figure 10). Due to collisions with an inert gas (such as nitrogen, argon or helium) covalent bonds of the peptide ions break resulting in fragmentation of the molecular ion into smaller fragments and thus the tandem MS spectrum (MS/MS or MS^2) is acquired[160]. The ion that is fragmented is called “precursor ion” and the ions in the tandem-MS spectrum are called “product ions”[160]. When a fixed number of precursor ions are selected automatically from the ions detected in a survey scan and analyzed by tandem mass spectrometry, this process is referred to as data-dependent analysis (DDA)[150]. Whereas, when all ions within a selected m/z range are fragmented and analyzed, it is called data-independent acquisition (DIA)[167]. Most commonly fragmentation takes place at the amide bond between amino acids and the resulting ions are called b-ions when the charge is retained by the amino-terminal part and y-ions if the charge is retained by the carboxy-terminal part[160] (figure 12).

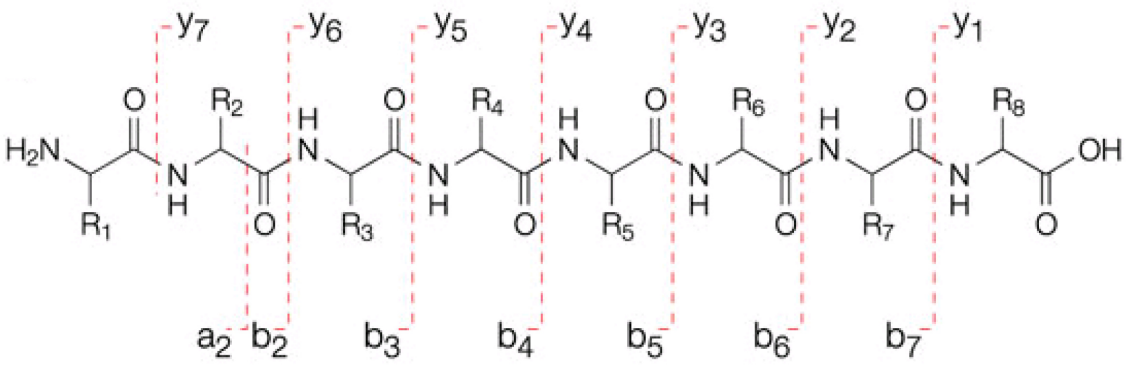

Figure 12: Peptide fragmentation as published in Steen and Mann [160]. By collisions with residual gas, bond breakage mainly occurs at the amide bonds. The resulting ions are called b-ions when the charge is retained by the amino-terminal part and y-ions if the charge is retained by the carboxy-terminal part.

Theoretically, the amino-acid sequence of the precursor ions can be determined because each peptide fragment in a series differs from its neighbor by one amino acid[160]. Yet the tandem-MS spectra are often not complete. Therefore, peptide-fragmentation spectra are matched to peptide sequences in a database on the basis of the observed and expected fragment ions[160]. The origin of the investigated sample has to be considered and is digested *in silico* under the respective workflow settings concerning the chosen enzyme and introduced modifications. One exemplary search algorithm to search sequence databases with MS/MS-spectra data is Mascot, which was also used in this study. In Mascot the accuracy of peptide identification is reported in terms of a probability score and by searching against a decoy sequence database the false discovery rate (FDR) can be calculated. Low FDR values can be obtained by using high-quality data, characterized by high mass accuracy, high number of fragments and high signal-to-noise ratios. Furthermore, the number of unique peptides identified for a specific protein is also an important parameter.

A typical proteomic study compares protein expression under different conditions and thus quantitative proteomics are fundamental. Many different quantitation techniques have been invented in the last years and incorporated into proteomic workflows. Proteins can for instance be metabolically labeled with heavy or light isotope-containing growth media or labeled proteins may be spiked in following lysis (figure 13)[168]. Enzymatic labeling can be done during digestion and chemical labeling or isobaric

tagging of peptides may occur further downstream. These protein identification strategies permit relative (comparison to a reference sample) or absolute quantification[154]. Label-free quantification is performed during or after data analysis and relies on advanced software analysis[168]. There are two major categories of label-free methods: extracted ion chromatogram (XIC)-based quantitation and spectral counting[168]. Spectral counting is based on the expectation that the number of peptide-identifying MS/MS spectra correlates directly with the abundance of protein[168]. XIC-based quantitation, which was used in this thesis, assumes that higher peptide concentrations will generate greater area-under-the-curve values in the MS spectra[168]. By measuring the relative concentrations of individual precursor ions within two or more samples and matching these abundances proteomic differences between biological conditions can be revealed. Absolute quantification can be done by use of internal standard peptides that have been synthetically prepared for selected or multiple reaction monitoring (SRM, MRM)[168].

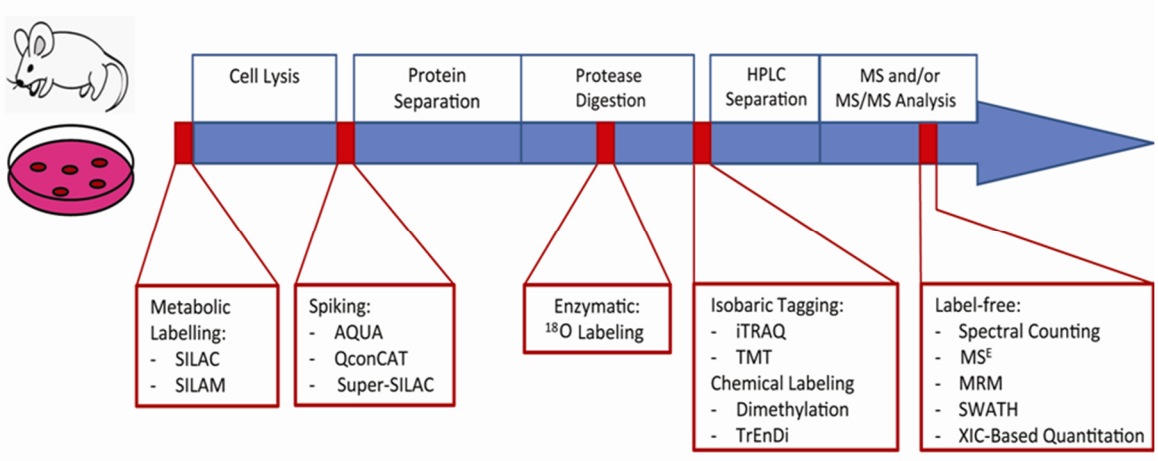

Figure 13: Quantitation strategies in a proteomic workflow as published in Smith [168]. Cell culture or animal model samples can be labeled metabolically at the protein level. Further down-stream labeled proteins can be spiked in or peptides can be enzymatically labeled during digestion. Following digestion, chemical labeling or isobaric tagging of peptides may be done. Label-free quantitation occurs during or after data analysis.

5.5. Aims of the study

Proliferative vitreoretinopathy (PVR) is one of the most common failures after retinal detachment surgeries and is characterized by the migration, adhesion and epithelial-to-

mesenchymal transition (EMT) of retinal pigment epithelial cells (RPE) and the subsequent formation of sub- and epiretinal fibrocellular membranes[1-3]. Currently there is no pharmacological adjuvant for preventing or treating PVR. In this PhD project the carbohydrate-binding proteins Gal-1 and Gal-3 were investigated as potential therapeutic agents for PVR with respect to modulated glycomic surface fingerprints of RPE cells upon PVR development. This work can be subdivided into 2 parts:

(1) Characterization of EMT processes and glycomic fingerprints of RPE cells during dedifferentiation

EMT is one of the key cellular events in PVR development. During EMT RPE cells convert from epithelial into mesenchymal cells and lose their epithelial characteristics and acquire migratory mesenchymal properties[10]. Here we analyzed changes in phenotype, proteome and cell surface glycan structures of RPE cells undergoing EMT *in vitro*. The impact of the glycomic shift associated with acquisition of a myofibroblastic phenotype of RPE cells for the pathogenesis of PVR was analyzed and interpreted and its relevance for the high efficacy of Gal-1 and Gal-3 in preventing PVR-associated cellular events was determined. A further aim was to develop a stable cell culture model for epithelial RPE cells.

(2) Functional impact of galectin treatment in correlation with glycomic surface fingerprints

a. Impact of galectins on the cellular behavior of RPE cells

In correlation of changed glycomic surface fingerprints upon EMT, functional impact of galectin treatment on RPE cells was analyzed. Furthermore Gal-1 and Gal-3 knockdown cells were established and investigated based on their glycan structure on the cell surface and on the reactivity to exogenously added galectin.

b. Identification of galectin-specific glycoprotein ligands in RPE cells

The cell surface proteins targeted by specific galectins on RPE cells are largely unknown. Here, we aimed to identify galectin ligands to unravel the functional effects of galectins on cellular behavior and to get new insights in the highly specific binding of galectins to dedifferentiated but not native RPE cells and the following prevention of PVR-associated cellular events. Relevance of glycosylation of these interactors for the functional galectin binding and the crosslinking activity was also analyzed.

6. Materials

6.1. Chemicals

Chemicals	**Manufacturer**
Acetid acid	Merck Millipore, Darmstadt, Germany
acetonitrile (ACN)	Sigma Aldrich, Steinheim, Germany
Acrylamide/Bis	Serva, Heidelberg, Germany
Ammonium bicarbonate	Sigma Aldrich, Steinheim, Germany
Ammonium persulphate (APS)	Bio-Rad, Munich, Germany
Asialofetuin	Sigma Aldrich, Steinheim, Germany
Biotinamidohexanoic acid N-hydroxysuccinimide ester (NHS)	Sigma Aldrich, Steinheim, Germany
β-lactose	Sigma Aldrich, Steinheim, Germany
β-mercaptoethanol	Sigma Aldrich, Steinheim, Germany
bromphenolblue	Merck Millipore, Darmstadt, Germany
Bovine serum albumin (BSA) Fraction V	Biomol, Hamburg, Germany
Complete	Sigma Aldrich, Steinheim, Germany
Coomassie Brilliant Blue R250	Serva, Heidelberg, Germany
Cyanogen bromide-activated Sepharose 4B	GE Healthcare, Uppsala, Sweden
L-Cystein	Roth, Karlsruhe, Germany
dimethyl sulfoxide (DMSO)	Sigma Aldrich, Steinheim, Germany
Dithiotreitol (DTT)	Merck Millipore, Darmstadt, Germany
DMNJ	Sigma Aldrich, Steinheim, Germany
Ethanol	Merck Millipore, Darmstadt, Germany
Ethanolamin	Sigma Aldrich, Steinheim, Germany
ethylenediaminetetraacetic acid (EDTA)	Merck Millipore, Darmstadt, Germany
Forskolin	Biomol, Hamburg, Germany
FluorSave	VWR, Radnor, USA
Glycerin	Merck Millipore, Darmstadt, Germany
Goat serum	Thermo Fisher Scientific, Waltham, USA

HCl	Merck Millipore, Darmstadt, Germany
Hoechst	Thermo Fisher Scientific, Waltham, USA
HPLC grade H20	Merck Millipore, Darmstadt, Germany
Iodacetamide	Merck Millipore, Darmstadt, Germany
Kifunensine	Sigma Aldrich, Steinheim, Germany
Lipofectamine 2000	Life Technologies, Carlsbad, USA
Methanol	Merck Millipore, Darmstadt, Germany
MTT	Thermo Fisher Scientific, Waltham, USA
NaCl	Sigma Aldrich, Steinheim, Germany
Na_2CO_3	Sigma Aldrich, Steinheim, Germany
NH_4HCO_3	Sigma Aldrich, Steinheim, Germany
Na_2HPO_4	Sigma Aldrich, Steinheim, Germany
NaN_3	Sigma Aldrich, Steinheim, Germany
NaOH	AppliChem, Darmstadt, Germany
Non-fat dried milk	Bio-Rad, Munich, Germany
NP-40	Roche, Basel, Switzerland
PageRuler™ Prestained Protein Ladder	Thermo Fisher Scientific, Waltham, USA
Paraformaldehyde	Sigma Aldrich, Steinheim, Germany
Phosphatase inhibitor cocktail 2 and 3	Sigma Aldrich, Steinheim, Germany
Plus Reagent	Life Technologies, Carlsbad, USA
ProteinG-Sepharose beads	GE Healthcare, Uppsala, Sweden
SB 431542 TGFβ inhibitor	R&D systems, Minneapolis, USA
Sodium dodecyl sulfate (SDS)	Sigma Aldrich, Steinheim, Germany
Sodium acetate	Sigma Aldrich, Steinheim, Germany
Sodium Deoxycholate	Sigma Aldrich, Steinheim, Germany
Sodium hydrogencarbonate	Merck Millipore, Darmstadt, Germany
Sodium orthovanadate	Sigma Aldrich, Steinheim, Germany
Swainsonine	Sigma Aldrich, Steinheim, Germany
Tetramethylethylenediamine (TEMED)	Bio-Rad, Munich, Germany
Trifluoroacetic acid (TFA)	Applied Biosystems, Foster City, USA
Tris	GE Healthcare, Uppsala, Sweden

Triton X-100	Sigma Aldrich, Steinheim, Germany
Tween20	Sigma Aldrich, Steinheim, Germany
Urea	Sigma Aldrich, Steinheim, Germany
yeast extract	Roth, Karlsruhe, Germany
Y-27632 ROCK-inhibitor	Biomol, Hamburg, Germany

6.2. General lab equipment

Lab equipment	**Manufacturer**
Centrifuge 5424	Eppendorf, Hamburg, Germany
Electrophoresis & blotting chamber	Bio-Rad, Munich, Germany
Electrophoresis chamber SubCell GT	Bio-Rad, Munich, Germany
Ibidi heating systems	Ibidi, Munich, Germany
Incubator Heracell 150i	Thermo Fisher Scientific, Waltham, USA
Incubator/Shaker E.coli	Memmert, Schwabach, Germany
Laminar flow	Weiss Pharmatechnik GmbH, Sonnenbühl, Germany
Magnetic Stirrer	IKA Labortechnik, Staufen, Germany
Multichannel Electronic Pipette	Mettler-Toledo, Greifensee, Switzerland
PCR machine Peqstar	Peqlab, Erlangen, Germany
pH Electrode inlab micro	Mettler-Toledo, Greifensee, Switzerland
Pipette 1 ml, 200 µl, 20 µl, 10 µl	Eppendorf, Hamburg, Germany
Power supply PowerPac HC	Bio-Rad, Munich, Germany
Power supply PowerPac 300	Bio-Rad, Munich, Germany
Thermomixer comfort	Eppendorf, Hamburg, Germany
Tube Rollers	Stuart, Staffordshire, UK
Tube Rotator	Stuart, Staffordshire, UK
Vortex Genius 3	IKA Labortechnik, Staufen, Germany

6.3. Consumables

Consumables	**Manufacturer**
Cell culture flask, 75 cm^2, 25 cm^2	Greiner, Frickenhausen, Germany
Cell culture dishes, 10 cm^2	Greiner, Frickenhausen, Germany
Cell scraper 25 cm	Sarstedt, Nümbrecht, Germany
Falcon conical tubes	BD Bioscience, San Jose, USA
Filter 0.2 µm, 0.45 µm	Merck Millipore, Darmstadt, Germany
Glass coverslips	VWR, Radnor, USA
Hybond-P PVDF membrane	Amersham, Little Chalford, UK
Pipette 5 ml, 10 ml, 25 ml, 50 ml	Greiner, Frickenhausen, Germany
Pipette tips	Thermo Fisher Scientific, Waltham, USA
Pipette tips	Eppendorf, Hamburg, Germany
Slide-a-lyzer dialysis cassettes	Thermo Fisher Scientific, Waltham, USA
Six well plates	Nunc, Wiesbaden, Germany
U-shaped 96 well plates	Corning, New York, USA
96 well plates	BD Bioscience, San Jose, USA
30kDa cut-off centrifuge filter	Pall Corporation, New York, USA

6.4. Kits and Standards

Kit	**Manufacturer**
ECL Plus enhanced chemiluminescence kit	GE Healthcare, Uppsala, Sweden
Human Phospho-Kinase Array	R&D systems, Minneapolis, USA
Pierce™ BCA (bicinchoninic acid assay) Protein Assay Kit	Thermo Fisher Scientific, Waltham, USA
Pierce™ NHS-Fluorescein Antibody Labeling Kit	Thermo Fisher Scientific, Waltham, USA
Plasmid DNA MiniPrep Kit	Thermo Fisher Scientific, Waltham, USA

6.5. Enzymes

Enzyme	**Manufacturer**
BsmBI	Thermo Fisher Scientific, Waltham, USA
Fast Alkaline Phosphatase	Thermo Fisher Scientific, Waltham, USA
Lys-C	Wako Chemicals GmbH, Neuss, Germany
Papain	Worthington, Lakewood, USA
Trypsin-EDTA 0.05% (w/v)	Gibco, Paisley, UK
Trypsin (Sequencing grade modified trypsin)	Promega, Mannheim, Germany
T4 Polynucleotide Kinase	New England Biolabs, Massachusetts, USA

6.6. Cell culture reagents and media

Medium or Reagent	**Manufacturer**
Bovine serum albumin (BSA) for cell culture	GE Healthcare, Uppsala, Sweden
DMEM high glucose	Gibco, Paisley, UK
FCS	Gibco, Paisley, UK
Kanamycin	Sigma Aldrich, Steinheim, Germany
LB Medium	Self-made (10 g/l NaCl, 10 g/l Tryptone, 5 g/l Yeast extract)
MEMα	Sigma Aldrich, Steinheim, Germany
MEGM	PromoCell, Heidelberg, Germany
OptiMEM	Life Technologies, Carlsbad, USA
PBS without Ca^{2+}/Mg^{2+}	Gibco, Paisley, UK
Penicillin/Streptomycine 10,000 U/mL	Gibco, Paisley, UK
Puromycin	Sigma Aldrich, Steinheim, Germany
Trypsin-EDTA 0.05% (w/v)	Gibco, Paisley, UK
ZYM 5052 auto-induction medium	Self-made, based on Studier [169]

6.7. Buffers

Buffer	**Manufacturer**
Acetate buffer	Self-made, 0.1 M NaAc, 0.5 M NaCl, pH 3-4
Ammonium bicarbonate buffer	Self-made, 50 mM ABC in H_2O
Buffer for galectin expression and purification	Self-made, 20 mM Tris-HCl, 150 mM NaCl, 0.03% (v/v) CHAPS, pH 7.5
Coupling buffer	Self-made, 0.1 M $NaHCO_3$, 0.5 M NaCl, pH 8.3
E.coli lysis buffer	Self-made, 20 mM Tris-HCl, 150 mM NaCl, 10 mM $MgSO_4$, 10 µg/ml DNaseI, 1 mM AEBSF.HCl, 0.03% (v/v) CHAPS, 1 mg/ml lysosyme, pH 7.5
FACS buffer	Self-made, PBS +1% BSA
Fast digestion buffer	Thermo Fisher Scientific, Waltham, USA
Fixing solution Coomassie staining	Self-made, 50% methanol, 12% acetic acid
Laemmli buffer	Self-made, 5% (w/v) SDS, 250 mM Tris-HCl pH 6,8, 50% (v/v) glycerol, 500 mM β-Mercaptoethanol, 0,025% (w/v) bromphenol-blue
RIPA	Self-made, 50 mM Tris-HCl pH 7.4, 150 mM NaCl, 0.1%(w/v) SDS, 0.5% (w/v) Sodium Deoxycholate, 1% (v/v) NP-40, Complete 1X
Solubilisation solution MTT assay	10% SDS in 0.01 M HCl
T4 DNA Ligase Puffer	New England Biolabs, Massachusetts, USA
Urea Buffer	Self-made, 8 M urea in 0.1 M Tris/HCl pH 8.5

6.8. Analytical instruments

Instrument	**Manufacturer**
Digital Developer Fusion FX	VilberLourmat, Eberhardzell, Germany
EMax Plus Microplate Reader	Molecular Devices, Sunnyvale, USA
FACS Fortessa	BD Biosciences, Heidelberg, Germany
RSLC Ultimate 3000	Dionex, Idstein, Germany
Lactose-agarose column	J-Oil Mills, Tokyo, Japan
Mass spectrometer Orbitrap XL	Thermo Fisher Scientific, Waltham, USA
Mass spectrometer Q Exactive HF	Thermo Fisher Scientific, Waltham, USA
Microscope DMI8	Leica Microsystems, Wetzlar, Germany
Nano trap column	LC Packings, Sunnyvale, USA
PepMap100 C18 HPLC column	LC Packings, Sunnyvale, USA
AcquityM UPLC, HSST3 column	Waters, Eschborn, Germany
Plate Reader Synergy HT	Biotek, Bad Friedrichshall, Germany

6.9. Antibodies

Primary antibody	**host species**	**Manufacturer**
anti-E-Cadherin, ab15148	rabbit	Abcam, Cambridge, UK
anti-GAPDH, MAB374	mouse	Merck Millipore, Darmstadt, Germany
anti-Gal-1, 25B11	mouse	Monoclonal Antibody Core Facility, HMGU, Germany
anti-Gal-3, 15B6	rat	Monoclonal Antibody Core Facility, HMGU, Germany
anti-ITGB1, AIIB2	rat	DSHB, Iowa, USA
anti-LRP1, ab92544	rabbit	Abcam, Cambridge, UK
anti-PDGFRB, ab32570	rabbit	Abcam, Cambridge, UK
anti-phospho-ERK p44/p42, #4370	rabbit	Cell signaling, Danvers, USA
anti-Vimentin, V6630	mouse	Sigma Aldrich, Steinheim, Germany

Secondary antibody	**Host species**	**Manufacturer**
anti-rabbit AlexaFluor647, #111-607-008	goat	Dianova, Hamburg, Germany
anti-rat AlexaFluor568, #112-297-020	goat	Dianova, Hamburg, Germany
anti-rabbit AlexaFluor488, #111-547-008	goat	Dianova, Hamburg, Germany
anti-mouse AlexaFluor568, #115-297-003	goat	Dianova, Hamburg, Germany
HRP-coupled secondary antibodies	rat, mouse, rabbit	Jackson ImmunoResearch, West Grove, USA

6.10. Lectins

Lectin	**Manufacturer**
Human Gal-1	Arie Geerlof, Institute of Structural Biology, HMGU, Germany
Human Gal-3	Arie Geerlof, Institute of Structural Biology, HMGU, Germany
Human Gal-8	Arie Geerlof, Institute of Structural Biology, HMGU, Germany
Human Gal-9	Arie Geerlof, Institute of Structural Biology, HMGU, Germany
Biotinylated PHAL	Vector laboratories, Burlingame, USA
Biotinylated ConA	Vector laboratories, Burlingame, USA
Biotinlyated Mal2	Vector laboratories, Burlingame, USA
Biotinylated PNA	Vector laboratories, Burlingame, USA

Secondary antibody	**Manufacturer**
Streptavidin-Alexa488	Thermo Fisher Scientific, Waltham, USA
Streptavidin-HRP	Vector laboratories, Burlingame, USA

6.11. Cell lines

Cell line	**Species**	**Supplier**
ARPE19 (CRL-2302™)	Human, eye	ATCC, Virginia, USA
HEK293T	Human, kidney	Life Technologies, Carlsbad, USA

6.12. Mammalian cells

Cell	**Species**	**Source**
RPE cells	Human, eye	Eye Bank of the Department of Ophthalmology, Linz General Hospital (Austria); Ludwig-Maximilians-University (Munich, Germany)
RPE cells	Porcine, eye	Schlachthof München, Munich, Germany

6.13. *E. coli* strains

Strain	**Supplier**
BL21 (DE3)	New England Biolabs, Massachusetts, USA
StbL3	Thermo Fisher Scientific, Waltham, USA

6.14. Guide RNAs

gRNA	**Sequence**
Gal-1	CCACCTCGCCTCGCACTCGA GTGCCTTCGAGTGCGAGGCG GATGGTGTTGGCGTCGCCGT
Gal-3	CATGATGCGTTATCTGGGTC
	GGCTGGTTCCCCCATGCGCC
	GCCCAGCAGGGGCGCCATAG

6.15. Plasmids

Construct	**Function**	**Resistance**	**Provided by**
lentiCRISPRv2	Transfer plasmid	Puromycin	lentiCRISPR v2 was a gift from Feng Zhang (Addgene plasmid # 52961)[170]
pETM-11	Expression vector	Kanamycin	Constructed by G. Stier, European Molecular Biology Laboratory
pMD2.G	Packaging plasmid	Ampicillin	pMD2.G was a gift from Didier Trono (Addgene plasmid # 12259)
psPAX2	Packaging plasmid	Ampicillin	psPAX2 was a gift from Didier Trono (Addgene plasmid # 12260)

6.16. Software

Software	**Version**	**Manufacturer**
ACAS	-	Ibidi + MetaviLabs, Germany + USA
CRISPR design tool	-	Zhang Lab, MIT, USA
Cytoscape	3.4.0	Institute of Systems Biology, Seattle, USA
FACS Diva	8.0.1	BD Biosciences, Heidelberg, Germany
FlowJo	7.6	TreeStar, Inc., Ashland, USA
FunRich	2.1.2	Open source, New York, USA
GeneRanker	2016	Genomatix, Munich, Germany
Huygens Essentials	16.05	Scientific Volume Imaging BV, Netherlands
ImageJ	1.50i	National Institute of Health, USA

Leica Appl. Suite	2.0	Leica Microsystems, Wetzlar, Germany
Mascot	2.5.1	MatrixScience, London, UK
Perseus	1.5.3.2	Computational Systems Biochemistry, Germany
Phobius	-	Karolinska Institutet, Sweden
Progenesis QI	2.0	Waters, Eschborn, Germany

7. Methods

7.1. Isolation of human and porcine RPE cells and RPE cell culture

Human cadaver eyes of organ donors were received by the Eye Bank of the Department of Ophthalmology at the Linz General Hospital (Linz, Austria) or at the Ludwig-Maximilians-University (LMU) (Munich, Germany) and were processed within 24 hours after death by an ophthalmologist in accordance with the institutions standard operating procedures. The securing process was authorized by the ethics committees of the hospital of the LMU Munich and of the Land Oberoesterreich and it was complied with the Declaration of Helsinki and approved by the relatives. Porcine eyes were provided by a local abattoir (Schlachthof München, Munich, Germany) and processed within 6 hours after slaughtering of the pics. As described in Priglinger et al. [118], Priglinger et al. [116] and Obermann et al. [171], porcine and human eyes were cleaned from periocular tissue and disinfected by incubation in 80% ethanol. After removal of the front segment of the eye, the vitreous body was also removed, the inner part of the eyecup was filled with phosphate-buffered saline (PBS, Gibco) and the retina was aspirated and removed. The eyecup was rinsed and incubated for 15-20 min at room temperature with pre-warmed 1 mM EDTA in PBS (37 °C), pH 7.4, to get rid of residual vitreous, remaining retina and photoreceptor outer segments. PBS/1 mM EDTA was discarded and the eyecup was filled with dissociation buffer (3 mM L-Cystein, 1 µg/µl BSA in PBS/1 mM EDTA), containing 45 µg papain (Worthington) per 1 ml dissociation buffer. After incubation for 23 minutes at 37 °C, the RPE cells were resuspended by pipetting up and down within the eyecup to dispense as much RPE cells as possible. To stop activity of papain, the loosened RPE cells were transferred in Dulbecco's modified Eagles medium (DMEM, Gibco) supplemented with 10% fetal calf serum (FCS, Gibco) and 1 % penicillin/streptomycine (P/S). After centrifugation for 5 minutes at 930 rpm at room temperature, the resulting cell pellet was resuspended and cultivated at high cell densities in DMEM, 10% FCS, 1% P/S at 37 °C and 5% CO_2. RPE cells isolated from one eye were cultivated in dishes with a surface area of 1.5 cm^2. If required, the cell culture medium was supplemented with 10 µM Kifunensine (Sigma Aldrich), 3 µM ROCK Inhibitor Y-27632 (biomol), 10 µM TGF-β inhibitor SB 431542 (R&D Systems), 10 µM Forskolin (biomol), 1 mM DMNJ (Sigma Aldrich) or 1 µg/ml Swainsonine (Sigma Aldrich)

for the respective time period. Passage numbers of 3 to 7 of the primary RPE cells were used for experiments. Regarding the limited availability of especially human RPE cells, the human RPE cell line ARPE19 (ATCC® CRL-2302™) was used for some experiments. ARPE19 cells are often used in RPE cell research, since they express RPE-specific markers such as the retinal pigment epithelium-specific 65kDa protein (RPE65) and having structural and functional RPE cell characteristics[172, 173]. ARPE19 cells were cultivated under the same cell culture conditions as primary human and porcine RPE cells, namely in DMEM, supplemented with 10% FCS and 1% P/S. Passage numbers between 10 and 20 were used for experiments. For some experiments FCS concentration in the medium was reduced to 3%.

To prevent EMT processes during cell culture, the minimum essential medium MEMα Sigma Aldrich), supplemented with 1% or 0% FCS, and the Mammary Epithelial Cell Growth Medium MEGM (PromoCell, 0% FCS) were tested as RPE cell culture media, compared to DMEM. As described in Maminishkis et al. [174] MEMα also contained: N1 supplement (Sigma Aldrich) 1:100 ml/ml, glutamine-penicillin-streptomycin (Sigma Aldrich) 1:100 ml/ml and nonessential amino acid solution (Sigma Aldrich) 1:100 ml/ml. Hydrocortisone (20 µg/l), taurine (250 mg/l), and triiodo-thyronin (0.013 µg/l) (THT) were dissolved in PBS to a final concentration of 1:500 (ml/ml) and added to the RPE medium.

7.2. Preparation of cell lysates

For preparation of protein lysates, ARPE19 and primary RPE cells were washed twice with ice-cold PBS and lysed in RIPA buffer (50 mM Tris-HCl pH 7.4, 150 mM NaCl, 0.1%(w/v) SDS, 0.5% (w/v) Sodium Deoxycholate, 1% (v/v) NP-40, Complete 1X) at 4 °C. For analysis of ERK phosphorylation 1 mM sodium orthovanadate and phosphatase inhibitor cocktail 2 and 3 (1:100, Sigma Aldrich) was added to RIPA buffer. After centrifugation at 12000 rpm for 15 minutes at 4 °C, the supernatant of the lysates was stored at -20 °C for further use.

7.3. Determination of protein concentrations

Protein concentrations were determined by Pierce™ BCA (bicinchoninic acid assay) Protein Assay Kit (Thermo Fisher, 23225). Bovine serum albumin (BSA) was used as a reference protein and a standard curve was used to calculate the unknown protein concentrations. 5 µl of the BSA dilutions (concentrations of 0.25 to 8 mg/ml) and of each unknown protein sample or dilutions thereof were pipetted into 96-well flat bottom plates. BCA working reagent (WR) was prepared by mixing 50:1 Reagent A:B. Reagent A contains sodium carbonate, sodium bicarbonate, BCA and sodium tartrate in 0.1M sodium hydroxide. Reagent B contains 4% cupric sulfate. 200 µl of WR was added to each well. After incubation at 37 °C for 30 min, absorbance was measured at 562nm on a plate reader. For each analysis a new standard curve was prepared based on the measured absorbance of the BSA dilutions and the protein concentrations were calculated by linear regression. As a blank the respective dilution buffer of the protein samples was used.

7.4. Expression and purification of human galectins

Recombinant human Gal-1, Gal-3, Gal-8 and Gal-9 were kindly produced and provided by Dr. Arie Geerlof (Protein Expression and Purification Facility, Institute of Structural Biology, Helmholtz Center Munich). As described in Priglinger et al. [118], Priglinger et al. [116] and Obermann et al. [171], the bacterial pETM-11 expression vector was used for cloning. pETM-11/hgalectin-1(-3, -8, -9) were transformed respectively into the *E. coli* strain BL21 (DE3). After cultivation at 20 °C in 2-L flasks containing 500 ml ZYM 5052 auto-induction medium[169] and 100 µg/ml kanamycin, *E. coli* cells were harvested by centrifugation when saturation was reached. Cells were divided in three pellets and stored at -20 °C. For lysis of the cells by sonication, the pellet was resuspended in 30 ml lysis buffer (20 mM Tris-HCl, 150 mM NaCl, 10 mM $MgSO_4$, 10 µg/ml DNaseI, 1 mM AEBSF.HCl, 0.03% (v/v) CHAPS, 1 mg/ml lysosyme, pH 7.5). After centrifugation (40,000 x g) and filtration (0.2 µm), the supernatants were applied to 2 ml lactose-agarose columns (J-Oil Mills, Tokyo, Japan), equilibrated in buffer A (20 mM Tris-HCl, 150 mM NaCl, 0.03% (v/v) CHAPS, pH 7.5). Before elution, the columns were washed three times with 25 ml buffer A. Bound proteins were eluted twice with 5 ml buffer A supplemented with 0.2 M β-lactose and protein containing fractions were pooled. His_6-

tagged hGalectin-1 was dialyzed against 1 L PBS containing 5 mM β-mercaptoethanol over night at 4 °C, his_6-tagged hGalectin-3, hGalectin-8 and h-Galectin-9 against 1 L PBS without β-mercaptoethanol. After filtration (0.2 µm), the dialysates were stored at 4 °C. Protein concentrations were calculated after measuring the absorbance at 280 nm by the following formula:

$$Protein\ concentration\ (M) = \frac{A_{280}}{\varepsilon_{protein} * b} * dilution\ factor$$

A_{280}: absorbance at 280nm

b: path length [cm]

$\varepsilon_{protein}$ = protein molar extinction coefficient [$\frac{l}{mol*cm}$]

ε_{Gal-1} = 8855 $M^{-1}cm^{-1}$

ε_{Gal-3} = 35870 $M^{-1}cm^{-1}$.

7.5. Biotinylation of human Gal-1 and Gal-3

For biotinylation, 150 mM β-lactose was added to 1 mg of purified Gal-1 and Gal-3, respectively, to stabilize the galectins. The proteins were dialyzed at 4 °C in Slide-A-lyzer dialysis cassettes (3.5 kDa cut off, Thermo Fisher) against 0.1 M sodiumhydrogencarbonate with 50 mM ß-Lactose, pH 9.2., for 2 hours. After a following 1 hour biotinylation at RT with 100 µg biotinamidohexanoic acid N-hydroxysuccinimide ester (NHS) according to the manufacturer´s instructions (Sigma Aldrich), the galectins were dialyzed again overnight at 4 °C against PBS. Activity of the biotinylated galectins was monitored by agglutination assay.

7.6. NHS-Fluorescein galectin labeling

Galectins were labeled with Fluorescein for FACS analysis with the Pierce™ NHS-Fluorescein Antibody Labeling Kit (Thermo Fisher). Based on the manufacturer's instructions, 1 mg of Gal-1 and Gal-3 was coupled to Fluorescein via N-hydroxysuccinimide ester (NHS) respectively. Protein concentration was calculated by the following formula after measuring the absorbance at 280 nm and 495 nm:

$$Protein\ concentration\ (M) = \frac{A_{280} - (A_{495} * CF)}{\varepsilon_{protein}} * dilution\ factor$$

A_{280}: absorbance at 280 nm

A_{495}: absorbance at 495 nm

CF: Correction Factor = $\frac{A_{280}}{A_{495}} = 0.3$

$\varepsilon_{protein}$ = protein molar extinction coefficient [$\frac{l}{mol*cm}$]

ε_{Gal-1} = 8855 $M^{-1}cm^{-1}$

ε_{Gal-3} = 35870 $M^{-1}cm^{-1}$

7.7. Activity control of human Gal-1 and Gal-3

Activity of purified and biotinylated galectins was determined semi-quantitatively by hemagglutination assays, adapted from Nowak et al. [175] and St-Pierre et al. [176]. Type 0 blood samples were kindly provided by Dr. Stefanie Hauck and Dr. Christine von Törne (Research Unit Protein Science, Helmholtz Centre Munich). 6 ml whole blood samples were collected in EDTA tubes and centrifuged at 3500 rpm for 5 min. The resulting transparent layer was removed and the red blood cells (RBC) were washed three times with PBS. After 10-fold dilution in PBS-3% glutaraldehyde, RBCs were rotated for 1h at RT and washed five times in PBS-0.0025% NaN_3. Resuspended in 4% PBS-0.0025 NaN_3, RBCs were stable for up to three months when stored at 4°C. For hemagglutination assay, serial dilutions of galectins in PBS were put in U-shaped 96 well plates and 10 µl RBCs were added per well. The minimum active concentration of each galectin, that prevented sedimentation of the RBCs, was evaluated visually, after incubation at 37 °C for 30 min (figure 14). For all experiments the respective Gal-1 and Gal-3 preparations were used in sufficiently active concentrations, as indicated.

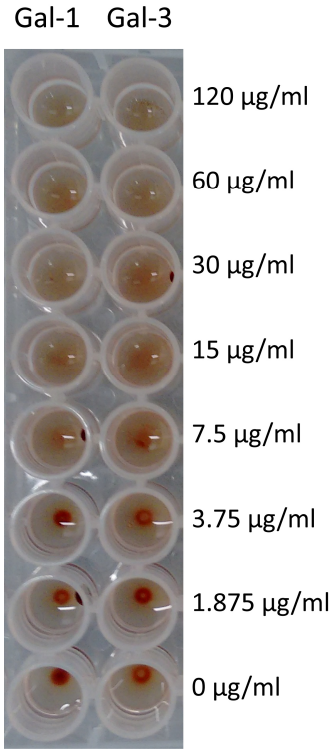

Figure 14: Activity of Gal-1 and Gal-3 determined semi-quantitatively by hemagglutination assays[175, 176]. Serial dilutions of galectins in PBS were put in U-shaped 96 well plates and 10 µl red blood cells (RBCs) were added per well. After incubation at 37 °C for 30 min, the minimum active concentration of each galectin, that prevented sedimentation of the RBCs, was evaluated visually.

7.8. MTT Assay

Cells were cultivated in 96-Well plates until 90% confluence was reached and then treated for 48h with 0, 6.25, 12.5, 25, 31, 62.5, 75 µg/ml Gal-1, Gal-3, Gal-8 and Gal-9 respectively, in DMEM plus 2% FCS. To 100 µl DMEM medium 10 µl MTT (3-(4, 5-dimethylthiazolyl-2)-2, 5-diphenyltetrazolium bromide, 5 mg/ml in PBS) was added for 4 hours at 37 °C. The yellow tetrazolium MTT was reduced by metabolically active cells to purple formazan, which could be solubilized by adding 100 µl of the solubilisation solution (10% SDS in 0.01 M HCl) to each well and incubating at 37 °C overnight. The absorbance was measured at 580 nm and color formation is a useful and convenient marker of the viable cells[177]. Thus, the viability of the cells correlated with the absorbance: the lower the absorbance at 580 nm, the lower cell viability.

7.9. Induction of Gal-1 and Gal-3 knockdown in ARPE19 cells by Lenti-CRISPR/Cas9

The CRISPR/Cas9 system (clustered regularly interspaced short palindrome repeats) was used to induce knockdown of Gal-1 and Gal-3 in ARPE19 cells. Based on publications from the Zhang group[170, 178, 179], lentiviral particles were used as vectors to integrate an expression cassette in the genome of ARPE19 cells and to introduce frame shift mutations in the coding sequence of the target genes. The expression cassette includes the guide RNA (gRNA - guides the Nuclease to the respective gene), the Nuclease Cas9 and a marker protein for puromycin resistance.

7.9.1. Target guide sequence cloning protocol

The CRISPR design tool (http://crispr.mit.edu/) was used to select appropriate gRNAs. The algorithm underlying this tool was published in Hsu et al. [178]. The sequences of the gRNAs of Gal-1 were

CCACCTCGCCTCGCACTCGA

GTGCCTTCGAGTGCGAGGCG

GATGGTGTTGGCGTCGCCGT

and for Gal-3

CATGATGCGTTATCTGGGTC

GGCTGGTTCCCCCATGCGCC

GCCCAGCAGGGGCGCCATAG.

In order to clone the target sequence into the lentiCRISPRv2 vector (addgene #52961), two oligonucleotides were created for each gRNA expression vector. Based on protocols described in Sanjana et al. [170] and published at http://genome-engineering.org/gecko/, a CACCG sequence was added to the 5’ end of the forward oligonucleotide (oligo-1) and an AAAC sequence to the 5’ end and a C to the 3’ end of the reverse oligonucleotide (oligo-2). 10 µg of lentiCRISPRv2 was digested and dephosphorylated at 37 °C for

30 minutes with 3 µl fast digest BsmBI (Thermo Fisher), 1 µl Fast Alkaline Phosphatase (FastAP, Thermo Fisher) in 7 µl 10x Fast digestion buffer (Thermo Fisher) and 0.7 µl 100 mM DTT with 6.3 µl H_2O. For the phosphorylation and annealing of the two oligonucleotides, 1 µl of oligo-1 (100 µM) and 1 µl of oligo-2 (100 µM) were merged with 1 µl of 10x T4 DNA Ligase Puffer (NEB), 6.5 µl H_2O and 0.5 µl T4 Polynucleotide Kinase (PNK, NEB) and put in a thermocycler for 30 minutes at 37 °C, followed by 5 minutes at 95 °C and ramped down to 25 °C at 5 °C/min. As negative control two forward or two reverse primers were used. Annealed oligos were diluted 1:200 in sterile H_2O. 3 µl of the BsmBI digested lentiCRISPRv2 vector and 1 µl of the 1:200 dilution of the annealed oligo mix were ligated in 1 µl T4 DNA Ligase buffer (10x) with 4 µl H_2O and 1 µl T4 DNA Ligase (NEB) at room temperature for 1 hour. Afterwards, 3 µl of the lentiviral transfer plasmids were transformed in 50 µl chemically competent cells StbL3 (E.coli) on ice for 30 minutes. After a heat shock for 30 seconds at 42 °C and a following incubation on ice for 2 minutes, 950 µl of lysogeny broth (LB) medium was added and the mixture was centrifuged for 45 minutes at 37 °C (300 rpm) and afterwards for 2 minutes at 4000 rpm at RT. The pellets were resuspended in 100 µl LB medium and plated on LB-Agar-plates (with Ampicillin). Plasmid DNA was amplified with a Plasmid DNA MiniPrep Kit (Thermo Fisher), following the manufactorer's instruction. The correct sequences of the vectors were verified by sequencing.

7.9.2. Lentivirus production

By co-transfection of three plasmids lentiviruses were created in 80% confluent HEK293T cells (Life Technologies)[170, 179]. In a 75cm^2 flask, 5 µg of packaging plasmids pMD2.G (addgene #12259) and 7.5 µg of psPAX2 (addgene #12260) were co-transfected with 10 µg of the respective created transfer plasmid "lentiCRISPRv2", using 100 µl Plus Reagent (Life Technologies) and 50 µl Lipofectamine 2000 (Life Technologies) in 8 ml OptiMEM (Life Technologies). As control, a virus was created with the two packaging plasmids and the "empty" plasmid lentiCRISPRv2 (addgene #52961) not coding for a functional gRNA (this plasmid contains a 2 kb "filler" sequence, which is not incorporated into a functional ribonucleoprotein complex of RNA and Cas9). A medium change after 6 hours to DMEM (Life Technologies) with 10 % fetal bovine serum (Life Technologies) and 1% bovine serum albumin (GE Healthcare) followed and after

60 hours lentiviral supernatants were harvested by centrifugation at 4 °C, 2000 g for 15 minutes and purified by 0.45 µm filtering. Lentiviral supernatant was stored at -80 °C and 750 µl of this supernatant was used to transduce 40% to 50% confluent ARPE19 cells in 10 cm² dishes. To select for transduced cells, 2 µg/ml puromycin was added to the cell culture media after one day. Gal-1 and Gal-3 knockdown was verified by Western Blot analysis. FACS analyses for galectin binding studies were performed between 12 to 20 days after transfection in order to allow sufficient knock-down.

7.10. Galectin pull-down experiments

Galectin pull-down assays were performed as described in Obermann et al. [171]. 1 mg Gal-1 and 1 mg Gal-3 were respectively coupled to 300 mg cyanogen bromide-activated Sepharose 4B (GE Healthcare). To activate the sepharose beads, they were washed 15 times with 1 mM HCl, followed by a single washing step in coupling buffer (0.1 M $NaHCO_3$, 0.5 M NaCl, pH 8.3), including a centrifugation step at 3000 rpm for 1 minute after each washing step. To couple the respective galectin isoforms to the beads, they are mixed 1:1 with coupling solution and were incubated on a rotating wheel with the activated beads at 4 °C overnight. Unreacted binding sites were blocked with 1 M ethanolamine (pH 8) for 2 hours at RT, after washing in a 5-fold volume of coupling buffer. The galectin-beads were washed several times at different pH values (3x coupling solution, 3x acetate buffer (0.1 M NaAc, 0.5 M NaCl, pH 3-4), 3x coupling buffer, 3x acetate buffer, 3x PBS). Stored in 20% ethanol, the beads were stable for several months. For each galectin pull-down experiment, activity of galectins, coupled to the beads, was tested. 100 µl beads-slurry (50% beads) was incubated with 200 µg asialofetuin (Sigma Aldrich) for 1 h at RT in absence and presence of 0.1 M ß- lactose. By incubation with 3x Laemmli buffer at 95 °C for 5 min, bound proteins were eluted and eluates were separated by SDS-PAGE (10% gels) and asialofetuin was detected by Coomassie staining. For galectin pull-downs, galectin-beads were washed three times with PBS to get rid of 20% ethanol and 20 µl beads-slurry (galectin-beads and ProteinG control beads (GE Healthcare)) were respectively incubated with 250 µg total proteins from human mesenchymal RPE cell lysates in PBS for 1h at 37 °C, with gentle mixing every 10 min. To get rid of weak bound proteins, beads were washed 4 times with PBS including centrifugation at 1000 rpm for 5 minutes. Bound proteins were eluted by 0.5

M β-lactose (Sigma Aldrich) and eluates were analysed by label-free quantitative LC-MS/MS. Five independent Gal-3 and five independent Gal-1 as well as the corresponding control ProteinG pull-down experiments with 3 or 4 technical replicates each were performed using RPE cell lysates derived from nine different human donors.

7.11. Sample preparation for mass spectrometry

10 µg of whole cell extracts and complete ß-lactose eluates of the Gal-1, Gal-3 and ProteinG pull-down experiments were proteolysed with Lys-C and trypsin (Promega, Mannheim, Germany) using a modified filter aided sample preparation protocol[180], as also described in Obermann et al. [171]. Protein samples were diluted to a final volume of 100 µl with ammonium bicarbonate buffer (ABC, Sigma Aldrich) and reduced for 30 min at 60 °C using 1 µl 1M dithiothreitol (DTT). When samples reached room temperature, 100 µl 8 M Urea Buffer (UA, Sigma Aldrich), pH 8.5, was added, followed by alkylation with 10 µl 300 mM iodoacetamide (Merck) for 30 min at RT in the dark. To quench unreacted iodacetamide 2 µl 1 M DTT was again added. 30 kDa cut-off centrifuge filter (Pall Corporation, NY) were equilibrated with UA buffer and protein samples were transferred to filters. Three washing steps with 400 µl UA buffer and two with 100 µl 50 mM ABC followed. Proteins were digested on the filters for 2h at RT with 1 µg Lys-C and afterwards with 2 µg trypsin overnight at 37 °C. By centrifugation through the filters, peptides were collected and after acidification with trifluoroacetic acid (TFA) (pH 2), samples were restored at -20 °C until mass spectrometry analysis.

7.12. Liquid chromatography and mass spectrometry (LC-MS/MS)

LC-MS/MS analysis for galectin pull-down samples was performed on a LTQ OrbitrapXL (Thermo Fisher Scientific Inc.) as also described previously[171, 181-184]. Every sample was automatically loaded onto an Ultimate3000 nano RSLC system (Dionex) with a nano trap column (300 µm inner diameter × 5 mm, packed with Acclaim PepMap100 C18, 5 µm, 100 Å; LC Packings, Sunnyvale, CA) in HPLC buffer containing 0.1% trifluoroacetic acid (TFA). The flow rate was 30 µl/min for 5 minutes. Using increasing acetonitrile (ACN) concentrations in 0.1% formic acid, peptides were separated on a reversed phase chromatography (PepMap, 25 cm, 75 µm ID, 1 µm/100 Å pore size, LC Packings) over 80 or 140 minutes at a flow rate of 300 nl/min. Maximal injection time for MS spectra was

100 ms, for MSMS spectra 500 ms. From the high resolution MS prescan the 10 most abundant peptide ions for fragmentation in the HCD trap were acquired. Yet, they had to be at least doubly charged and to have an intensity of 200 counts or more. The dynamic exclusion was 45 seconds and the isolation width was 2 amu. MS spectra were recorded within a mass range from 300 to 1500 m/z at a resolution of 60,000 full widths at half-maximum.

LC-MS/MS analysis for native and mesenchymal whole cell extracts was performed on a Q Exactive HF (Thermo Fisher Scientific Inc.). Samples were automatically loaded onto an Ultimate300 nano RSLC system (Thermo Fisher Scientific/Dionex) with a nano trap column (300 µm inner diameter × 5 mm, packed with Acclaim PepMap100 C18, 5 µm, 100 Å; LC Packings, Sunnyvale, CA) in HPLC buffer containing 0.1% trifluoroacetic acid (TFA). The flow rate was 30 µl/min for 5 minutes. Different concentrations of buffer A (2% ACN in 0.1% FA) and buffer B (100% ACN in 0.1% FA) were used to separate the peptides by increasing ACN concentrations on a reversed phase chromatography (AcquityMST3 column, 25 cm, 1.8 µm, Waters) over 130 minutes at a flow rate of 250 nl/min. The gradient was as followed:

0-5min: 3% buffer B
5min: 3% - 5% buffer B
5-85min: 25% buffer B
85-100min: 40% buffer B
100-105 min: 85% buffer B
105-110 min: 85% buffer B
110-112min: 85% - 3% buffer B
112-130min: 3% buffer B

Maximal injection time for MS and MS/MS spectra was 50 ms. From the high resolution MS prescan the 10 most abundant peptide ions for fragmentation in the HCD cell were acquired. Yet they had to be at least doubly charged, but not higher than 7 times charged and the AGC target was set to $1*10^5$. The dynamic exclusion was 30 seconds and the isolation width was 1.6 m/z. MS spectra were recorded within a mass range from 300 to 1500 m/z at a resolution of 60,000 for MS spectra and 15,000 for MS/MS spectra.

7.13. Protein identification and label-free quantification

Progenesis QI software for proteomics (Version 2.0, Nonlinear Dynamics, Waters, Newcastle upon Tyne, U.K.) was used to analyze the acquired spectra of the different samples for precursor intensity-based label-free quantification, as previously described[181-184]. Out of the profile data of the MS scans peak lists incorporating m/z values, intensities, abundances and m/z width were generated. Additionally, MS/MS spectra were transformed and stored in peaks lists with respective m/z values and abundance. The retention times of all samples were aligned to one reference sample. After automatic and manual alignment to a maximal overlay of all 2D features and exclusion of features without charges between 2 and 7, samples were grouped according to experimental groups. Raw abundances of all features were normalized. Using the Ensembl human protein database (homo sapiens, release: 75, 105287 sequences; release: 80, 100208 sequences) peptide identification was performed with Mascot (MatrixScience, London, UK; version 2.5.1). 10 ppm peptide mass tolerance and 0.6 Da (20 mmu for samples measured on Q Exactive HF) fragment mass tolerance were the used search parameters. Carbamidomethylation was set as fixed modification, and methionine oxidation and deamidation of asparagine and glutamine as variable modifications and one missed tryptic cleavage was allowed. When searches were performed with a mascot score cut-off of 15 and an appropriate significance threshold p, an average false discovery rate (FDR) of <1.25% was calculated by the Mascot-integrated decoy database search. After reimporting peptide assignments into Progenesis QI, all normalized abundances of unique peptides of an identified protein were summed to calculate the total cumulative normalized abundance of the respective protein. Based on these abundances, the enrichment factors of the quantified proteins to respective control samples were calculated. For all other settings the default values were used.

7.14. Statistics

Statistical analysis was performed using normalized abundances of all identified proteins as determined by Progenesis QI (see 10.13). Proteins without unique peptides were excluded of the analysis. The enrichment factors of distinct proteins were calculated with the determined protein abundances compared to the respective control samples. Normal distribution was assumed and significance was determined by Student's t-test

(galectin pull-downs) or by q-value determination by Progenesis QI software (nat/ded). Proteins with p-values/q-values lower than 0.05 were regarded as significantly changed, and lower than 0.01 as highly significantly changed.

7.15. Proteomic tools

MS data were analyzed and illustrated by different proteomic and statistical tools. Volcano plot representations were done with Excel. The log2 transformed ratios between normalized abundances of distinct proteins in two comparable groups were plotted against the negative log10 transformed p- or q-value of the respective same two comparisons. Infinite fold changes were set to the highest measured ratio plus 1 and were equalized to the lowest measured ratio.

Cluster analysis of log2 transformed normalized abundances of all identified proteins was done with Perseus[185] applying hierarchical clustering based on Euclidean distance. Missing values were excluded. Principal Component analysis (PCA) was also done in Perseus[185] based on log2 transformed normalized abundances of all identified proteins.

Phobius analysis was used to predict based on the amino acid sequence of a protein, how many signal peptides and transmembrane domains a respective protein has[186].

Identified proteins were analyzed based on their cellular components or molecular functions for example by Genomatix (GO) software suite. Cellular component analysis of the 15 identified Gal-1 interactors and the 131 Gal-3 interactors was performed based on the gene ontology (GO) annotation “cellular component” in FunRich[187]. For protein network generation, the Cytoscape App ClueGO-CluePedia[188] was used. The corresponding gene names of the Gal-1 and Gal-3 interactors were clustered by the GO term “molecular function” using *homo sapiens* as the organism for background list. The respective functional groups are represented by their most significant (leading) term and the network reflects the relationship between them. The size of the nodes represents the enrichment significance of the respective terms based on the predefined kappa score threshold of 0.4.

7.16. Scratch assay

Cells were cultivated in 24 well plates until 100% confluence was reached. Before treatment with 60 µg/ml Gal-3 and 120 µg/ml Gal-1, cells were starved at least 4 hours in serum-free DMEM. Medium was aspirated and a linear scratch was made in the confluent cell layer. To get rid of cell debris, cells were washed with PBS and DMEM + 3% FCS was added with the respective galectin concentrations. Cells were transferred to the ibidi heating systems (ibidi, Germany) for multi-well plates coupled to the Leica DMi8 microscope with a HCX PL APO 10x/1.20 objective lens. Cells were cultivated at 37 °C at 5% CO_2 and life cell imaging was performed, taking pictures every 20 minutes of the defined scratch region over a time period of up to 5 days. Migration of the cells into the scratch wound healing area could be analyzed over time with ACAS (Automated Cellular Analysis System, ibidi, MetaviLabs) by measuring the gap covered area.

7.17. FACS analysis

ARPE19 or human and porcine RPE cells were cultivated up to a confluence of 80% and washed with PBS. Cells were detached by incubation with 0.05% trypsin-EDTA (Thermo Fisher) for 3 minutes at 37 °C and then transferred to DMEM+10% FSC to inhibit activity of trypsin. After centrifugation at 930 rpm for 5 minutes, cells were washed with and resuspended in PBS. Cells were counted and divided to $1*10^5$ cells per reaction tube. After centrifugation at 1000g for 3 minutes, cells were washed with 170 µl FACS buffer (PBS + 1% BSA). The binding compounds were prepared in the respective concentrations in FACS buffer and cells were incubated with them for 20 minutes at 4 °C, followed by a washing step with 170 µl FACS buffer. The used compounds were:

- 60 µg/ml biotinylated Gal-1
- 60 µg/ml biotinylated Gal-3
- 3 µg/ml of the biotinylated plant lectins PHAL, ConA, Mal2, PNA (vector laboratories)

After incubation with Streptavidin-Alexa488 (1:200, Thermo Fisher) for 20 minutes at 4 °C, cells were again washed with 170 µl FACS buffer and resuspended in 500 µl FACS buffer for measuring. FACS analysis was performed using a BD Fortessa (BD Biosciences) flow cytometer with FACSDiva software (BD Biosciences). Flow cytometry data were

exported in the format 3.0 and analyzed using FlowJo 7.6 cell analysis software (Tree Star, Inc.).

For the analysis of endocytosis of Gal-1 and Gal-3, ARPE19 cells were treated with Fluorescein-labeled galectins for 5, 15 and 30 minutes or with Fluorescein-transferrin (Thermo Fisher, T2871) for 30 minutes at 37 °C to enable endocytosis. Prior to that, ARPE19 cells were treated with 10 µM kifunensine to inhibit α-mannosidase I or with 400 µM dynasore (abcam) to inhibit dynamin-mediated endocytosis. After trypsinisation of the cells to get rid of transferrin, Gal-1 and Gal-3, bound on the cell surface, but not endocytosed, FACS analysis was performed as described above.

7.18. Immunocytochemical staining

7.18.1. EMT analysis

Porcine RPE (pRPE) cells were treated with 3 µM ROCK Inhibitor Y-27632, 10 µM TGF-β inhibitor SB 431542, 10 µM Forskolin, 30 µg/ml Gal-1, 30 µg/ml Gal-3 or with 1 µg/ml of the mannosidase-inhibitor Swainsonine directly after isolation of the eyes up to passage 6. pRPE cells were cultivated on glass coverslips (VWR) until 80-90% confluence in DMEM+10% FCS. After fixation with 4% paraformaldehyde, coverslips were blocked with Tris-buffered saline with 0.1% Tween20 (TBS-T) + 1% bovine serum albumin (BSA) + 0.5% goat serum for 45 minutes at RT and incubated with the respective antibody mouse anti-Vimentin (1:50, Sigma Aldrich) and rabbit anti-E-Cadherin (1:50, abcam) at 4 °C overnight. After two washing steps in TBS-T, an incubation with the secondary antibodies goat-anti-rabbit-AlexaFluor488 and goat anti-mouse AlexaFluor568 (1:1000, Dianova) followed for 1h at RT. Coverslips were washed again two times with TBS-T, counterstained with Hoechst (1:5000, ThermoFisher) for 8 minutes at RT, mounted with FluorSave (VWR) and photographed on a Leica DMi8 microscope with a HCX PL APO 20x/1.20 objective lens. Filter cubes for GFP, TXR and DAPI detections were used (JH Technologies). All images were captured using a Leica DFC365 FX camera and constant settings for gain and exposure time were maintained for all samples within an experimental set-up. Images were processed by the Leica Application Suite LASX (version 2.0, Leica). As control, cells were stained under equal conditions without primary antibodies and only with secondary antibodies. No unspecific labeling was observed. The

immunocytochemical staining of pRPE cells treated with different components was repeated at least three times. Phase-contrast microscopy was also done with cultivated RPE cells on a Leica DMi8 microscope with HC PL FL 10x/0.3 or 20x/0.4 objective lenses.

7.18.2. Co-localisation of galectin with ITGB1, LRP1 and PDGFRB

Mesenchymal human RPE cells were cultivated on glass coverslips (VWR) upon 60-70% confluence in DMEM+10% FCS with or without 10 µM Kifunensine (Sigma Aldrich) up to passage 4-7. Cells were washed and starved for at least two hours in serum-free DMEM medium before Galectin-treatment. 120 µg/ml Gal-1 and 60 µg/ml Gal-3 were incubated with the cells for 30 minutes at 37 °C. As control no galectin was added. Cells on the coverslips were fixed with 4% paraformaldehyde, washed with TBS-T and incubated with blocking solution (Tris-buffered saline with 0.1% Tween20 (TBS-T) + 1% bovine serum albumin (BSA) + 0.5% goat serum) for 45 minutes at RT. Galectin binding was visualized by incubation with Streptavidin-Alexa488 (1:500, ThermoFisher) for 1h at RT. Immunocytochemical staining with rabbit anti-LRP1 (1:50, abcam), rabbit anti-PDGFRB (1:50, abcam) or rat anti-ITGB1 (1:60, DSHB) diluted in TBS-T was performed overnight at 4 °C. After washing twice with TBS-T, coverslips were incubated with the secondary antibodies goat-anti-rabbit-AlexaFluor647 or goat anti-rat AlexaFluor568 (1:1000, Dianova) for 1h at RT. Nuclei were stained with Hoechst (1:5000, ThermoFisher) for 8 minutes at RT and coverslips were mounted with FluorSave (VWR) and photographed on a Leica DMi8 microscope with a HCX PL APO 63x/1.20 objective lens. Filter cubes for GFP, Y5, TXR and DAPI detections were used (JH Technologies). All images were captured under constant settings for gain and exposure time within an experimental set-up using a Leica DFC365 FX camera. Images were processed by the Leica Application Suite LASX (version 2.0, Leica) and the deconvolution software Huygens Essential using the classic maximum likelihood estimation (CMLE) algorithm with a signal to noise ratio of 40 and 50 iterations (version 16.05, Scientific Volume Imaging B.V., Netherlands, http://svi.nl). As control, cells were stained under equal conditions without primary antibodies and only with secondary antibodies. No unspecific labeling was observed (data not shown). Immunocytochemical staining of human RPE cells was repeated at least three times with cells from three different donors.

7.19. Western blot analysis

10 µg of the respective whole cell extracts were used for Western Blot analysis. For the analysis of the phosphorylation of ERK 15 µg of the respective protein sample were used. For the galectin pull-down experiments with lysates of mesenchymal RPE cells from three different donors, treated or untreated with 10 µM Kifunensine for up to 4 weeks, whole protein eluates were applied. Protein samples were separated by SDS-PAGE (10% gels) and blotted onto PVDF membranes. After blocking with 3% BSA in TBS-T for Western blots using phospho-specific antibodies or with 5% non-fat dried milk in TBS-T for 1h at RT, blots were incubated with antibodies against rabbit anti-LRP1 (1:20,000, abcam), rabbit anti-PDGFRB (1:1,000, abcam), mouse anti-GAPDH (1:10,000, Millipore), mouse anti-Vimentin (1:500, Sigma Aldrich), rabbit anti-E-Cadherin (1:200, abcam), rabbit anti-phospho-ERK p44/p42 (1:2,000, cell signaling, #4370), mouse anti-Gal-1 (1:2, in house), rat anti-Gal-3 (1:2, in house) or with the biotinylated plant lectin PHAL (1:1,000, vector laboratories) at 4 °C overnight. After washing three times with TBS-T, blots were incubated with the appropriate HRP-coupled secondary antibodies (1:7,500, Jackson ImmunoResearch) or with Streptavidin-HRP (1:20,000, vector laboratories) for 1h at RT and binding was visualized by signal development with ECL Plus enhanced chemiluminescence kit (GE Healthcare). All Western Blot experiments were repeated at least 3 times.

7.20. Coomassie staining

For Coomassie staining of a SDS-PAGE, Coomassie Brilliant Blue R250 Powder (Serva) was used. The gel was fixed for 30 minutes in the fixing solution (50% methanol, 12% acetic acid). 0.4% Brilliant BlueR250 was diluted in fixing solution. A 1:10 dilution thereof was used to stain the gel for 30 minutes. After destaining the gel with fixing solution for 30 minutes, it was washed at least twice for 15 minutes in H_2O.

7.21. Analysis of phosphorylation profiles

For the simultaneous analysis of changes in relative site-specific phosphorylation profiles of 43 kinases and 2 related total proteins after galectin treatment, the Human Phospho-Kinase Array (R&D Systems, ARY003B) was used. Selected phospho-specific capture antibodies are spotted in duplicate on nitrocellulose membranes. According to the

manufacturer´s instructions (R&D systems), 300 µg of whole cell extracts of ARPE19 cells untreated or treated for 15 minutes with 120 µg/ml Gal-1 or 60 µg/ml Gal-3 were incubated with the nitrocellulose membranes overnight at 4 °C. After subsequent incubation with a cocktail of biotinylated detection antibodies and Streptavidin-Horseradish Peroxidase, the amount of phosphorylated protein bound at the respective capture spot was visualized by signal development with chemiluminescent detection reagents. Pixel density of each spot was determined with ImageJ[189] considering background subtraction[189]. Mean pixel density, standard deviation and statistical significance (Student's t-test) were determined. P-values lower than 0.05 were considered as significant (*), p-values lower than 0.01 as highly significant (**).

8. Results

8.1. Characterization of EMT processes and glycomic fingerprints of RPE cells during dedifferentiation

Epithelial-to-mesenchymal transition (EMT) is one of the key cellular events in PVR development. To get deeper insights in cellular processes underlying EMT, we analyzed changes in phenotype, proteome and cell surface glycan structures of RPE cells undergoing EMT *in vitro*. We also examined the impact of glycomic shifts on binding of Gal-1 and Gal-3 on epithelial and mesenchymal RPE cells. To prevent EMT *in vitro* and to develop a stable cell culture model for epithelial RPE cells, we tried to interfere with both phenotype transition and glycan synthesis.

8.1.1. Primary RPE cells undergo morphologic changes during sub-cultivation

Because of the limited availability of human RPE cell samples derived from patients suffering PVR, cultured primary human or porcine RPE cells were used as a well-accepted *in vitro* model system for early PVR[45]. Dulbeccos modified Eagle Medium (DMEM, high glucose, pyruvate) with 10% FCS was routinely used to cultivate primary RPE cells on tissue culture plastic. After isolation of RPE cells from eyes, they were routinely plated at a high density to keep the cells in a homogenous cell monolayer. 100% confluence was normally reached after 5 days.

Directly after isolation, the cells were pigmented and had a well-differentiated epithelial morphology (passage 1, figure 15). During sub-cultivation, from passage 2 or 3 on, the RPE cells began to dedifferentiate and transformed into a mesenchymal-like phenotype (figure 15). 6^{th}- or higher passage-cells had totally lost their epithelial characteristics, their cell-cell contacts and spreading was increased (figure 15). Changes in the cytoskeleton structure were also visible. Cell culture conditions with lower cell densities enabled higher degrees of cell spreading and faster dedifferentiation of the cells.

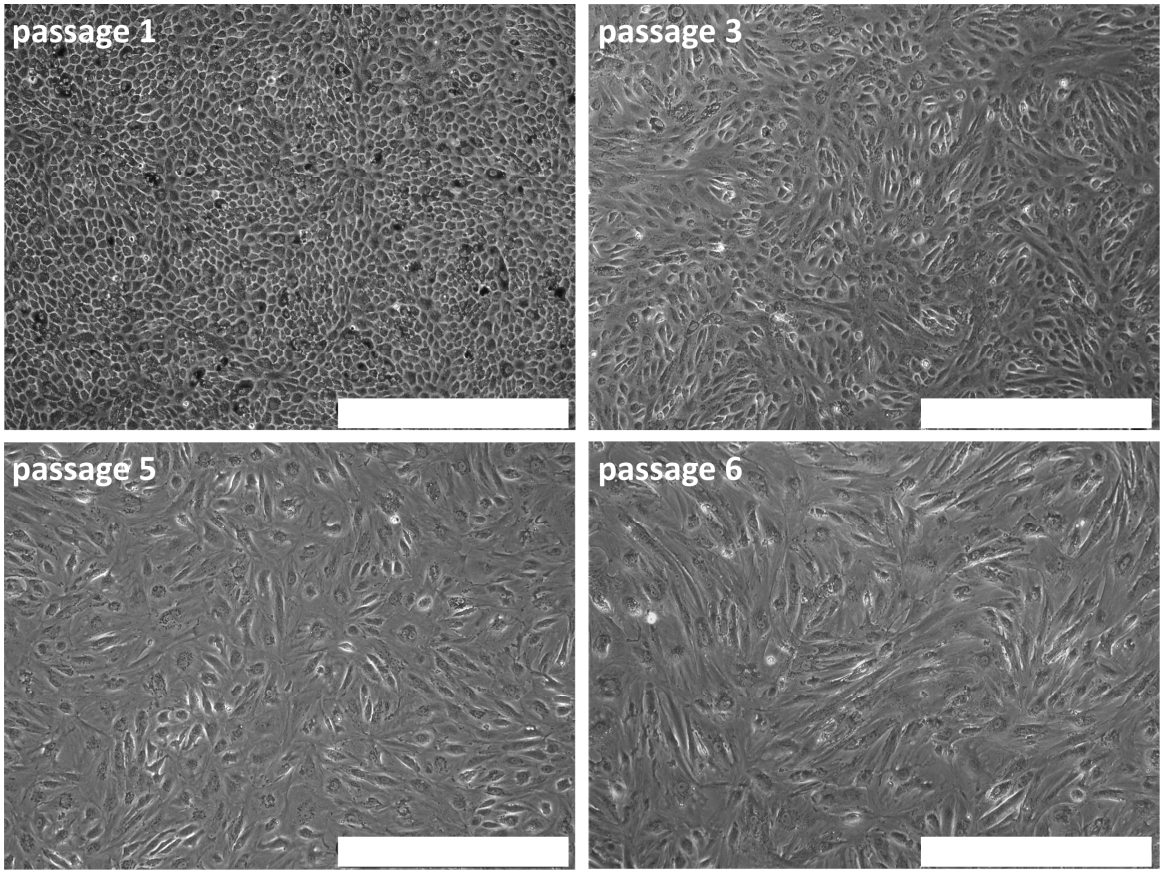

Figure 15: Primary RPE cells undergo EMT during culture. Phase-contrast images (10x objective lense) of porcine RPE cells at different passages cultivated in Dulbeccos modified Eagle Medium (DMEM, high glucose, pyruvate) with 10% FCS, scale bar 500 µm.

8.1.2. Clear differences in protein expression of native and mesenchymal RPE cells

To get deeper insights into epithelial-to-mesenchymal transition (EMT) processes during sub-cultivation of RPE cells, a proteome-wide screening approach was done. Whole cell extracts of native RPE cells, freshly isolated of human cadaver eyes, or of cultivated human RPE cells (passage number 5-7) were analyzed by label-free quantitative LC-MS/MS. Four different human donors for native RPE cells and four different donors for mesenchymal RPE cells were used. To identify those proteins that were up- or downregulated in mesenchymal RPE cells compared to native ones, ratios of the means of all protein abundances in all native and all mesenchymal RPE cells were calculated. Statistical analysis was done using FDR adjusted p-values (q-values). Proteins with a q-value <0.01 and enrichment factors (fold change, FC) of ≥ 5 or ≤ 0.2 in native cells compared to mesenchymal RPE cells were regarded as highly significantly changed.

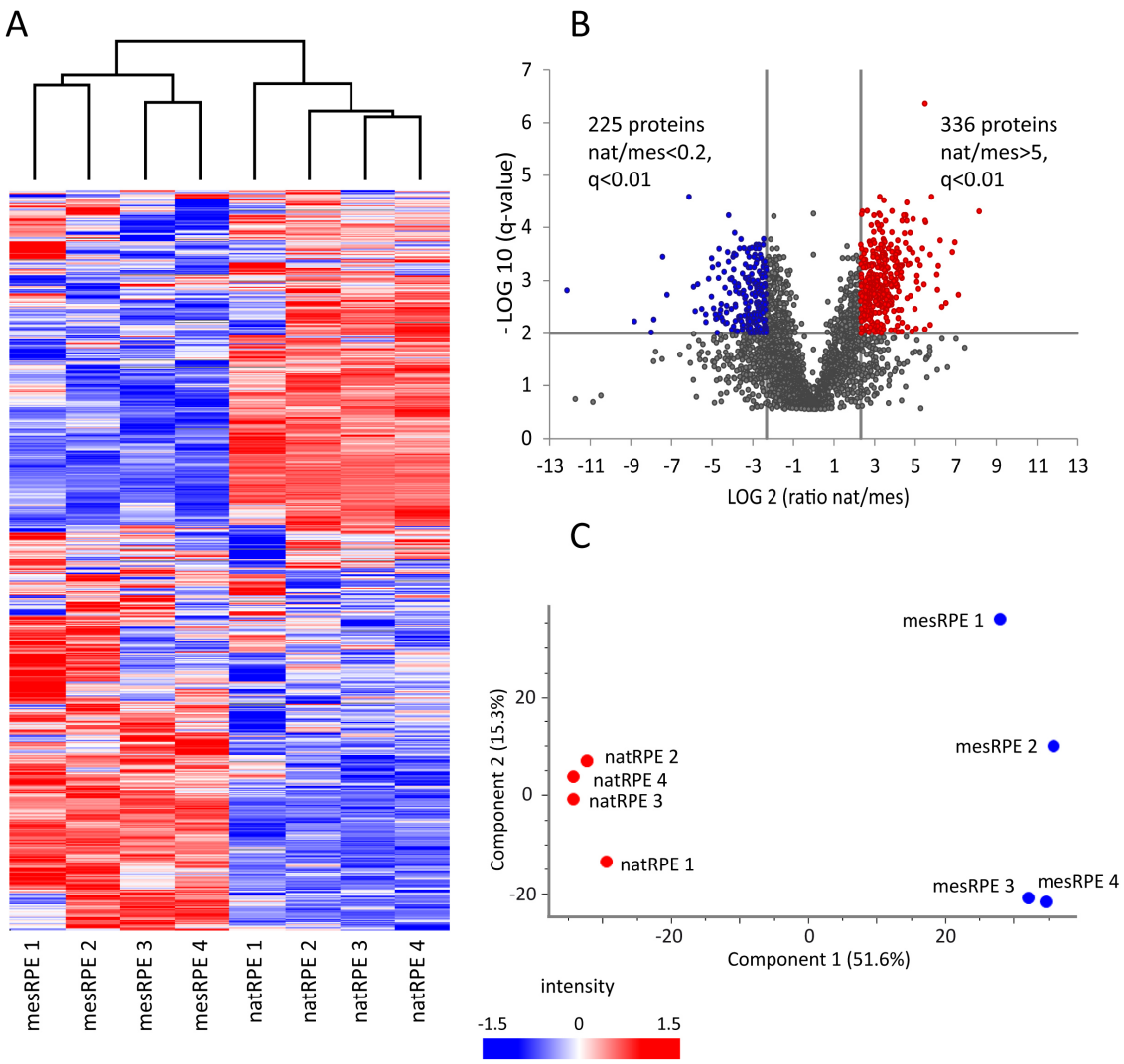

Figure 16: Proteomic analysis of native and mesenchymal human RPE cells reveals clear differences in protein expression. A: Cluster analysis based on the normalized abundances of all identified proteins of 4 different human mesenchymal RPE samples (passage number 5-7) and 4 different human native RPE samples. High abundant proteins were colored in red, low abundant proteins in blue. B: Volcano Blot analysis: ratios of the means of all protein abundances in all native and all mesenchymal RPE cells were calculated and plotted against the corresponding negative log10 transformed FDR adjusted p-values (q-values). Those proteins with a q-value <0.01 and enrichment factors of ≥ 5 (red dots) or ≤ 0.2 (blue dots) in native cells compared to mesenchymal RPE cells were regarded as significantly changed. C: Principal Component Analysis of the 4 native RPE and the 4 mesenchymal RPE cell samples. nat: native, mes: mesenchymal.

Clustering of the identified and relatively quantified proteins showed a clear difference in protein expression in native and mesenchymal human RPE cells (figure 16A). 2454 proteins could be identified in all 8 samples. 336 proteins were highly significantly

(q<0.01) over five-fold upregulated (FC nat/mes>5) in native RPE cells (red dots, figure 16B). Using the corresponding cut-off, 225 proteins were over five-fold upregulated (FC<0.2) in mesenchymal RPE cells (blue dots, figure 16B). Even though there was a biological variance in the human samples, a clear difference in protein expression was visible between native and mesenchymal RPE cells in Principal Component Analysis (figure 16C). Only 174 of 2454 proteins were expressed at similar levels in native and mesenchymal cells (enrichment factor between 0.8 and 1.2), which means that 93% of all identified proteins were changed upon sub-cultivation of RPE cells. Epithelial cell markers like Claudin-19 and E-Cadherin were downregulated in mesenchymal cells as expected, whereas mesenchymal cell markers like Vimentin and N-Cadherin were upregulated in mesenchymal cells (figure 17). Thus, sub-cultivation of RPE cells led not only to a complete change of phenotype of RPE cells, but also to an impressive change in protein expressions.

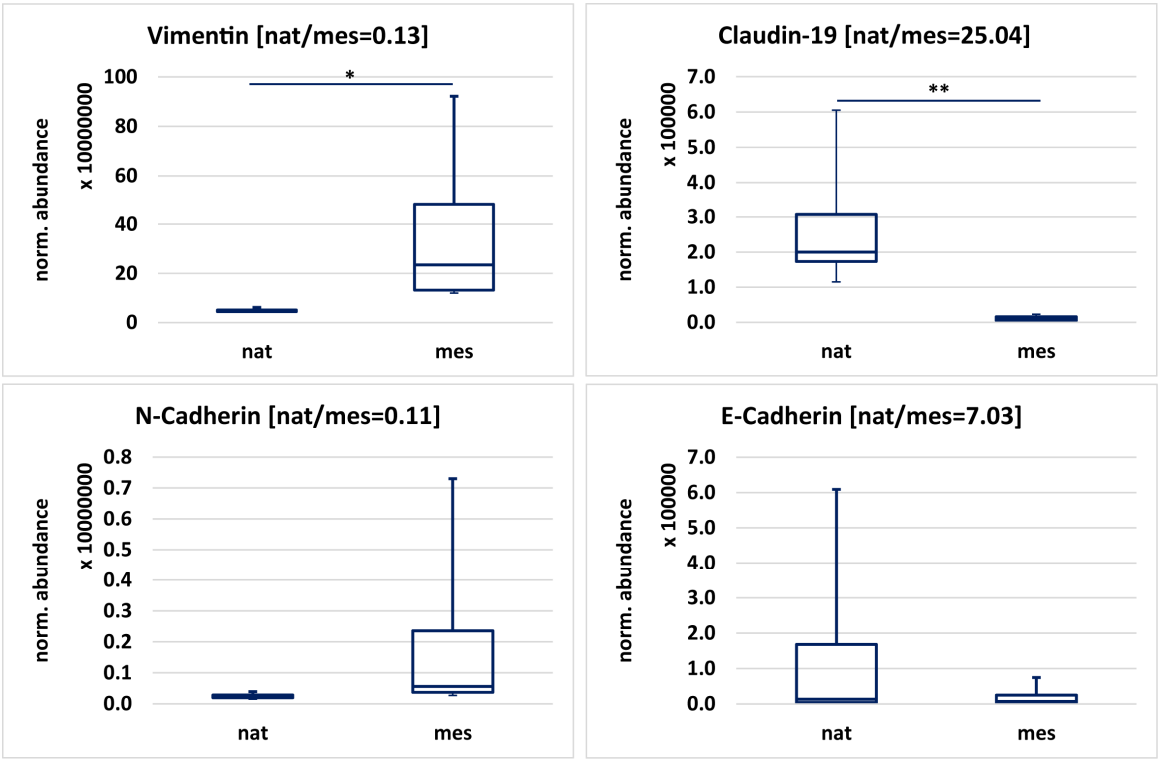

Figure 17: Epithelial cell markers are downregulated, mesenchymal cell markers are upregulated in cultured RPE cells of passage 5-7. Box plot analysis of normalized abundances of Vimentin, Claudin-19, N-Cadherin and E-Cadherin in 4 human native RPE cell samples and 4 human mesenchymal RPE cell samples; *significantly changed (q<0.05), **highly significantly changed (q<0.01). nat: native, mes: mesenchymal.

8.1.3. Expression of complex-type N-glycans increases upon EMT conferring increased Gal-1 and Gal-3 binding on mesenchymal RPE cells

Besides a complete change of the proteome, we have identified that EMT of RPE cells leads to increased β-1,6-N-glycosylation on the cell surface and thus increased binding of Gal-3, as published in Priglinger et al. [116]. The specificity of the plant lectin phytohemagglutinin-L (PHAL) for complex-type N-glycans was used to visualize an increased expression of β1,6-N-acetylglucosamine (GlcNAc)-branched tri- and tetraantennary complex-type N-glycans upon EMT (figure 18A).

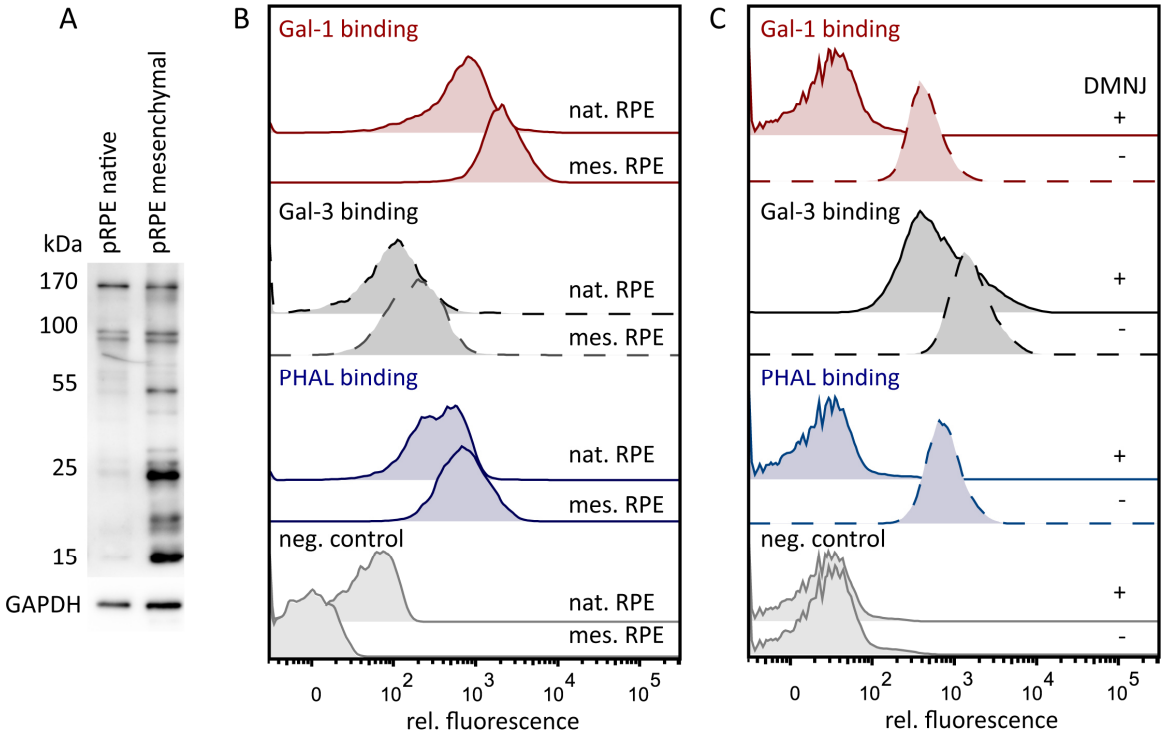

Figure 18: Expression of complex-type N-glycans increases upon EMT conferring increased Gal-1 and Gal-3 binding on mesenchymal RPE cell. A: 10 µg of native (nat) and mesenchymal (mes) porcine RPE (pRPE) whole cell extracts were separated respectively by SDS-PAGE and Lectin Blot analysis was performed with the biotinylated plant lectin phytohemagglutinin-L (PHAL). GAPDH was used as loading control. A representative blot of at least three different experiments is shown. B+C: Flow cytometric analysis of binding of Gal-1, Gal-3 and PHAL to native (nat) and mesenchymal (mes) porcine RPE cells (B) and to mesenchymal RPE cells untreated or treated with deoxymannojirimycin (DMNJ) (C). Representative results of at least two independent FACS experiments are shown. rel: relative.

This glycomic change during EMT came along with increased binding of Gal-1 and Gal-3 to mesenchymal RPE cells (figure 18B). By FACS analysis it could be confirmed that

native RPE cells exhibited little binding of PHAL, Gal-1 and Gal-3 compared to the unstained cells (neg. control), whereas PHAL, Gal-1 and Gal-3 binding to mesenchymal RPE cells was evident (figure 18B). Native RPE cells showed increased background fluorescence compared to mesenchymal RPE due to their intense pigmentation (see neg. control panel in figure 18B).

To proof that complex-type N-glycans are required for Galectin binding, mesenchymal RPE cells were treated with deoxymannojirimycin (DMNJ) to block N-glycan elongation, followed by staining with Gal-1, Gal-3 or PHAL (figure 18C). Effectiveness of 1 mM DMNJ treatment was measurable by decreased staining with the plant lectin PHAL compared to untreated cells (figure 18C, blue solid line). Reduction of complex-type N-glycans on RPE cells resulted also in decreased Gal-1 and Gal-3 binding (figure 18C, red and black solid line), verifying that tetra- or triantennary complex type N-glycans (β1,6-(GlcNAc)-branched N-glycans) were necessary for effective Galectin binding on the RPE cell surface.

8.1.4. Gal-3 binds to the RPE cell surface via complex-type N-glycans but not O-glycans

Gal-3 binding was less decreased by inhibition of N-glycan synthesis by DMNJ than Gal-1 binding. To determine potential further oligosaccharide preferences of Gal-3 on myofibroblastic RPE cells, dedifferentiated human RPE cells were treated besides DMNJ with BenzylGalNAc to inhibit elongation of O-glycans (figure 19C). BenzylGalNAc can also compete with sialyltransferases resulting in decreased O-glycan sialylation. Decreased O-glycan sialylation was verified by increased staining with the plant lectin peanut agglutinin (PNA) compared to untreated controls (figure 19C, black dotted line). Treatment of RPE cells with Vibrio cholera neuraminidase resulted in removal of sialic acids on glycoproteins as shown by reduced binding of Maackia Amurensis Lectin-2 (Mal-2, specific for α2,3 sialic acid residues) after treatment with neuraminidase (figure 19B, black dotted line). Reduction of complex-type N-glycans on RPE cells, as shown before in figure 18C, resulted in decreased Gal-3 and PHAL binding (figure 19A, red and black dotted line), whereas decreased accessibility of branched O-glycans didn't alter binding of Gal-3 to RPE cells (figure 19C, red line). Binding of Gal-3 to RPE was increased

by removal of sialic acids by Vibrio cholera neurominidase (figure 19B, red line). These results indicate, that binding of Gal-3 to the RPE cell surface strongly depends on the interaction of Gal-3 with complex-type N-glycans (β1,6-(GlcNAc)-branched N-glycans) but not on complex-type O-glycans and sialylation of glycans.

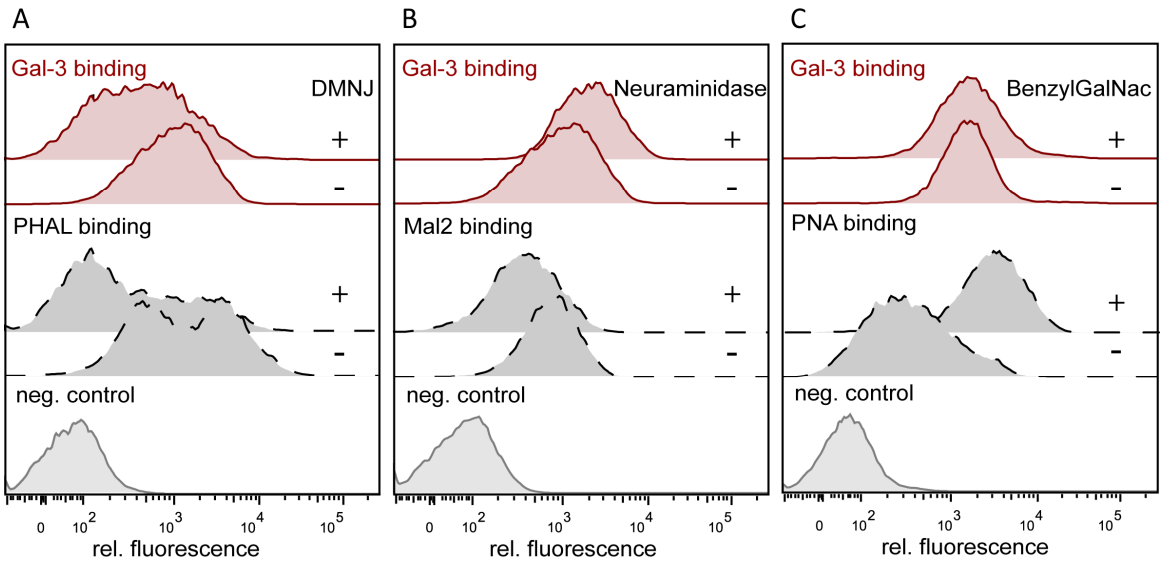

Figure 19: Gal-3 binds to the RPE cell surface via complex-type N-glycans but not complex-type O-glycans. Flow cytometric analysis of binding of Gal-3 compared to binding of different plant lectins (PHAL: phytohemagglutinin-L, Mal2: Maackia Amurensis Lectin-2, PNA: peanut agglutinin) to human RPE cells untreated or treated with deoxymannojirimycin (DMNJ), Vibrio cholera neuraminidase or BenzylGalNac. Representative results of at least three independent experiments are shown.

8.1.5. EMT inhibitors maintain the epithelial phenotype of RPE cells *in vitro*

As shown in figure 15, it was difficult to keep primary RPE cells in their epithelial state under routinely used cell culture conditions. Because of the limited availability of native RPE cells in adequate amounts to analyze the impact of galectins on cellular processes – especially EMT –, it was necessary to create a stable cell culture model of epithelial RPE cells. Different cell culture media – suitable for cultivation of epithelial cells – were tested to prevent EMT processes during cultivation: the minimum essential medium MEMα and the mammary epithelial cell growth medium MEGM, compared to the standardly used DMEM. Besides, different concentrations of FCS were tested.

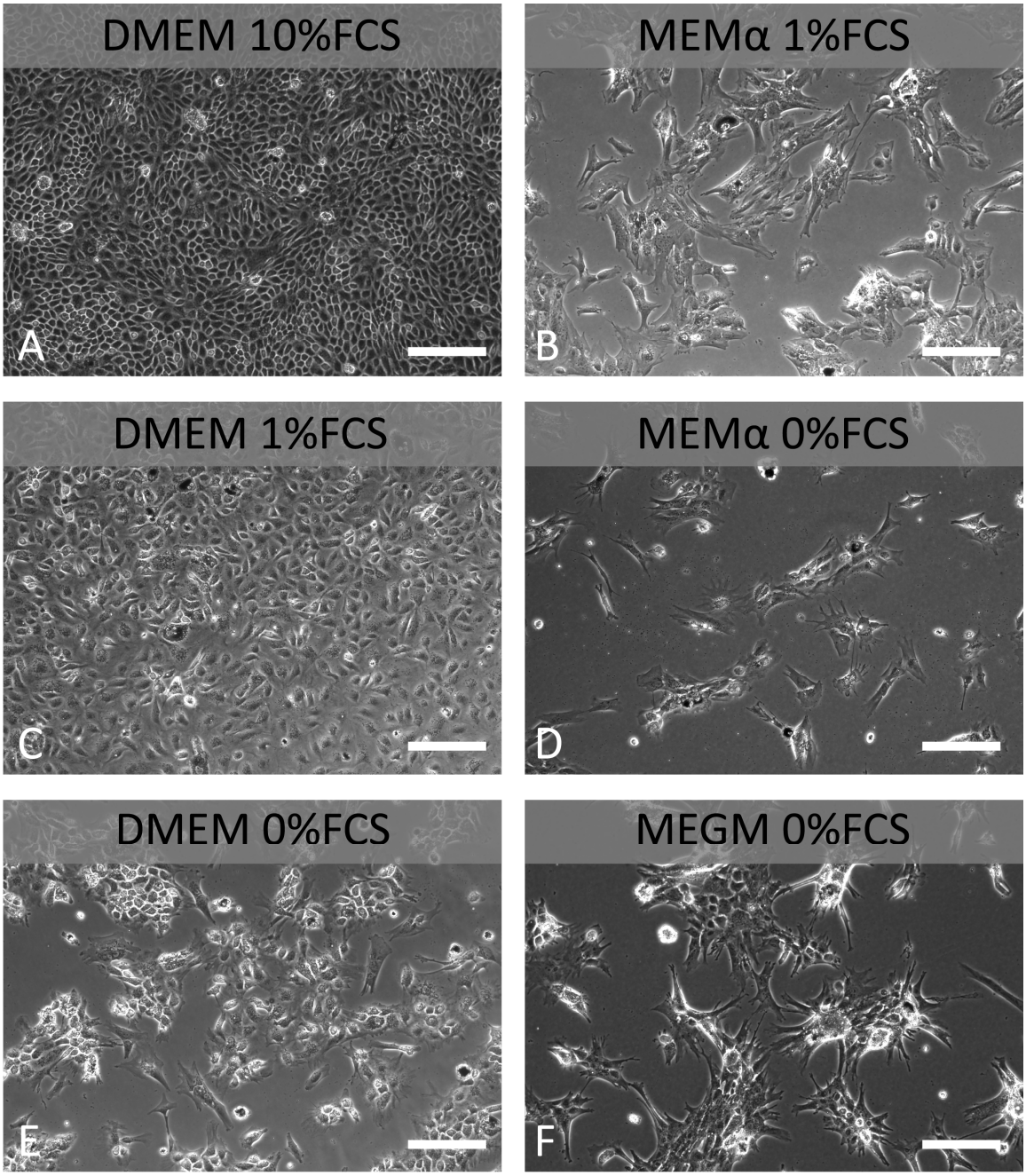

Figure 20: RPE cells are only able to attach and proliferate when cultivated in DMEM. Phase-contrast images of porcine RPE cells (passage 1) cultivated in DMEM supplemented with 10% FCS (A), 1% FCS (C), 0% FCS (E) or in MEMα with 1%FCS (B), 0% FCS (D) or in MEGM with no FCS (F). FCS: fetal calf serum, DMEM: Dulbeccos modified Eagle Medium, MEMα: Minimum Essential Medium, MEGM: Mammary Epithelial Cell Growth Medium. Scale bar 200 µm.

RPE cells were only able to attach and proliferate when they were cultured in DMEM medium (figure 20A and 20C) with at least 1% FCS. When no FCS was added to the medium, RPE cells didn't attach to the surface of the cell culture dishes, they died and

strong morphologic changes took place (figure 20E). Both, MEMα and MEGM, were also not suitable to cultivate RPE cells, even with higher concentrations of FCS (figures 20B, 20D, 20F). Cultivation in DMEM with 1% FCS was possible for shorter periods of 1 or 2 days, but for long-term cultivation 10% FCS was necessary to prevent cell growth arrest of the RPE cells. Consequently, RPE cells were cultivated in DMEM added with 10% FCS and for short-term experiments the FCS concentration was reduced to 3% or 0%. Yet, during sub-cultivation EMT took place under these conditions (figure 15).

As the tested epithelial cell culture media MEMα and MEGM were not suitable for primary RPE cell culture and especially not suitable for prevention of EMT, different EMT inhibitors were tested to keep RPE cells in their epithelial phenotype during RPE cell cultivation: 3 µM ROCK Inhibitor Y-27632, 10 µM TGF-β inhibitor SB 431542 and 10 µM Forskolin (figure 21). Immunocytological staining of untreated porcine RPE cells (passage 5) revealed high expression of vimentin (mesenchymal cell marker) and very low expression of E-Cadherin (epithelial cell marker) (figure 21AE). A clear E-Cadherin expression on the cell membrane could be detected, when the cells were treated with ROCK Inhibitor Y-27632 (figure 21AG), TGF-β inhibitor SB 431542 (figure 21AF) or Forskolin (figure 21AH). Even at passage 5 (in DMEM, 10%FCS) porcine RPE cells maintained epithelial cell characteristics, including cell-cell contacts, by treatment with the EMT inhibitors. These results could be verified by Western Blot analysis, showing a clear E-Cadherin expression in these cells (figure 21C).

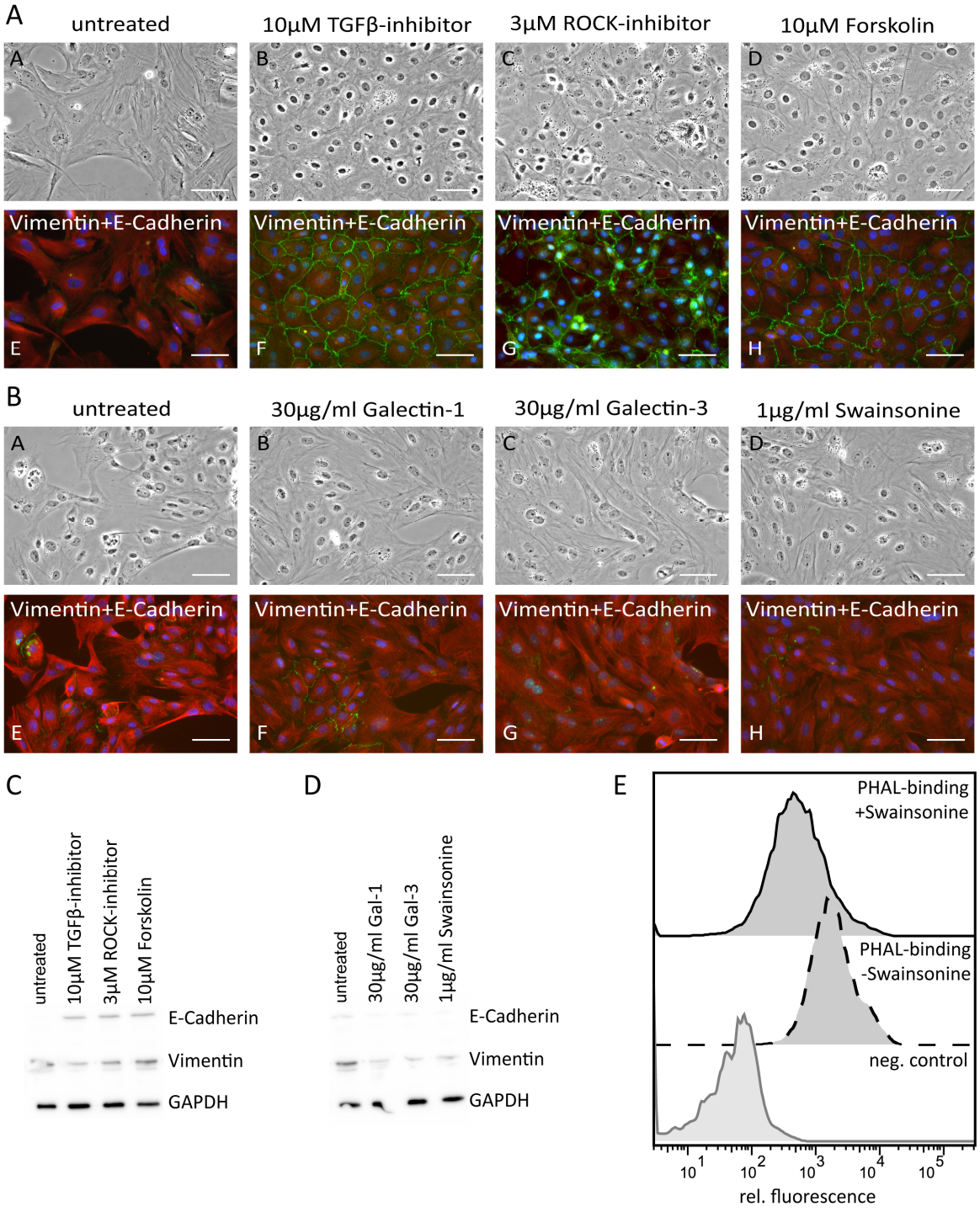

Figure 21: EMT inhibitors stabilize the epithelial phenotype of RPE cells *in vitro*. A+B: Immunocytochemical staining of porcine RPE cells (A: passage 5; B: passage 3) with anti E-Cadherin Alexa488 (green) and anti-Vimentin Alexa568 (red) after treatment with 10 µM TGF-β inhibitor SB 431542, 3 µM ROCK Inhibitor Y-27632 and 10 µM Forskolin (A) or with 30 µg/ml Gal1, Gal-3 or 1 µg/ml Swainsonine (B). Scale bar: 50 µm. C+D: Western Blot analysis of pRPE cell lysates (C: passage 5; D: passage 3) untreated or treated with 10 µM TGF-β inhibitor SB 431542, 3 µM ROCK Inhibitor Y-27632 and 10 µM Forskolin (C) or with 30 µg/mlGal1, Gal-3 or 1 µg/ml Swainsonine (D) against E-Cadherin and

Vimentin. GAPDH was used as a loading control. E: Flow cytometry analysis of PHAL binding to pRPE cells untreated or treated with 1 µg/ml Swainsonine. Representative results of at least three independent experiments are shown.

8.1.6. Gal-1, Gal-3 and complex-type N-glycan inhibitors are not able to prevent EMT

As shown in figure 18, EMT of RPE cells is accompanied by a glycomic shift to complex-type N-glycans on the cell surface. To analyze if there is a correlation in inhibiting N-glycan synthesis and thus EMT processes, RPE cell were treated with 1 µg/ml of the mannosidase-inhibitor Swainsonine directly after isolation. Additionally, to test if Gal-1 or Gal-3 binding has an impact on EMT of RPE cells, porcine RPE cells were also treated with 30 µg/ml Gal-1 or Gal-3. After passage 3 the cells developed a stable mesenchymal phenotype. No E-Cadherin expression was identified by immunocytochemistry and Western Blot analyses, verifying that neither Gal-1 and Gal-3 nor Swainsonine were suitable to prevent EMT processes (figure 21B and 21D). Inhibition of mannosidase I and reduced N-glycan synthesis by Swainsonine treatment could be confirmed by reduced PHAL binding in FACS analysis (figure 21E).

8.1.7. EMT-inhibitors do not influence glycomic change of RPE cells and galectin-binding

To analyze the impact of EMT inhibition by the ROCK Inhibitor Y-27632, TGF-β inhibitor SB 431542 or Forskolin on the glycosylation pattern of the cells and on galectin binding, pRPE (treated and untreated with EMT inhibitors) were stained with PHAL, Concanavalin A (ConA), Gal-3 or Gal-1 (figure 22A-D). PHAL, ConA, Gal-1 and Gal-3 binding was evident to mesenchymal pRPE cells (figure 22A-D, black solid lines). Treatment of pRPE cells with 10 µM Kifunensine reduced PHAL, Gal-1 and to a lesser extend Gal-3 binding, ConA (specific for mannose and glucose) binding was not influenced (figure 22A-D, red lines). Gal-1, Gal-3 and PHAL bound slightly less to RPE cells treated with TGFβ-inhibitor (figure 22A-D, blue solid lines), whereas the EMT-inhibitors Forskolin and the ROCK-inhibitor exhibited no change in binding of Gal-1 and Gal-3 (figure 22A-D, blue and black dotted lines). Additionally, clear PHAL binding to EMT-inhibitor treated cells revealed that the glycomic shift to complex-type N-glycans couldn't be prevented by all three tested EMT-inhibitors (figure 22E). Consequently, EMT-inhibitor treatment of native RPE cells

stabilized the epithelial phenotype of RPE cells, but the glycosylation pattern didn't correlate to the pattern of native RPE cells.

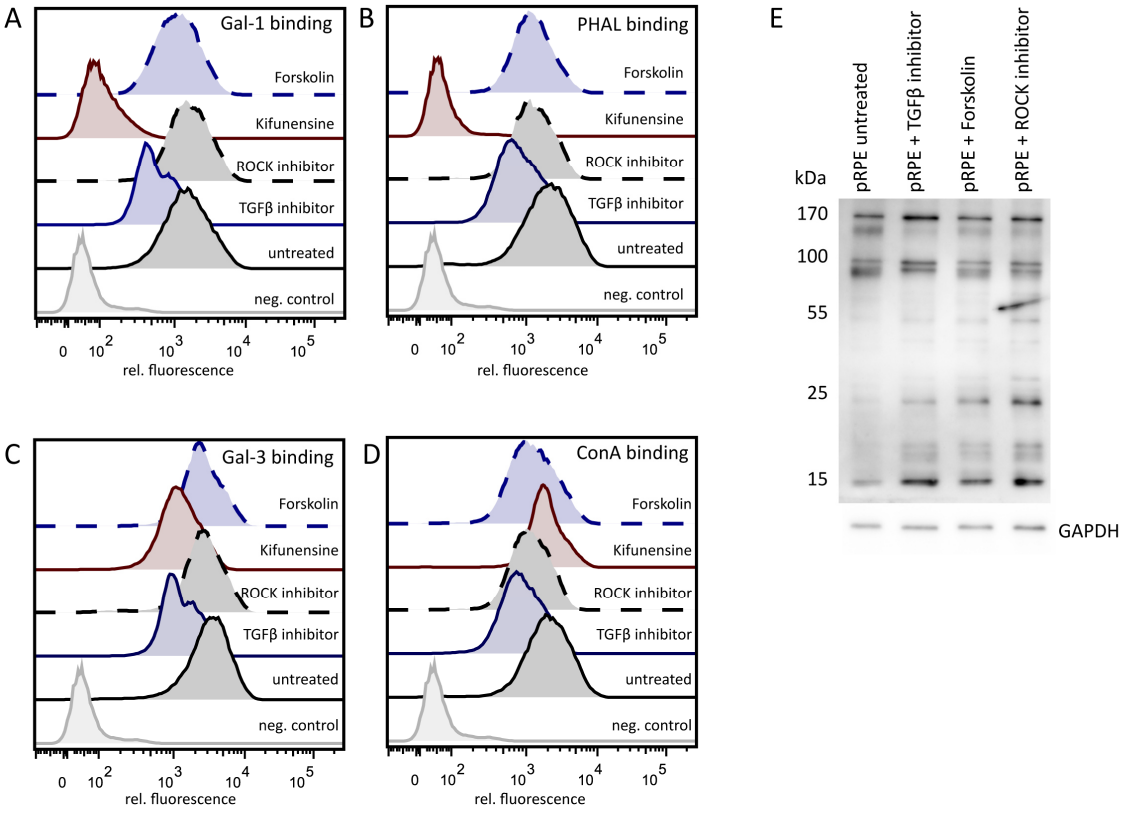

Figure 22: EMT-inhibitors do not influence glycomic change of RPE cells and Galectin-binding. A-D: Flow cytometric analysis of Gal-1, Gal-3, PHAL and Concanavalin (ConA) binding on pRPE cells untreated or treated with 10 µM TGF-β inhibitor SB 431542, 3 µM ROCK Inhibitor Y-27632, 10 µM Kifunensine and 10 µM Forskolin. E: Lectin Blot analysis with the plant lectin PHAL binding to pRPE cells untreated or treated with 10 µM TGF-β inhibitor SB 431542, 3 µM ROCK Inhibitor Y-27632 and 10 µM Forskolin. GAPDH was used as a loading control. Representative results of at least three independent experiments are shown.

8.2. Functional impact of galectin treatment on RPE cells in correlation with surface glycome

To analyze functional impact of galectin treatment on RPE cells in correlation of changed glycomic surface fingerprints upon EMT, influence of Gal-1 and Gal-3 on migration of RPE cells was examined in scratch-wound-healing assays. Furthermore, we established Gal-1 and Gal-3 knockdown cells and investigated based on their glycan structure on the cell surface their reactivity to exogenously added galectin.

8.2.1. Gal-1 and Gal-3 are not cytotoxic to RPE cells

Gal-1, Gal-3, Gal-8 and Gal-9 are expressed in RPE cells. To test if the respective isoforms have cytotoxic effects on RPE cells when added exogenously, a MTT assay was performed with the ARPE19 cell line as well as with primary human and porcine RPE cells. The yellow tetrazolium MTT (3-(4, 5-dimethylthiazolyl-2)-2, 5-diphenyltetrazolium bromide) was reduced by metabolically active cells to purple formazan, which was solubilized and quantified by spectrophotometry[177]. Viability of the cells correlated with color formation: the lower the absorbance at 580 nm, the lower cell viability. Gal-1 and Gal-3 were not toxic towards ARPE19, human and porcine RPEs up to a concentration of 70 µg/ml after a 48h treatment (figures 23A and 23B). A modest toxicity towards those cells could be seen with Gal-8 (>31µg/ml) (figure 23C), while Gal-9 was highly toxic at concentrations above 12.5 µg/ml (figure 23D). With respect to potential application of galectins in therapeutic approaches, Gal-8 and Gal-9 were considered too toxic and all subsequent analysis and experiments were performed only with Gal-1 and Gal-3.

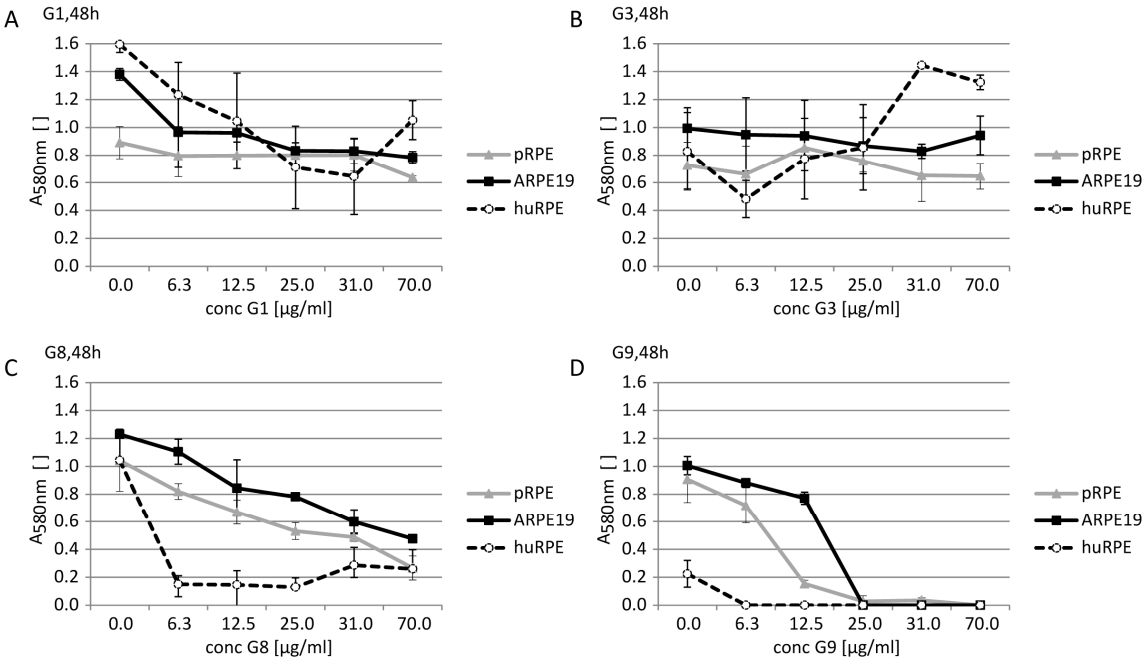

Figure 23: Gal-1 and Gal-3 are not cytotoxic to RPE cells. MTT assay was done with the ARPE19 cell line, primary human (huRPE) and porcine RPE cells (pRPE) treated with increasing concentrations of Gal-1 (A), Gal-3 (B), Gal-8 (C) or Gal-9 (D) (in triplicates). After 48h treatment MTT (5 mg/ml in PBS) was added for 4 hours at 37 °C and the formed crystals were solubilized at 37 °C overnight with 10% SDS in 0.01M HCl. The viability of the cells positively correlated with the absorbance (580 nm) .

8.2.2. Gal-1 and Gal-3 inhibit migration of RPE cells in a carbohydrate-dependent manner

Gal-1 and Gal-3 are known to inhibit attachment and spreading of mesenchymal RPE cells [114, 117]. Here we performed scratch-wound-healing assays to analyze the effect of Gal-1 and Gal-3 on RPE cell migration. A confluent layer of RPE cells was scratched and directly treated with Gal-1 and Gal-3. Migration of RPE cells into the scratch area was monitored by live-cell imaging over time and normalized gap covered area was determined. Gal-1 and Gal-3 diminished migration of RPE cells in scratch-wound-healing assays (figures 24B and 24C). This effect was rescued by treatment of the cells with 10 µM Kifunensine. Inhibition of complex-type-N-glycan formation by Kifunensine led to less galectin and PHAL binding on the cell surface (figure 24A) and thus to decreased inhibition of migration by Gal-1 and Gal-3 in scratch-wound-healing assays (figures 24B and 24C).

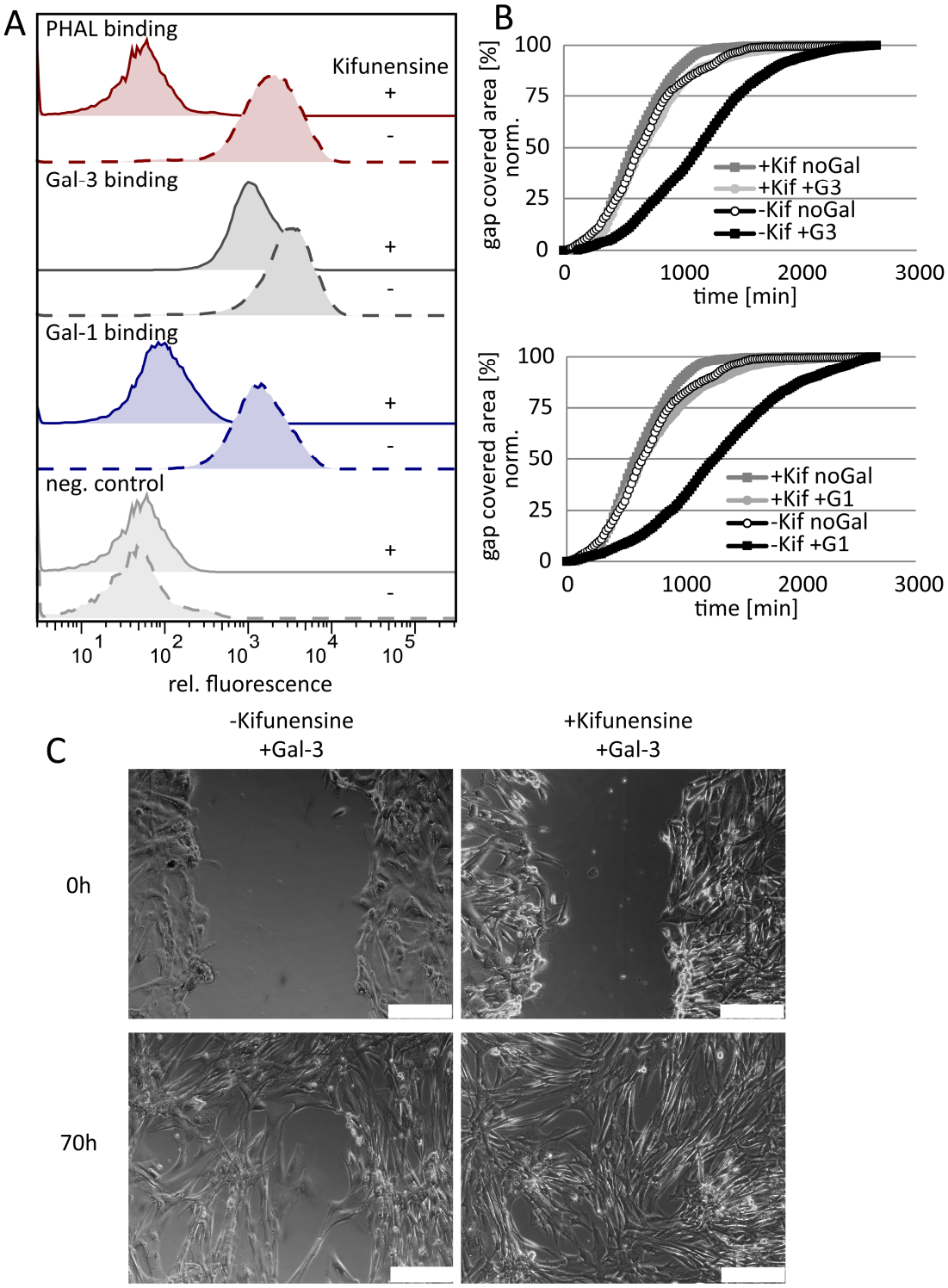

Figure 24: Gal-1 and Gal-3 diminished migration of RPE cells in a carbohydrate-dependent manner. A: Flow cytometry analysis of PHAL, Gal-1 and Gal-3 binding on human RPE cells untreated or treated with 10 µM Kifunensine to inhibit complex-type-N-glycan formation. B+C: Scratch-wound healing assay with human RPE cells treated with or without Kifunensine. RPE cells were scratched and directly treated with 60 µg/ml Gal-3 or 120 µg/ml Gal-1. Migration of RPE cells into the scratch area was monitored over time and the normalized gap covered area [%] was determined. Scale bar: 250 µm. Kif: Kifunensine, PHAL: phytohemagglutinin-L. Representative results of at least three independent experiments are shown.

8.2.3. Knockdown of endogenous Gal-1 and Gal-3 has no impact on galectin-binding

Endogenous Gal-1 and Gal-3 are by trend upregulated in mesenchymal RPE cells compared to native ones (figure 25A)[113] and Cao et al. [190] describe that exogenous Gal-3 stimulates re-epithelialization of corneal wounds in wildtype mice but not in Gal-3 knockout mice[190]. Thus, we wanted to analyze if intrinsic expression of Gal-1 and Gal-3 has any effects on surface glycosylation and galectin-binding. Gal-1 and Gal-3 knock-down cells were produced by the Lenti-CRISPR/Cas9 system, and knock-down was verified by Western Blot analysis (figure 25B). FACS analysis revealed that knock-down of Gal-1 and Gal-3 induced no change on Galectin-binding compared to non-infected cells or cells transduced with the lentiviral vector expressing a non-coding filler guide RNA (LV) (figure 25C). Besides, Gal-1 and Gal-3 knock-down had no influence on complex type-N glycans on the cell surface, since no change of PHAL-binding could be observed (figure 25C).

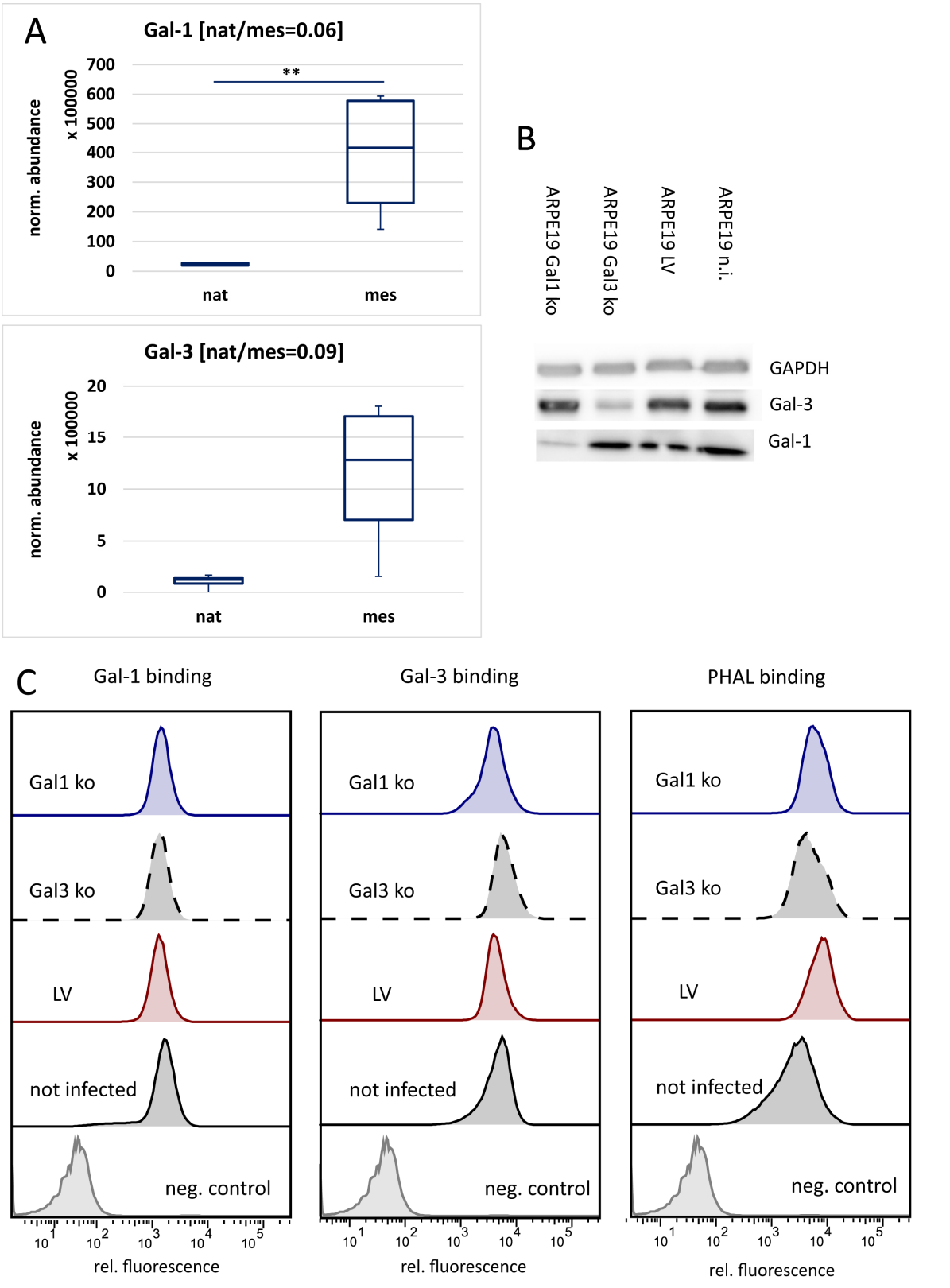

Figure 25: Knock-down of endogenous Gal-1 and Gal-3 has no impact on Galectin-binding. A: Box-plot analysis of normalized abundances of Gal-1 and Gal-3 in native (nat) and mesenchymal (mes) human RPE cells, revealed by proteomic analysis of native and mesenchymal human RPE cells (results 8.1.2, figure 16). B: ARPE19 cells were not infected (n.i.) or infected with lentiviral vectors expressing

"lentiCRISPRv2" plasmids coding for functional gRNAs to knockdown Gal-1 (Gal1 ko) and Gal-3 (Gal3 ko) or without functional gRNA (LV). Knock-down of Gal-1 and Gal-3 in ARPE19 cells by the LentiCRISPR/Cas9 system was verified by Western Blot analysis with antibodies against Gal-1 (25B11) and Gal-3 (15B6). GAPDH was used as a loading control. C: FACS analysis of Gal-1, Gal-3 and PHAL binding on ARPE19 cells not transduced or transduced with lentiviral vectors expressing "lentiCRISPRv2" plasmids coding for functional gRNAs to knockdown Gal-1 (Gal1 ko) and Gal-3 (Gal3 ko) or without functional gRNA (LV). Nat: native, mes: mesenchymal, norm: normalized, PHAL: phytohemagglutinin-L. Representative results of at least three Western Blot analyses and three FACS analyses are shown.

8.3. Proteome-wide identification of glycosylation-dependent interactors of Gal-1 and Gal-3 on mesenchymal RPE cells

The cell surface proteins targeted by specific galectins on RPE cells are largely unknown. To identify Gal-1 and Gal-3 specific interactors on the RPE cell surface, a galectin pull-down assay was established and we analyzed the cellular component distribution and molecular functions of the identified galectin ligands. Relevance of glycosylation of galectin interactors for the functional galectin binding and the crosslinking activity was also determined. To analyze functional and signal modulating effects of galectins on RPE cells, simultaneous determination of changes in phosphorylation profiles of distinct proteins due to galectin binding was performed.

8.3.1. Gal-3 revealed more interacting binding partners than Gal-1

To identify Gal-1 and Gal-3 specific interactors on the RPE cell surface, a galectin pull-down assay was established. For the pull-down experiments, Gal-1 and Gal-3 were coupled to CnBr-activated sepharose beads. To test if the galectins are still active after coupling to Sepharose beads, galectin-beads were incubated with asialofetuin, a known interactor of galectins, in absence and presence of 0.1 M ß- lactose, which act as a competitor. Bound asialofetuin was eluted with Laemmli buffer and eluates were separated by SDS-PAGE. Asialofetuin was detected by Coomassie staining (figure 26), verifying active Gal-1 and Gal-3 coupled to the beads.

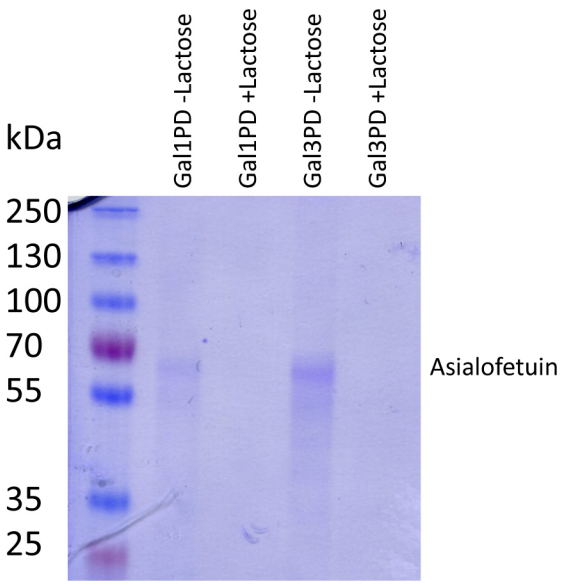

Figure 26: Gal-1 and Gal-3 are still active after coupling to sepharose beads. After incubation of Gal-1 (Gal1PD) and Gal-3 (Gal3PD) sepharose beads with asialofetuin in absence and presence of 0.1 M β-lactose (-/+ Lactose), eluates were separated by SDS-Page and asialofetuin was detected by Coomassie staining.

To identify Gal-1 and Gal-3 interacting binding proteins, whole cell extracts of dedifferentiated mesenchymal human RPE cells were incubated with the respective galectin-sepharose beads. Specific galectin binding proteins were eluted by β-lactose as a competitor for specific carbohydrate binding. The same pull-down experiments were done with ProteinG-coupled sepharose beads to exclude unspecific ligands. A subsequent proteomic screening of all lactose eluates was performed. In 5 independent Gal-3 pull-down experiments (with 3 or 4 technical replicates each) 1429 different proteins and in 5 independent Gal-1 pull-down experiments (3 or 4 technical replicates per experiment) 1528 proteins with an overlay of 1272 proteins were identified (figure 27A). Those proteins, that were significantly ($p<0.05$) at least 2-fold (fold-change (FC)≥2) enriched in Gal-1 or Gal-3 eluates compared to the unspecific control, were selected as the most promising Gal-1 and Gal-3 interacting proteins. In Gal-3 pull-down experiments, more significant interacting binding partners were revealed, as shown in volcano plot analysis of one exemplary Gal-1 (figure 27D) and one exemplary Gal-3 (figure 27E) pull-down experiment. While 771 proteins were over 2-fold enriched in Gal-3 eluates (FC≥2), 332 of these proteins could also be determined as significantly bound to Gal-3 (FC≥2, $p<0.05$) (figure 27B). Compared to that, 698 proteins were specifically

enriched in Gal-1 lactose eluates (FC≥2) but only 60 of these proteins reached also significance (FC≥2, p<0.05) (figure 27B). For further analysis and validation we only used those proteins, that could be detected in 2 or more independent experiments (FC≥2, p<0.05, n≥2) (figure 27C), which were 15 Gal-1 interactors (table 1) and 131 Gal-3 interactors (table 2) fulfilling these strict criteria.

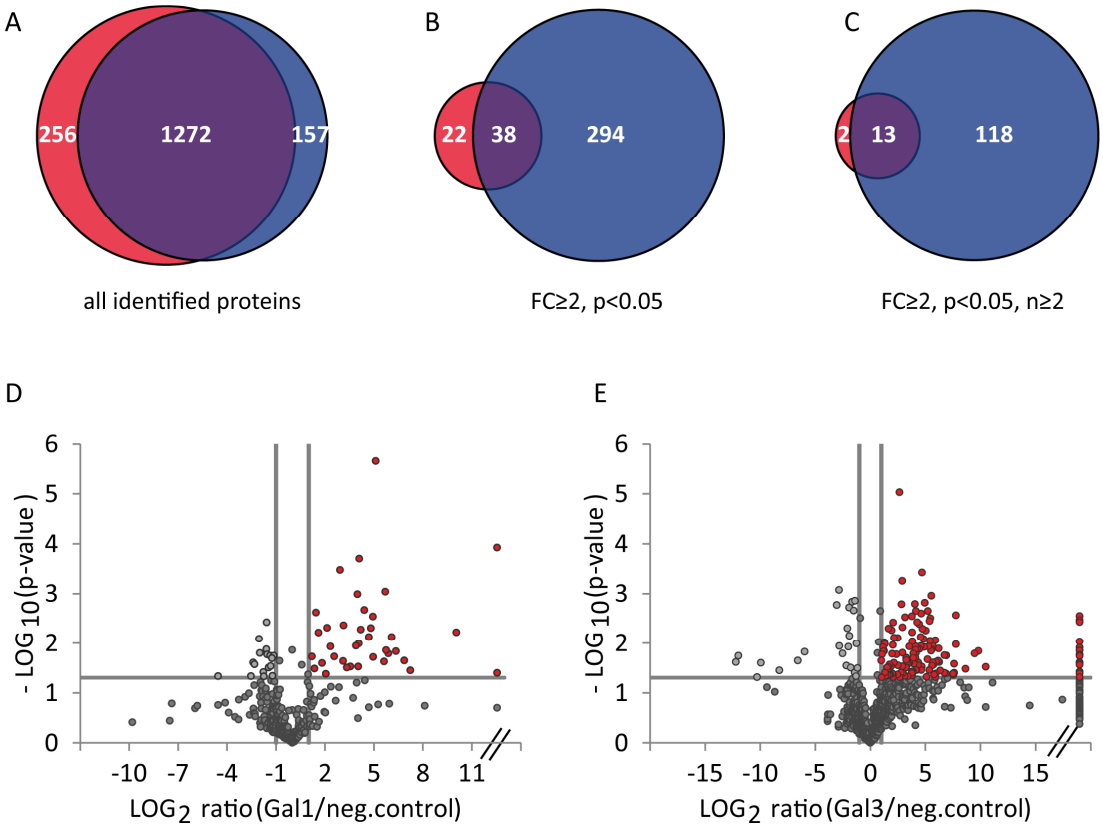

Figure 27: Gal-3 reveals more significant interacting binding partners than Gal-1. A-C: Numbers of protein identifications in all Gal-1 (red) and Gal-3 (blue) pull-down experiments (A); numbers of protein identifications of all significantly enriched (p<0.05) proteins with an enrichment factor over or equal 2 in the galectin ß-lactose eluates compared to negative control (FC≥2) (B) and of all significantly enriched proteins (p<0.05, FC≥2), that could be detected in 2 or more independent pull-down experiments (C). Numbers of overlapping protein identifications are represented (violet). D+E: Volcano plot representation of one exemplary Gal-1 (D) and one exemplary Gal-3 (E) pull-down experiment (with 3 replicates each). The log2 transformed ratios between normalized abundances of all proteins identified in lactose eluates of galectin pull-down compared to unspecific control (Protein-G pull-down) are plotted against the respective negative log10 transformed p-values of the t-test. P-values of p<0.05 and additional regulation of ≥ two fold were regarded as significant (red dots). Infinite fold changes were set to the highest measured ratio plus 1 (dots on the right site of the plot), fold changes with a value of 0 were equalized with the lowest measured ratio (dots on the left site of the plot).

Table 1: List of RPE cell proteins with high affinity to Galectin-1.

1st Accession Number	Gene name	Ratio Gal1/neg. control	P-value	TMD	SP	Protein name
ENSP00000333298	LAMP1	1065.8	0.006	1	Y	lysosomal-associated membrane protein 1
ENSP00000307513	MRC2	136.4	0.049	1	0	mannose receptor, C type 2
ENSP00000007722	ITGA3	104.6	0.021	1	Y	integrin, alpha 3
ENSP00000261023	ITGAV	59.2	0.016	1	Y	integrin, alpha V
ENSP00000303351	ITGB1	53.9	0.014	1	Y	integrin, beta 1
ENSP00000233714	LANCL1	52.2	0.001	0	0	LanC l antibiotic synthetase component C-like 1 (bacterial)
ENSP00000314508	GBA	34.8	0.000	0	Y	glucosidase, beta, acid
ENSP00000331544	FBLN1	34.1	0.018	0	Y	fibulin 1
ENSP00000243077	LRP1	31.1	0.019	1	Y	low density lipoprotein receptor-related protein 1
ENSP00000258341	LAMC1	21.3	0.002	0	Y	laminin, gamma 1 (formerly LAMB2)
ENSP00000262776	LGALS3BP	19.0	0.043	0	Y	lectin, galactoside-binding, soluble, 3 binding protein
ENSP00000228506	MLEC	18.1	0.037	1	Y	malectin
ENSP00000265304	SSBP1	6.1	0.045	0	0	single-stranded DNA binding protein 1, mitochondrial
ENSP00000200639	LAMP2	5.9	0.001	1	Y	lysosomal-associated membrane protein 2
ENSP00000258733	GPNMB	5.3	0.049	1	Y	glycoprotein (transmembrane) nmb

15 identified Gal-1 interactors in order of their enrichment factors in the ß-lactose eluates of galectin pull-downs compared to unspecific controls. For calculation the mean of all technical replicates within one experiment was used. Significance was determined by Student's t-test. Proteins with p-values of $p<0.05$, enrichment of ≥ two-fold in galectin pull-down eluates (FC ≥ 2) and additional identification in two or more independent pull-down experiments (n ≥ 2), were regarded as significant. The ratios represent the maximum fold changes of all experiments and the corresponding p-values. TMD: transmembrane domain. SP: signal peptide. FC: fold change.

Table 2: List of RPE cell proteins with high affinity to Galectin-3.

1st Accession Number	gene name	Ratio Gal3/neg. control	P-value	TMD	SP	Protein name
ENSP00000273784	AHSG	infinity	0.016	0	Y	alpha-2-HS-glycoprotein
ENSP00000222374	CADM4	infinity	0.047	1	Y	cell adhesion molecule 4
ENSP00000312435	DAG1	infinity	0.004	1	Y	dystroglycan 1 (dystrophin-associated glycoprotein 1)
ENSP00000321573	DCBLD2	infinity	0.007	3	Y	discoidin, CUB and LCCL domain containing 2
ENSP00000334145	F3	infinity	0.003	1	0	coagulation factor III (thromboplastin, tissue factor)
ENSP00000314508	GBA	infinity	0.014	0	Y	glucosidase, beta, acid
ENSP00000282588	ITGA1	infinity	0.002	1	Y	integrin, alpha 1
ENSP00000264106	ITGA6	infinity	0.015	1	Y	integrin, alpha 6
ENSP00000266041	ITIH4	infinity	0.014	0	Y	inter-alpha-trypsin inhibitor heavy chain family, member 4
ENSP00000258341	LAMC1	infinity	0.016	0	Y	laminin, gamma 1 (formerly LAMB2)
ENSP00000231004	LOX	infinity	0.046	0	Y	lysyl oxidase
ENSP00000374135	LRP1B	infinity	0.029	1	Y	low density lipoprotein receptor-related protein 1B
ENSP00000199940	MAP2	infinity	0.035	0	0	microtubule-associated protein 2
ENSP00000217939	MXRA5	infinity	0.012	0	Y	matrix-remodelling associated 5
ENSP00000294785	NCSTN	infinity	0.009	1	Y	nicastrin
ENSP00000324270	OXTR	infinity	0.041	7	0	oxytocin receptor
ENSP00000319782	PODXL	infinity	0.020	1	Y	podocalyxin-like
ENSP00000356572	QSOX1	infinity	0.007	0	Y	quiescin Q6 sulfhydryl oxidase 1
ENSP00000266771	SLC15A4	infinity	0.014	13	0	solute carrier family 15 (oligopeptide transporter), member 4
ENSP00000444408	SLC1A5	infinity	0.017	9	0	solute carrier family 1 (neutral amino acid transporter), member 5
ENSP00000004531	SLC7A2	infinity	0.042	14	0	solute carrier family 7 (cationic amino acid transporter, y+ system), member 2
ENSP00000335300	TPCN1	infinity	0.002	12	0	two pore segment channel 1
ENSP00000351190	ITIH2	527961.6	0.006	0	Y	inter-alpha-trypsin inhibitor heavy chain 2
ENSP00000418725	ITGB1	20223.9	0.011	0	Y	integrin, beta 1 (fibronectin receptor, beta polypeptide, antigen CD29 includes MDF2, MSK12)
ENSP00000269141	CDH2	4103.6	0.003	1	Y	cadherin 2, type 1, N-cadherin (neuronal)
ENSP00000257857	CD63	3186.1	0.032	4	0	CD63 molecule
ENSP00000329797	CADM1	2304.6	0.003	1	Y	cell adhesion molecule 1
ENSP00000333298	LAMP1	1591.0	0.003	1	Y	lysosomal-associated membrane protein 1
ENSP00000231368	LNPEP	1439.2	0.031	1	0	leucyl/cystinyl aminopeptidase
ENSP00000257879	ITGA7	1433.6	0.000	1	0	integrin, alpha 7
ENSP00000256689	SLC38A2	910.1	0.015	11	0	solute carrier family 38, member 2
ENSP00000268613	CDH13	900.6	0.008	0	0	cadherin 13
ENSP00000368752	PRNP	737.3	0.024	2	Y	prion protein
ENSP00000263398	CD44	581.2	0.017	1	Y	CD44 molecule (Indian blood group)
ENSP00000382340	ABCC1	521.0	0.002	10	0	ATP-binding cassette, sub-family C (CFTR/MRP), member 1

ENSP00000293379	ITGA5	477.1	0.002	1	Y	integrin, alpha 5 (fibronectin receptor, alpha polypeptide)
ENSP00000230418	PTK7	231.3	0.005	1	Y	protein tyrosine kinase 7
ENSP00000261978	LTBP2	219.4	0.002	0	Y	latent transforming growth factor beta binding protein 2
ENSP00000280527	CRIM1	218.6	0.003	1	Y	cysteine rich transmembrane BMP regulator 1 (chordin-like)
ENSP00000308727	SUSD5	218.1	0.001	1	Y	sushi domain containing 5
ENSP00000336888	SLC44A2	208.8	0.006	10	0	solute carrier family 44 (choline transporter), member 2
ENSP00000258733	GPNMB	202.7	0.007	1	Y	glycoprotein (transmembrane) nmb
ENSP00000256997	ACP2	198.2	0.026	1	Y	acid phosphatase 2, lysosomal
ENSP00000357190	PTPRK	197.0	0.040	1	Y	protein tyrosine phosphatase, receptor type, K
ENSP00000356787	ATP1B1	188.5	0.044	1	0	ATPase, Na+/K+ transporting, beta 1 polypeptide
ENSP00000310206	SEZ6L2	184.0	0.041	1	Y	seizure related 6 homolog (mouse)-like 2
ENSP00000306864	VASN	180.9	0.024	1	Y	vasorin
ENSP00000348307	SIRPA	146.7	0.044	1	Y	signal-regulatory protein alpha
ENSP00000421922	LRPAP1	141.9	0.001	0	Y	low density lipoprotein receptor-related protein associated protein 1
ENSP00000320084	CD276	121.5	0.010	1	Y	CD276 molecule
ENSP00000305988	ALCAM	121.5	0.007	1	Y	activated leukocyte cell adhesion molecule
ENSG00000125730	C3	119.1	0.042	0	Y	complement component 3
ENSP00000290401	NPTN	115.6	0.002	1	Y	neuroplastin
ENSP00000378392	PSAP	111.3	0.002	0	Y	prosaposin
ENSP00000264036	MCAM	109.0	0.022	1	Y	melanoma cell adhesion molecule
ENSP00000311502	HEG1	101.8	0.003	0	0	heart development protein with EGF-like domains 1
ENSP00000331544	FBLN1	100.3	0.015	0	Y	fibulin 1
ENSP00000311402	SLC4A2	96.9	0.046	13	0	solute carrier family 4 (anion exchanger), member 2
ENSP00000228506	MLEC	96.6	0.000	1	Y	malectin
ENSP00000053867	GRN	85.3	0.013	0	Y	granulin
ENSP00000296181	ITGB5	84.8	0.001	1	Y	integrin, beta 5
ENSP00000265077	VCAN	83.4	0.003	0	Y	versican
ENSP00000295633	FSTL1	77.8	0.008	0	Y	follistatin-like 1
ENSP00000413922	ITIH3	76.7	0.024	0	Y	inter-alpha-trypsin inhibitor heavy chain 3
ENSP00000352288	PLXNB2	75.0	0.005	1	Y	plexin B2
ENSP00000318557	SLC12A4	74.5	0.013	14	0	solute carrier family 12 (potassium/chloride transporter), member 4
ENSP00000324101	CD151	72.1	0.028	4	0	CD151 molecule (Raph blood group)
ENSP00000266718	LUM	65.3	0.001	0	Y	lumican
ENSP00000273258	ARL6IP5	60.8	0.049	4	0	ADP-ribosylation-like factor 6 interacting protein 5
ENSP00000269228	NPC1	60.7	0.009	13	Y	Niemann-Pick disease, type C1
ENSP00000347596	EFEMP1	57.1	0.004	0	Y	EGF containing fibulin-like extracellular matrix protein 1
ENSP00000333697	TMEM17 9B	52.2	0.007	3	Y	transmembrane protein 179B
ENSP00000312506	CSPG4	44.1	0.003	1	Y	chondroitin sulfate proteoglycan 4

ENSP00000188790 FAP	43.6	0.022	0	Y	fibroblast activation protein, alpha
ENSP00000323534 FN1	43.3	0.002	0	Y	fibronectin 1
ENSP00000262776 LGALS3BP	41.9	0.004	0	Y	lectin, galactoside-binding, soluble, 3 binding protein
ENSP00000243077 LRP1	41.5	0.001	1	Y	low density lipoprotein receptor-related protein 1
ENSP00000315130 CLU	39.7	0.002	0	Y	clusterin
ENSP00000206423 CCDC80	38.8	0.001	0	Y	coiled-coil domain containing 80
ENSP00000318646 RPS15A	37.8	0.003	0	0	ribosomal protein S15a
ENSP00000200639 LAMP2	37.6	0.004	1	Y	lysosomal-associated membrane protein 2
ENSP00000307513 MRC2	37.5	0.002	1	0	mannose receptor, C type 2
ENSP00000261023 ITGAV	32.1	0.015	1	Y	integrin, alpha V
ENSP00000341730 RPL10	31.6	0.003	0	0	ribosomal protein L10
ENSP00000371626 TRA2B	31.4	0.006	0	0	transformer 2 beta homolog (Drosophila)
ENSP00000323929 A2M	30.9	0.002	0	Y	alpha-2-macroglobulin
ENSP00000333769 BSG	26.8	0.000	1	Y	basigin (Ok blood group)
ENSP00000007722 ITGA3	26.7	0.001	1	Y	integrin, alpha 3 (antigen CD49C, alpha 3 subunit of VLA-3 receptor)
ENSP00000349437 IGF2R	26.5	0.003	1	Y	insulin-like growth factor 2 receptor
ENSP00000084795 RPL18	25.6	0.000	0	0	ribosomal protein L18
ENSP00000222399 LAMB1	24.9	0.000	0	Y	laminin, beta 1
ENSP00000226359 AFP	22.1	0.013	0	Y	alpha-fetoprotein
ENSP00000252804 PXDN	21.3	0.006	0	Y	peroxidasin
ENSP00000275730 SLC12A9	20.8	0.003	13	0	solute carrier family 12, member 9
ENSP00000359602 LMBRD1	19.6	0.013	7	0	LMBR1 domain containing 1
ENSP00000366460 PLXDC2	19.2	0.007	1	Y	plexin domain containing 2
ENSP00000286371 ATP1B3	18.8	0.035	1	0	ATPase, Na+/K+ transporting, beta 3 polypeptide
ENSP00000264896 SCARB2	15.7	0.026	1	Y	scavenger receptor class B, member 2
ENSP00000340815 SLC3A2	15.6	0.012	1	0	solute carrier family 3 (amino acid transporter heavy chain), member 2
ENSP00000327290 ITGA11	15.2	0.016	1	Y	integrin, alpha 11
ENSP00000260356 THBS1	15.2	0.002	0	Y	thrombospondin 1
ENSP00000341861 SERPING1	13.7	0.041	0	Y	serpin peptidase inhibitor, clade G (C1 inhibitor), member 1
ENSP00000376899 PTGFRN	13.3	0.016	1	Y	prostaglandin F2 receptor inhibitor
ENSP00000377047 PTPRZ1	13.1	0.048	1	Y	protein tyrosine phosphatase, receptor-type, Z polypeptide 1
ENSP00000296585 ITGA2	12.1	0.003	1	Y	integrin, alpha 2 (CD49B, alpha 2 subunit of VLA-2 receptor)
ENSP00000261799 PDGFRB	11.7	0.012	1	Y	platelet-derived growth factor receptor, beta polypeptide
ENSP00000355330 TGM2	11.4	0.001	0	0	transglutaminase 2
ENSP00000222247 RPL18A	10.2	0.001	0	0	ribosomal protein L18a
ENSP00000344456 CTNNB1	9.1	0.000	0	0	catenin (cadherin-associated protein), beta 1, 88kDa
ENSP00000272317 RPS27A	8.8	0.006	0	0	ribosomal protein S27a
ENSP00000264832 ICAM1	6.7	0.000	1	Y	intercellular adhesion molecule 1
ENSP00000296674 RPS23	6.4	0.016	0	0	ribosomal protein S23

ENSP00000346015 RPL27A	5.9	0.000	0	0	ribosomal protein L27a
ENSP00000369743 RPS6	4.8	0.001	0	0	ribosomal protein S6
ENSP00000253788 RPL27	4.8	0.003	0	0	ribosomal protein L27
ENSP00000416293 SLC2A1	4.5	0.010	12	0	solute carrier family 2 (facilitated glucose transporter), member 1
ENSP00000311430 RPL4	4.3	0.027	0	0	ribosomal protein L4
ENSP00000277865 GLUD1	4.2	0.036	0	Y	glutamate dehydrogenase 1
ENSP00000345689 RAB5C	4.2	0.026	0	0	RAB5C, member RAS oncogene family
ENSP00000363018 RPL10A	3.8	0.006	0	0	ribosomal protein L10a
ENSP00000348849 RPS26	3.8	0.024	0	0	ribosomal protein S26
ENSP00000225698 C1QBP	3.4	0.027	0	0	complement component 1, q subcomponent binding protein
ENSP00000346022 RPL9	3.4	0.011	0	0	ribosomal protein L9
ENSP00000295598 ATP1A1	3.3	0.003	8	0	ATPase, Na+/K+ transporting, alpha 1 polypeptide
ENSP00000379888 RPS8	3.2	0.026	0	0	ribosomal protein S8
ENSP00000305920 GLB1	3.1	0.047	0	Y	galactosidase, beta 1
ENSP00000325136 HADHB	3.1	0.030	0	Y	hydroxyacyl-CoA dehydrogenase/3-ketoacyl-CoA thiolase/enoyl-CoA hydratase (trifunctional protein), beta subunit
ENSP00000346027 RPL21	3.1	0.036	0	0	ribosomal protein L21
ENSP00000366156 SRM	3.1	0.038	0	0	spermidine synthase
ENSP00000251453 RPS16	2.5	0.040	0	0	ribosomal protein S16
ENSP00000342070 CTSB	2.5	0.004	0	Y	cathepsin B

131 identified Gal-3 interactors in order of their enrichment factors in the lactose eluates of galectin pull-downs compared to unspecific controls. For calculation the mean of all technical replicates within one experiment was used. Significance was determined by Student's t-test. Proteins with p-values of $p<0.05$, enrichment of ≥ two-fold in galectin pull-down eluates (FC ≥ 2) and additional identification in two or more independent pull-down experiments (n ≥ 2), were regarded as significant. The ratios represent the maximum fold changes of all experiments and the corresponding p-values. TMD: transmembrane domain. SP: signal peptide. FC: fold change.

8.3.2. Gal-1 and Gal-3 interactors play a role in multiple binding processes and are mainly localized in membranes

To analyze the cellular component distribution of the 131 identified Gal-3 and the 15 Gal-1 interactors, GeneRanker analysis was performed (table 3) and visualized by FunRich classifications[187] (figure 28A). Classifications to subcellular localizations of interactors of both galectins are equally spread. Both, Gal-1 and Gal-3 interacting proteins were mainly localized in membranes, exosomes and lysosomes (figure 28A). Gal-1 interactors are represented on the inner ring, Gal-3 interactors are represented on the outer ring in figure 28A.

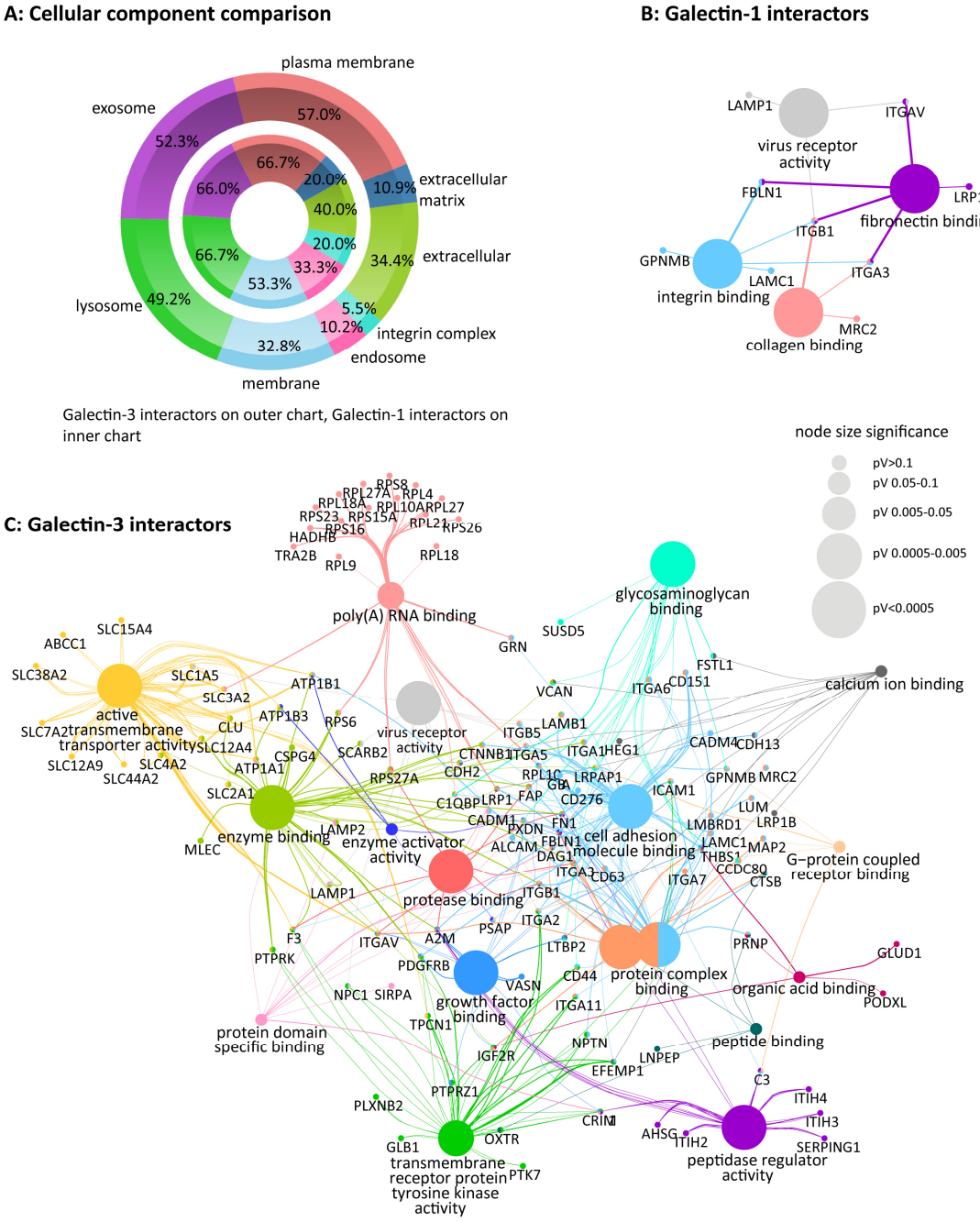

Figure 28: Galectin interactors play a role in multiple binding processes and are mainly localized in membranes. A: Comparison of the 15 Galectin-1 interactors (inner chart) and the 131 Galectin-3 interactors (outer chart), based on the gene ontology (GO) annotation "cellular component" in FunRich[187]. B+C: Network of Galectin-1 (B) and Galectin-3 (C) interactors, clustered by the GO term "molecular function" in the cytoscape app ClueGo-CluePedia[188]. The size of the nodes represents the statistical significance of the enrichment of the terms. The group heading term is the most significant within a group (default). The color code reflects the functional groups. The edges show the connection of distinct genes to specific molecular functions. Not connected to other proteins in the Gal-1 interactor network: LGALS3BP, LAMP2, GBA, LANCL1, MLEC, SSBP1. Not connected to other proteins in the Gal-3

interactor network: PLXDC2, TGM2, BSG, SRM, RAB5C, QSOX1, PTGFRN, ACP2, MCAM, LOX, LGALS3BP, SEZ6L2, MXRA5, NCSTN, AFP, DCBLD2, ARL6IP5, TMEM179B.

GeneRanker analysis revealed that 7 Gal-1 interactors and 67 of the 131 identified Gal-3 interactors are localized to the plasma membrane or on the cell surface. Additionally, 9 of the 15 Gal-1 interactors and 71 Gal-3 interactors have at least one transmembrane domain, assigned by Phobius analysis (table 1 and table 2). Based on the GO term "molecular functions" (table 3), Gal-1 and Gal-3 interactors were clustered in the Cytoscape ClueGo-CluePedia[188] network (figures 28B and 28C). Both, Gal-1 and Gal-3 interactors play a role in multiple binding processes. Whereas Gal-3 interactors comprise functions like glycosaminoglycan and growth factor binding among others (figure 28C), Gal-1 interactors are more involved in integrin, collagen and fibronectin binding processes (figure 28B).

Besides known Gal-1 and Gal-3 interactors like for example LAMP1, basigin (BSG) and different members of the integrin family, many novel interactors could be identified with this approach. Two of them are of great interest: the low density lipoprotein receptor-related protein 1 (LRP1) and the platelet-derived growth factor receptor beta (PDGFRB). LRP1 is involved in the regulation of growth factor homeostasis, cell migration and invasion and mainly acts as an endocytotic receptor[191-194]. In PVR, LRP1 is overexpressed in RPE and RMG cells[194]. In this study, LRP1 was identified as significant Gal-1 interactor with an enrichment factor of 31.1 and of 41.5 as Gal-3 interactor (table 1 and table 2). It is known, that the PDGF receptor and LRP1 associate in endosomal compartments, which modulates signaling pathways like the MAPK and Akt/phosphatidylinositol 3-kinase pathways[195]. In PVR development, PDGF and PDGFR as key regulators of cell migration and proliferation play a significant role[196]. In this approach PDGFRB could only be identified as significant Gal-3 interactor with an enrichment factor of 11.7 (table 2).

Table 3: Galectin interactors play a role in adhesion and binding processes and are mainly localized in membranes.

	Gal-1 interacting proteins		Gal-3 interacting proteins	
	GO-Term	P-value	GO-Term	P-value
cellular components	integral component of plasma membrane	6.79E-05	intrinsic component of membrane	1.70E-18
	intrinsic component of plasma membrane	8.02E-05	integral component of membrane	9.26E-18
	integrin alpha3-beta1 complex	9.91E-05	intrinsic component of plasma membrane	7.08E-16
	receptor complex	2.51E-04	integral component of plasma membrane	6.09E-14
	integral component of membrane	2.99E-04	plasma membrane part	8.46E-13
	protein complex involved in cell adhesion	3.01E-04	cell surface	3.11E-12
	integrin complex	3.01E-04	membrane part	4.27E-10
	external side of plasma membrane	3.17E-04	external side of plasma membrane	6.21E-10
	intrinsic component of membrane	3.60E-04	protein complex involved in cell adhesion	1.12E-08
	invadopodium	5.88E-04	integrin complex	1.12E-08
molecular functions	fibronectin binding	2.47E-06	receptor activity	5.21E-09
	protease binding	1.19E-04	molecular transducer activity	1.44E-07
	integrin binding	1.82E-04	cell adhesion molecule binding	2.99E-07
	extracellular matrix binding	5.80E-04	collagen binding	3.54E-07
	receptor binding	6.86E-04	integrin binding	1.01E-06
	collagen binding	9.54E-04	transmembrane signaling receptor activity	1.81E-05
	receptor activity	1.04E-03	glycosaminoglycan binding	3.39E-05
	cell adhesion molecule binding	1.35E-03	receptor binding	4.83E-05
	macromolecular complex binding	2.10E-03	growth factor binding	5.95E-05
	lipoprotein particle receptor binding	2.77E-03	protein binding involved in cell-matrix adhesion	8.31E-05
signal transduction pathway associations	matrix metalloproteinase	1.75E-04	integrin	1.19E-11
	integrin	1.94E-04	low density lipoprotein receptor related protein	2.74E-06
	lysosomal	4.82E-04	matrix metalloproteinase	1.38E-05
	sphingomyelin phosphodiesterase 1, acid lysosomal	2.20E-03	focal adhesion kinase 1	5.88E-05
	endocytic	9.83E-03	lysosomal	8.62E-05
			interleukin 18 (interferon gamma inducing factor)	1.31E-03
			platelet derived growth factor	1.42E-03
			vascular endothelial growth factor receptor	1.65E-03
			endocytic	3.04E-03
			lymphotoxin alpha (tnf superfamily)	3.77E-03

biological processes	integrin-mediated signaling pathway	6.31E-05	cell adhesion	9.80E-12
	cellular defense response	1.04E-04	biological adhesion	1.88E-11
	negative regulation of Rho protein signal transduction	1.04E-04	extracellular structure organization	7.46E-11
	cell-substrate adhesion	1.91E-04	extracellular matrix organization	7.46E-11
	negative regulation of Ras protein signal transduction	3.08E-04	cell-substrate adhesion	3.27E-10
	negative regulation of small GTPase mediated signal transduction	3.08E-04	cell migration	1.89E-09
	formation of primary germ layer	5.91E-04	cell motility	7.36E-09
	regulation of body fluid levels	8.44E-04	localization of cell	7.36E-09
	negative regulation of intracellular signal transduction	8.48E-04	cell-matrix adhesion	9.67E-09
	cell adhesion	9.57E-04	locomotion	1.74E-08

GeneRanker analysis of Gal-1 and Gal-3 interacting proteins based on the GO terms "cellular component", "molecular function", "signal transduction pathway associations" and "biological processes". Top ten results with the according p-values are listed. GO: gene ontology.

8.3.3. Gal-1 induces cross-linking of LRP1, Gal-3 induces cross-linking of LRP1 and PDGFRB including ITGB1 on the surface of RPE cells

In order to validate LRP1 and PDGFRB as potential targets for Gal-1 and Gal-3 continuative functional experiments have been performed. It is known that Gal-1 and Gal-3 can form dynamic lattices on the cell surface by cross-linking and clustering of transmembrane glycoproteins and thus influence many cellular processes[85, 86, 102]. To check if LRP1 and PDGFRB are involved in these galectin lattices, mesenchymal human RPE cells were treated with biotinylated Gal-1 or Gal-3 for 30 minutes before fixation. Immunocytochemical staining of these cells revealed large speckle staining patterns of both galectins (figures 29B1, C1, E1), LRP1 (figures 29B2, C2), PDGFRB (figure 29E2) and ITGB1 (figures 29B3, C3, E3) in cells treated with Gal-1 and Gal-3 compared to diffuse staining patterns in untreated cells (figures 29A1-A3, 29D1-D3). The staining pattern of ITGB1 as a known galectin interactor indicated a clear overlay with Gal-1 and Gal-3 staining, visible by yellow speckles (figure 29B5, C5, E5). There was also a strong overlay of the staining patterns of Gal-1/Gal-3 and LRP1/PDGFRB, as shown by clear white speckles (figures 29B4, C4, E4). Cross-linking of the respective galectin, LRP1/PDGFRB and ITGB1 could also be verified by clear overlay of the staining patterns (figures 29B6, C6, E6). Without addition of exogenous galectin, no obvious cluster formation could be

seen (figures 29A6, D6), showing that exogenously added galectin induces the cross-linking of the respective interactors.

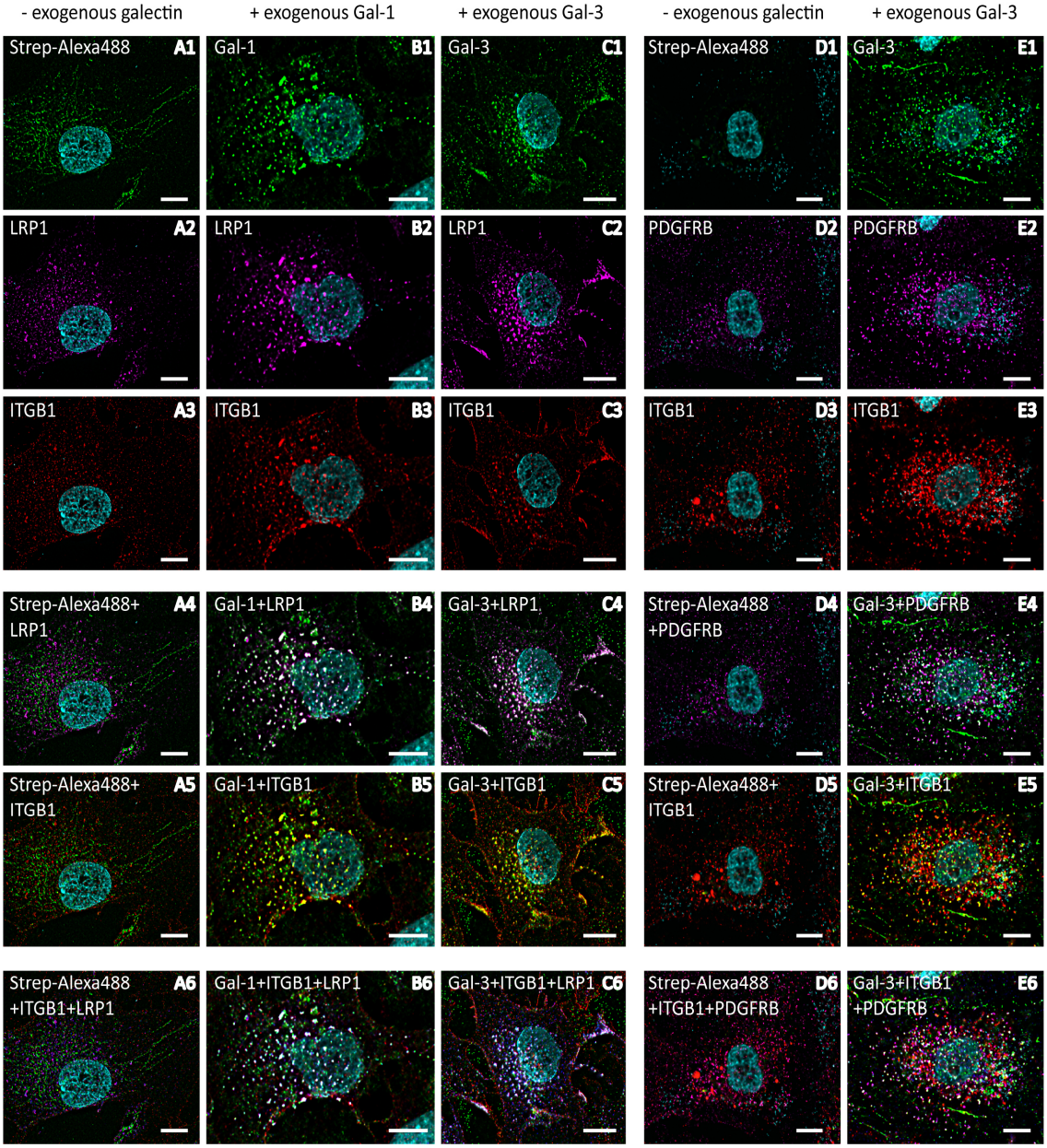

Figure 29: Exogenous Gal-1 and Gal-3 induce cross-linking of LRP1, PDGFRB and ITGB1 on the cell surface of human mesenchymal RPE cells. Immunocytochemical staining of human RPE cells, pretreated before fixation with or without biotinylated Gal-1 or Gal-3 for 30 min. Galectin-binding was visualized by Streptavidin-Alexa488 (green), LRP1 and PDGFRB by Alexa647 (magenta) and ITGB1 by Alexa568 (red). Gal-1 and Gal-3 (B1, C1 and E1), LRP1 (B2 and C2), PDGFRB (E2) and ITGB1 (B3, C3, and E3) stainings show a pronounced punctuate staining pattern. Double staining of RPE cells with Gal-1/Gal-3 and LRP1/PDGFRB as well as with Gal-1/Gal-3 and ITGB1 indicated a clear overlay of both staining patterns, visible by white (B4, C4 and E4) and yellow (B5, C5 and E5) spots. For visualization of the clustering of galectin, LRP1/PDGFRB and ITGB1, LRP1 and PDGFRB staining was changed in silico to blue

and the overlay is seen in white (B6, C6 and E6). Whereas exogenous addition of galectin led to clear co-localization of LRP1 and ITGB1 on human RPE cells, no crosslinking could be seen without exogenous galectin (A6 and D6). Representative images from 4 independent experiments are shown. Scale bar: 10 µm.

8.3.4. Binding of Gal-1 and Gal-3 on LRP1 and PDGFRB is glycosylation-dependent

As shown before, Gal-1 and Gal-3 bind preferentially to β1,6-(GlcNAc)-branched N-glycans (figure 18). To analyze if binding and cross-linking of Gal-1 and Gal-3 with LRP1 and PDGFRB are dependent on complex-type N-glycan structures on the glycoprotein ligands, human RPE cells were treated for up to 4 weeks with 10 µM Kifunensine to inhibit Golgi-class I α-mannosidases[197-199]. Galectin-pull down experiments were repeated with RPE cell lysates of cells, treated with or without 10 µM Kifunensine. Inhibition of complex-type-N-glycosylation led to weaker binding of LRP1 and PDGFRB to Gal-1 and Gal-3 (figure 30).

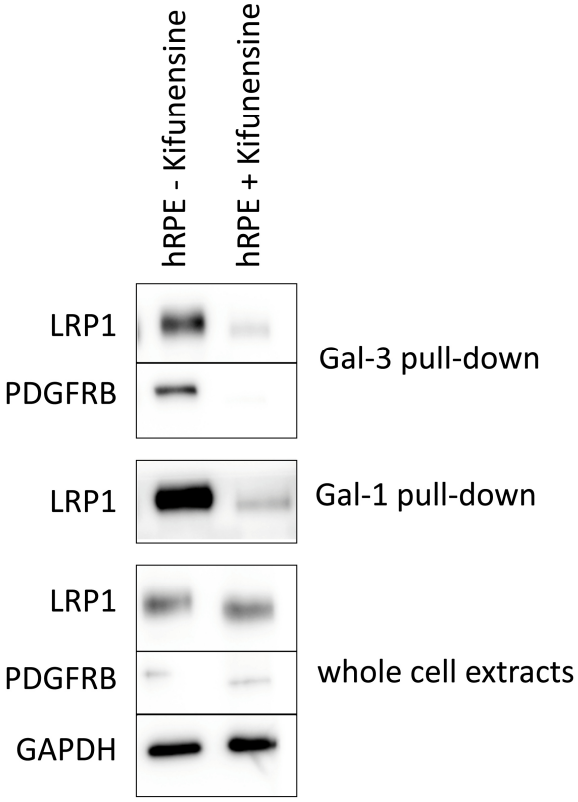

Figure 30: Complex-type N-glycosylation of Galectin-interactors is required for Galectin-binding. Gal-1 and Gal-3 pull-down experiments with lysates of human RPE cells, treated or untreated with 10 µM

Kifunensine. The eluates were analysed by Western Blot with antibodies against PDGFRB and LRP1. 10 µg of the whole cell extracts of the respective cell types were used as an input control for the pull-down experiments and probed for GAPDH as loading control. Representative blots from three independent experiments are shown.

Additionally, galectins bound less to cells treated with Kifunensine (figures 31A, C, E) and no lattice formation of the respective galectins with LRP1 (figures 31A4, C4), PDGFRB (figure 31E4) and ITGB1 (figures 31A3, C3, E3) was visible. Thus complex-type N-glycosylation of LRP1 and PDGFRB is necessary for galectin-binding.

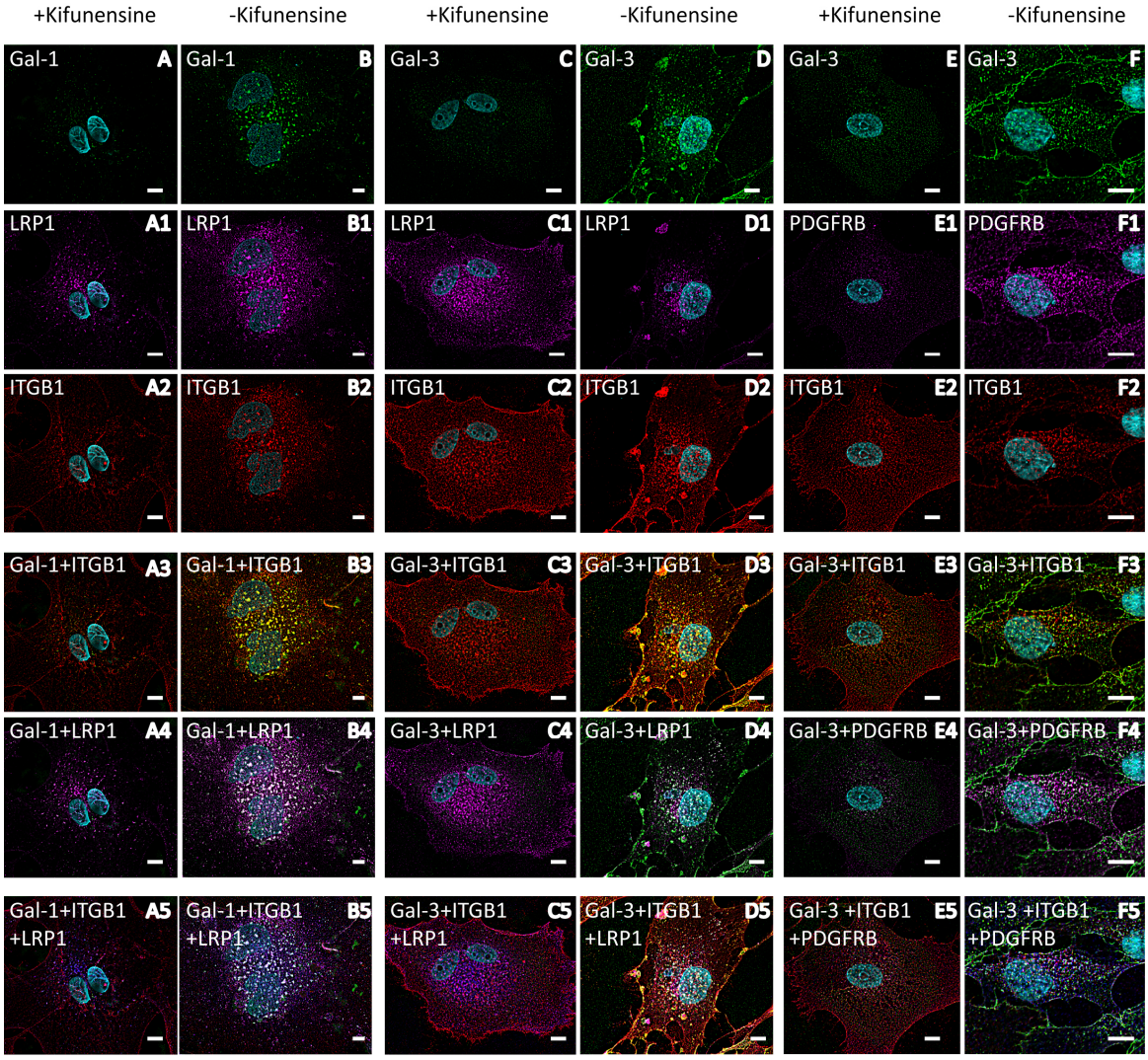

Figure 31: Complex-type N-glycosylation of Galectin-interactors is necessary for Galectin induced cross-linking of LRP1/PDGFR and ITGB1 on the cell surface of mesenchymal RPE cells. Immunocytochemical staining of human RPE cells, pretreated with 10 µM Kifunensine. Before fixation cells were pretreated with biotinylated Gal-1 or Gal-3 for 30 min. Galectin-binding was visualized with Streptavidin-Alexa488 (green) (A-F), LRP1 and PDGFRB by Alexa647 (magenta) (A1-F1) and ITGB1 by Alexa568 (red) (A2-F2).

Overlay of LRP1/PDGFRB and galectin staining patterns is visible in white (A4-F4), overlay of ITGB1 and galectin staining patterns in yellow (A3-F3). For visualization of the clustering of galectin, LRP1 and ITGB1, LRP1 and PDGFRB staining was changed in silico to blue and the overlay is seen in white (A5-F5). Whereas addition of exogenous galectin led to clear co-localization of LRP1 and ITGB1 on human RPE cells not treated with Kifunensine (B-B5, D-D5 and F-F5), no crosslinking could be observed in RPE cells treated with Kifunensine (A-A5, C-C5, E-E5). Representative images from 2 independent experiments are shown. Scale bar: 10 µm.

8.3.5. Endocytosis of Gal-1 and Gal-3 is glycosylation- and dynamin-dependent

LRP1 mainly acts as an endocytotic receptor and associates with PDGFR in endosomal compartments. To find out whether Gal-1 and Gal-3 undergo endocytosis after clustering with those receptors, Gal-1 and Gal-3 were covalently coupled to NHS-Fluorescein and ARPE19 cells were treated with those galectin-conjugates for 5, 15 and 30 minutes at 37 °C to enable endocytosis. After trypsinisation of the cells to get rid of excessive Gal-1 and Gal-3, which was bound on the cell surface but not endocytosed, FACS analysis was performed. Both Gal-1 and Gal-3 endocytosis increased over time (figures 32A and B, blue lines). However, by pre-treatment of the cells with Kifunensine to inhibit complex-type N-glycan elongation, endocytosis of Gal-1 was completely inhibited and endosomal uptake of Gal-3 was decreased (figures 32A and B, red lines). Dynasore, an inhibitor of dynamin-mediated endocytosis by rapidly blocking coated vesicle formation within seconds[200], decreased endosomal uptake of Gal-1 and Gal-3 (figure 32C, black and blue lines). Transferrin was used as a positive control to verify dynasore-mediated endocytosis inhibition and its uptake was reduced by inhibition of dynamin (figure 32C, red lines).

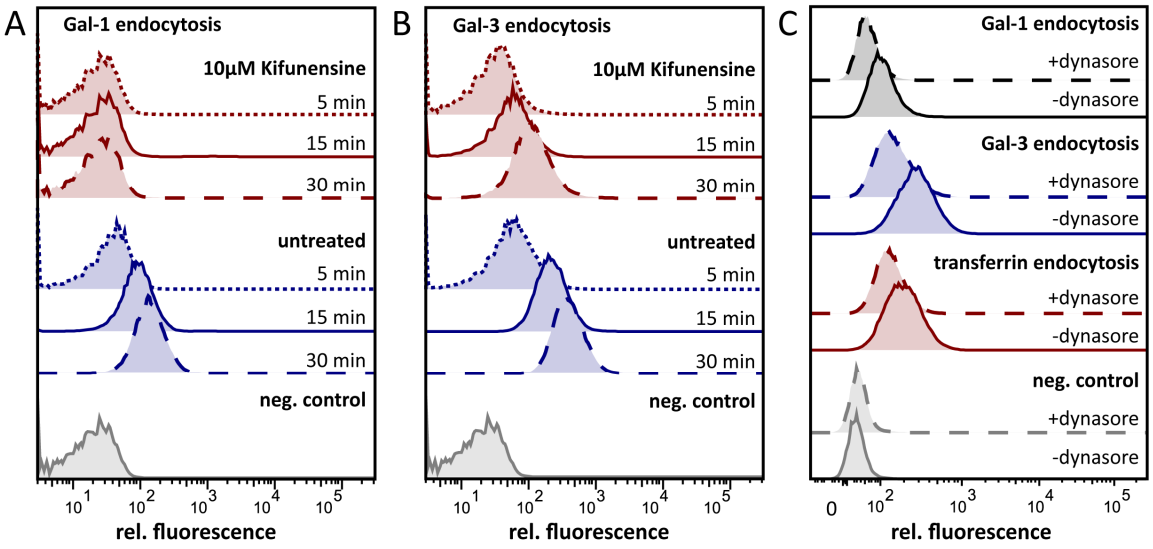

Figure 32: Endocytosis of Gal-1 and Gal-3 is glycosylation- and dynamin- dependent. Flow cytometry analysis of Gal-1, Gal-3 and transferrin endocytosis in ARPE19 cells, untreated or treated with 10 µM Kifunensine or 400 µM dynasore. ARPE19 cells were treated for 5, 15 or 30 minutes with Gal-1-Fluorescein-conjugates (A), Gal-3-Fluorescein-conjugates (B) or 30 minutes with Gal-1-, Gal-3- or transferrin-Fluorescein conjugates (C).

8.3.6. Enhanced phosphorylation of ERK-1/2 and AKT-1/2/3 by binding of Gal-1 and Gal-3

To analyze functional and signal modulating effects of galectins on RPE cells, simultaneous determination of changes in phosphorylation profiles of distinct proteins due to galectin binding was performed. ARPE-19 cells were untreated or treated with Gal-1 and Gal-3 for 1, 15 or 30 minutes. Both Gal-1 and Gal-3 treatment significantly enhanced phosphorylation of the extracellular signal regulated kinase ERK-1/2 and the serine-threonine protein kinase Akt-1/2/3 (S473) (figures 33A and B). ERK-1 was phosphorylated at the threonine residue T202 and at the tyrosine residue Y204, ERK-2 at T185 and Y187. The corresponding Western Blot analysis (figure 33C) showed that phosphorylation of ERK1/2 was already enhanced after one minute treatment of ARPE-19 cells with Gal-1 and Gal-3 and was still detectable after 30 minute treatment. The glycogen synthase kinase GSK-3α/β (S21/S9) and the proline-rich protein Pras-40 (T246) were also higher phosphorylated by galectin treatment (figures 33A and B).

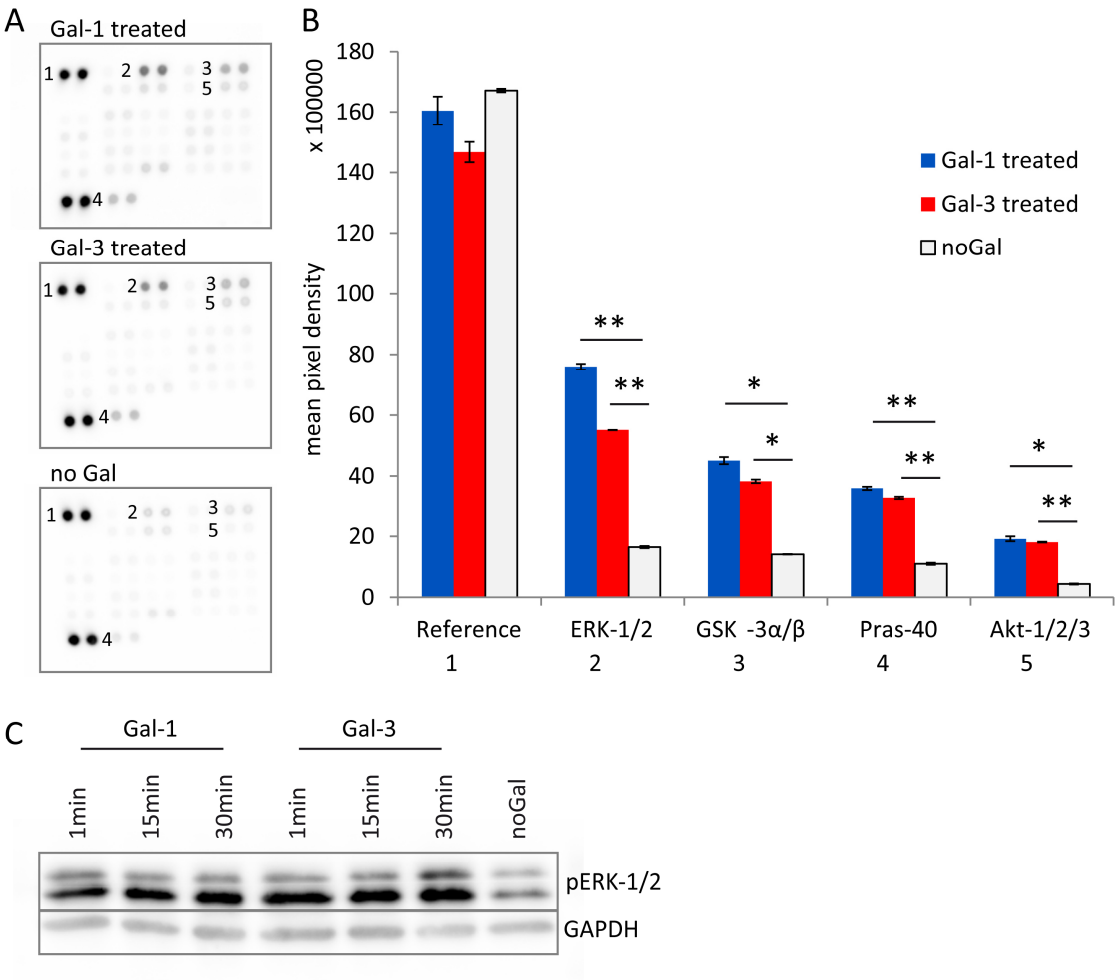

Figure 33: Enhanced phosphorylation of ERK-1/2 and AKT-1/2/3 by binding of Gal-1 and Gal-3. Analysis of phosphorylation levels induced by Gal-1 or Gal-3 treatment. A+B: 300 µg of ARPE19 cell extracts untreated or treated with Gal-1 or Gal-3 for 15 minutes were incubated with a nitrocellulose membrane of the Human Phospho-Kinase Array. Profiling of phosphorylation levels revealed significant induction of ERK1/2, GSK-3α/β, Pras-40 and Akt-1/2/3 phosphorylation after treatment with Gal-1 or Gal-3. The amount of phosphorylated protein bound at the respective capture spot was visualized by signal development with chemiluminescent detection reagents (A) and mean pixel density was determined in duplicates (B). P-values lower than 0.05 were considered as significant (*), p-values lower than 0.01 as highly significant (**). C: 15 µg of whole cell extracts of ARPE19 cells untreated or treated with Gal-1 or Gal-3 for 1, 15 or 30 minutes were separated by SDS-PAGE (10% gels) and blotted onto PVDF membranes. Blots were incubated with antibodies against phospho-ERK p44/p42 and GAPDH. Representative blots from three independent experiments are shown.

9. Discussion

9.1. *In vitro* cell culture models for epithelial and mesenchymal RPE cells

For studies of the physiology and pathophysiology of native tissue, cell culture models play an important role[174]. Especially investigating human RPE, where access to fresh native tissue is limited, suitable cell culture models are essential. Interestingly, RPE cells exhibit considerable phenotypic variation depending on their growth conditions[32, 201]. When cultivated in DMEM supplemented with 10% FCS at 37 °C, RPE cells lost their pigmentation, reduced their cell-cell contacts and changed their morphology into long, fibroblast-like cells during sub-cultivation (figure 15). This transition process from an epithelial to a mesenchymal-like phenotype is a natural process that occurs in the eye when the RPE is damaged to produce cells capable of propagating[32, 202]. Thus, cultivation of RPE cells on plastic in the presence of serum is an accepted *in vitro* model system for early PVR[45]. Here, we revealed in a proteome-wide screening approach that not only a complete change of phenotype, but also an entire expression level shift of 93% of all identified protein expression levels took place due to cultivation *in vitro* (figure 16). Accordingly, Hauck et al. [203] showed that retinal Müller glia (RMG) cells transdifferentiate from a multifunctional, differentiated glial cell to a dedifferentiated fibroblast-like phenotype in culture, which is accompanied by changes in the RMG proteome. Principal Component Analysis revealed that even though there was a biological variance in the different human samples, a clear difference in protein expression was visible between native and mesenchymal RPE cells (figure 16C). Yet, to reduce influence of biological variance and to analyze in more detail processes caused only by EMT, native and mesenchymal RPE cell samples deriving from the same human donor should be a better model. Therefore we tried to create a suitable cell culture method for cultivation of native RPE cells. In doing so it was important to keep the RPE cells in their epithelial phenotype for a long period of time – even over sub-cultivation – to get the required amount of cells and whole cell extracts as needed.

Important factors influencing the severity and speed of morphologic changes are for instance cell culture medium composition, freshness of the cells when isolated from the

tissue, cell seeding density, incubation conditions and passage number[32]. In this study the influence of these parameters was analyzed in detail. Different cell culture media with different FCS concentrations were tested to prevent EMT processes of freshly isolated RPE cells. MEMα supplemented with non-essential amino acids, N1 supplement and a mix of triiodo-thyronine, hydrocortisone and taurine was described in the literature as suitable culture medium of RPE cells[174]. As shown in Maminishkis et al. [174], RPE cells exhibited a confluent monolayer, an epithelial morphology with apical membrane microvilli and pigmentation, when cultivated in MEMα. Various tight junction proteins could be identified and VEGF was mainly secreted on the basal side, whereas PEDF was mainly secreted into the apical space[174]. In this study, cultivation of RPE cells in MEMα resulted in strong morphologic changes and RPE cells didn't attach to the surface of the cell culture dishes (figure 20). Yet, Maminishkis et al. [174] worked on the one hand with fetal RPE samples and on the other hand RPE cells were cultivated on cell culture inserts with extracellular matrix from human placenta as substrate coatings. Fetal RPE cell samples are not directly comparable with the human cadaver eyes of organ donors of unknown age, which we used in this study, regarding freshness and age-related tissue transformation. Furthermore Maminishkis et al. [174] subcultivated RPE cells only once and used the confluent monolayer, which arose after 3 to 4 weeks, for further experiments. We also tried to cultivate native RPE cells on cell culture inserts and epithelial phenotype was kept for a distinct time, but by this cultivation technique it is not possible to get the required amount of cells and whole cell extracts for FACS analysis, functional scratch-assay set-ups, MS-based analyses, Western Blot validation and analysis of signal modulating effects as needed in this approach, because in most of the experiments different conditions (e.g. treatment with galectins or N-glycan synthesis inhibitors) had to be analyzed in parallel. Unfortunately, MEGM, which is often used for different kinds of mammary epithelial cells[204], was also not suitable for long-lasting native RPE cell cultivation.

Another important parameter for RPE cell cultivation is the amount of FCS added to the medium[205]. FCS is the most widely used primary medium supplement for cell cultures. It contains several important ingredients like albumin, antichymotrypsin, apolipoproteins, biotin and growth stimulatory factors[205, 206]. As complex natural product, FCS may vary

from different manufacturers but also from lot to lot even from a single producer[205]. Exact composition as well as quality, type, and concentration of the components of FCS lots is not completely revealed, but has an immense influence on cellular processes during cell cultivation[205, 207]. Growth stimulatory factors including TGFβ and other growth factors contained in FCS trigger EMT and thus negatively affect maintenance of native epithelial morphology. Regarding RPE cell culture, RPE cells didn't attach to the surface of the cell culture dishes, they died and strong morphologic changes took place, when no FCS was added to the medium (figure 20).

Dedifferentiation and morphologic changes of RPE cells are also very dependent on cell-cell contacts. Disruption of such contacts triggers EMT, whereas intact and close cell-cell contacts maintain the epithelial phenotype of cells[43, 45]. In the RPE cell isolation protocol we used in this study, RPE cells were loosened and thus cell-cell-contacts were totally disrupted. Tamiya et al. [43] showed that mainly loss of cell-cell contacts initiates EMT in RPE cells and that TGFβ2 treatment promote EMT, but it has no effect on RPE cells when cell-cell contacts are retained. Therefore we seeded RPE cells at high cell densities, because cell culture conditions with lower cell densities enabled higher degrees of cell spreading and faster dedifferentiation of the cells. Establishing a stable cell culture model of epithelial RPE cells remains consequently challenging. By isolation of RPE cells from their native monolayer and following cultivation in cell culture dishes in DMEM (high glucose, pyruvate), which needs to be supplemented with a modest amount of FCS to verify cell attachment and growing, RPE cells are exposed to many different factors that trigger EMT.

Therefore we tested different EMT-inhibitors: ROCK Inhibitor Y-27632, TGF-β inhibitor SB 431542 and Forskolin and added them to the standardly used DMEM supplemented with 10% FCS. We could show that we can prevent the transition to a mesenchymal phenotype of RPE cells by EMT-inhibitors verified by clear E-Cadherin expression even upon several sub-cultivation cycles and higher passage numbers (figure 21). All of the three different used EMT-inhibitors had different points of action in EMT signaling processes.

The TGFβ inhibitor SB 431542 inhibits activin receptor-like kinase (ALK)5, which is the TGF-β type I receptor[208]. Besides, it inhibits also ALK4 and ALK7, but no other ALK family members[208]. Thus, SB 431542 is a specific inhibitor of TGFβ signaling and endogenous activin, but does not interfere with ERK, JNK or p38 MAPK pathways[208]. TGFβ has a predominant role in EMT induction[209] and TGFβ is often overexpressed as tumors evolve, which induces EMT of tumor cells, but TGFβ signaling can either suppress or promote tumor growth depending on the type of cancer[210]. Therefore, TGF-β receptor kinase inhibitors have been tested in preclinical studies as anti-tumor agents. Halder et al. [211] observed that SB 431542 inhibits TGF-β-induced transcription, gene expression, apoptosis, and growth suppression and attenuates the tumor-promoting effects of TGF-β, including TGF-β-induced EMT, cell motility, migration and invasion, and vascular endothelial growth factor secretion in human cancer cell lines. In the vitreous of patients suffering from PVR TGFβ is overexpressed and present in the PVR membranes[212, 213]. The concentration of TGFβ2 correlates with the severity of PVR and contractility of PVR membranes[30, 212]. Intravitreal injection of TGFβ1 in combination with fibronectin induced increased formation of tractional retinal detachments and intraocular fibrosis in rabbits[212]. By blocking TGFβ signaling EMT processes could be inhibited as shown in many approaches[214, 215]. In our *in vitro* model SB 431542 was able to prevent phenotype transition of RPE cells (figure 21).

Besides TGFβ itself we targeted a kinase downstream of TGFβ signaling: the ROCK kinase. EMT induced by TGFβ is mediated by a RhoA-dependent mechanism[216]. ROCK kinases are involved in proliferation, differentiation and apoptosis and play central roles in the organization of the actin cytoskeleton and thus are favored targets for the treatment of several human diseases[217]. Das et al. [218] showed for instance that a combination of ROCK inhibitor Y-27632 and TGF-β inhibitor SB 431542 led to reduced mesenchymal gene expression and increased E-Cadherin expression in renal tubular epithelial cells, which underwent EMT before. Reversal of EMT required both TGF-β inhibitor and ROCK inhibitor to re-establishing epithelial transcription and structural components[218]. Combinations of Y-27632, SB 431542 and Forskolin have also been tested in this study to prevent EMT of RPE cells (data not shown). Yet, combinations thereof were less successful in preventing EMT than single agents. In diverse studies the

inhibitory effect of Forskolin to TGFβ induced EMT could be shown in different cell types[219, 220]. Forskolin is a cAMP-elevating agent. It directly activates adenylate cylase to generate cAMP from ATP[221]. cAMP signaling has shown a number of antitumor effects, including the induction of mesenchymal-to-epithelial transition, inhibition of cell growth and migration[220, 222]. Concerning ophthalmology, forskolin has an antiglaucoma activity and is used as eye drops to reduce the intraocular pressure in clinical trials[222, 223]. Forskolin prevented in our study EMT of RPE cells *in vitro* (figure 21).

Concluding, a lot of effort was invested in establishing suitable cell culture models for human native tissue that is only limited available. Of course, it always has to be considered that every cell culture model is only a simulation of natural processes and many factors during cultivation need to be considered[32]. Pathological and physiological processes are very complex and hard to mimic *in vitro* under cell culture conditions. A transformed cell culture is for example characterized by such morphologic and growth changes that presumably make the cells too different from naturally transformed RPE. Yet, cultivated mesenchymal RPE cells mimic status of early PVR and thus those cells have been used to identify galectin interactors and analyze functional effects of galectins on RPE cells. Keeping RPE cells after isolation from their native tissue with their natural epithelial properties is very difficult as shown here. All three tested EMT-inhibitors stabilized the epithelial phenotype of native RPE cells. Yet the drawback of this cell culture model was that the glycosylation pattern didn't correlate to the pattern of native RPE cells as further discussed.

9.2. EMT in correlation with glycomic surface fingerprint

EMT is mainly driven by extracellular growth factors such as transforming growth factor-β (TGF-β), hepatocyte growth factor (HGF) and epidermal growth factor (EGF), but also by overexpression of transcription factors like for example SNAIL, SLUG and TWIST1 and intracellular signals of NFκB or WNT signaling activation for instance[41, 42, 224]. EMT is known to be accompanied by an aberrant expression of glycans for example in cancer development and progression[225]. Here, we could verify that in RPE cells a glycomic shift to complex-type β1,6-branched tri- and tetraantennary N-glycans took place upon EMT and that Gal-1 and Gal-3 bind preferentially to mesenchymal RPE cells (figure 18). In the

diversified field of glycan structures resulting from chain extensions with fucose, sulfate, polylactosamine or sialic acid residues as well as from glycan branching and modification by methylation or acetylation, only a small part of different glycan structures were analyzed here. Nevertheless our findings indicated that the glycomic profile of human RPE cells underwent a profound reorganization upon EMT *in vitro*[116]. And the finding that EMT is accompanied by an increase in complex-type N-glycan structures on the cell surface is consistent with other studies, showing a tissue-specific correlation of β1,6-(GlcNAc)-branched N-glycans accumulation and carcinoma progression[226-229]. In correlation to that, the Golgi β1,6N-acetylglucosaminyltransferase V (Mgat5), which is required in the biosynthesis of β1,6-(GlcNAc)-branched N-linked glycans, is upregulated in different pathological processes and may correlate with disease progression[227, 228]. In Priglinger et al. [116] we could show an upregulation of Mgat5 upon EMT of RPE cells. Yet, the knowledge about molecular mechanisms that explain the correlation of altered glycan patterns in context of EMT is very limited[225]. Demetriou et al. [228] assumed based on their findings that β1,6-GlcNAc branching of N-linked oligosaccharides directly contributes to growth controls and reduces substratum adhesion in premalignant epithelial cells. Thus, inhibition of Mgat5 might be useful in the treatment of malignancies, as also described in Granovsky et al. [227]. Still, Mgat5 is also named as a suppressor of both EMT and invasion in human lung cancer cells[230]. In the eye, Saravanan et al. [231] observed an increase of β1,6-GlcNAc branching and a downregulation of Mgat3 in healing corneas while Mgat5 expression was not changed. Mgat3 is also a Golgi N-acetylglucosaminyltransferase, which introduces bisecting β1,4GlcNAc and thereby suppresses β1,6GlcNAc branching by Mgat5. Thus, regulatory mechanisms for glycan expression seem to be tissue-specific and presumably different in both malignant and non-malignant tissues. In this study we could show that by treatment of RPE cells with N-glycosylation inhibitors the phenotype and thus EMT processes couldn't be influenced (figure 21). In more detail, by inhibition of α-mannosidase by treatment of the cells with Swainsonine directly after isolation, complex-type N-glycan synthesis could be prevented, but transition to a mesenchymal phenotype of RPE cells during cultivation could not. On the other hand, we could prevent the transition to a mesenchymal phenotype of RPE cells by EMT-inhibitors such as ROCK Inhibitor Y-27632, TGF-β inhibitor SB 431542 or Forskolin, yet a glycan change

to complex-type N-glycans nevertheless took place (figure 21). This leads to the conclusion that change of phenotype and change to an aberrant glycan-structure on the cell surface during EMT are independent multifactorial processes that can't be controlled by intervening single growth-factor pathways or single glycosyltransferase activities.

Galectins as carbohydrate-binding proteins with distinct glycan specificities could be the missing link between the complex-type N-glycans of cell surface glycoproteins and aberrant behavior of cells in malignant tissue. In previous studies, it could be shown that Gal-1 and Gal-3 are overexpressed in mesenchymal RPE cells and exogenously added Gal-1 and Gal-3 inhibit carbohydrate-dependent attachment and spreading of mesenchymal RPE cells[113, 114, 117]. Whether there is a link between the expression regulation of galectins and a glycomic shift on the cell surface to enhance galectin-binding and thus accessibility to galectin-induced functional effects, was also analyzed in this study and will be discussed later in detail. Unfortunately, no direct influence of galectin knockdown on cellular behavior or glycomic structures was amenable. Even though it is not fully clarified yet, if and how altered glycan patterns influence EMT processes, the changed glycan-structures on the cell surface of mesenchymal RPE cells can have a useful prognostic value with respect to identify early stages of PVR[229].

9.3. Functional impact of galectin in context of PVR

Most galectin ligands are branched N-glycans on transmembrane proteins[120]. Of note, these glycans are upregulated during EMT of human RPE cells and these changes lead to increased binding of Gal-3 to mesenchymal RPE cells (figure 18)[116]. Consequently it can be assumed that EMT sensitizes the susceptibility of cell surface receptors to galectins and that complex-type-N-glycan structures are very important for galectin binding. Analyzing the mechanisms of these glycan-galectin interactions will provide evidence whether these glycan structures are a prerequisite for galectin binding and how they influence interaction processes. Here we could show that Gal-1 and Gal-3 inhibit migration of RPE cells carbohydrate-dependent (figure 24). In previous studies, it could be shown that Gal-1 and Gal-3 inhibit carbohydrate-dependently the attachment and spreading of mesenchymal RPE cells[113, 114, 117]. By elimination of complex-type β1,6-

(GlcNAc)-branched N-glycans due to mannosidase inhibitor treatment, those cellular effects of galectins on RPE cells were reversed, pointing out the importance of glycomic structures of galectin interactors. Accordingly, we found that complex-type-N-glycosylation of the identified galectin interactors LRP1 and PDGFRB is required for galectin-binding and lattice formation on the RPE cell surface (figures 30, 31). A direct influence of galectins on prevention of EMT processes couldn't be proven here (figure 21). Yet, this can also strengthen the hypothesis that specific glycomic fingerprints are necessary for functional galectin binding, because binding on epithelial RPE cells is very weak due to lack of complex-type N-glycans.

Even though all members of the galectin family bind to galactose-β1,4-N-acetylglucosamine, it is assumed that the structural differences in their CRD domains not only lead to different specificities for distinct glycoproteins, but also to distinct biological activities[73-75]. Whereas Gal-1 induces apoptosis in several cell types, Gal-3 is associated with antiapoptotic effects [76, 77]. Yet, binding to different interactors does not necessarily mean that different downstream mechanisms are influenced. Gal-1 and Gal-3 can bind to distinct receptors but converge on similar downstream signaling in several analyses for induction of T cell death[73] or of neutrophil respiratory burst[79]. This assumption is further underscored by the finding that Gal-1 and Gal-3 don't show synergistic effects with respect to inhibition of RPE cell attachment and spreading when added simultaneously, suggesting that they may occupy a similar subset of cell surface receptors[114].

Interactome study revealed that Gal-1 and Gal-3 interactors are distributed in the same cellular components, mainly in membranes, and play a role in multiple binding processes (figure 28). GeneRanker analysis showed that both Gal-1 and Gal-3 interactors are involved in cell adhesion processes (table 3). Gal-3 interactors also play a role in ECM organization and cell migration, while Gal-1 interactors are involved in integrin-mediated signaling pathways. With respect to PVR, these biological processes are the key cellular processes in disease development, which is characterized by adhesion, migration and EMT of RPE and RMG cells[2, 5, 11]. The data monitored by our gene ranker analysis are of particular interest since target proteins of both Gal-1 and Gal-3 may play a role in the pathogenesis of PVR and thus be instrumental for influencing the disease process in

terms of a therapeutic approach. From recent studies it became evident that PVR is a multifactorial cellular process that can't be attenuated by inhibition of single growth factors and their downstream signaling pathways or by anti-inflammatory or anti-proliferative approaches alone[24-31]. As seen from our data, Gal-1 and Gal-3 may have the ability to orchestrate several cellular processes involved in PVR development simultaneously by interacting with a variety of distinct cell surface interactors, and thus provide a multimodal therapeutic concept.

9.4. Influence of intracellular expression of Gal-1 and Gal-3 on glycomic surface fingerprints

In former studies, it was found that only Gal-1, Gal-3, Gal-8 and Gal-9 are expressed in human RPE cells and only those galectin isoforms are able to bind to the RPE cells surface exogenously (data unpublished). We also found that Gal-1 and Gal-3 are upregulated in mesenchymal RPE cells compared to native RPE cells with an epithelial phenotype (figure 25) and could thereby verify former results[113]. One objective of this work was to find out, if there is a link between the expression of galectins and the induction of a glycomic shift on the cell surface to thereby enhance galectin-binding and thus galectin-induced cellular events. Cao et al. [190] describe that exogenous Gal-3 stimulates re-epithelialization of corneal wounds in wildtype mice but not in Gal-3 knockout mice[190]. Intracellular Gal-3 may thus contribute significantly to the process of wound healing[190]. Yet, whether intracellular Gal-3 influences the expression of specific cell surface or ECM receptors, which in turn influence cell-matrix interactions and cell migration, or whether Gal-3 has a direct or indirect influence on glycan patterns of these receptors and thus on specific lectin binding, remains to be solved[190]. Modulated expression levels of galectins can be associated with pathological conditions like in cancer, fibrosis and inflammation[66, 68, 81]. Interestingly, mainly those cell types, that express low levels of galectins under normal physiological conditions, overexpress galectins in disease state[66, 68, 81]. In contrast to that, when cells normally express high levels of a specific galectin isoform, these galectins are downregulated when those cells become abnormal[66]. In breast carcinoma cells for instance Gal-3 was stably overexpressed and this was accompanied by increased levels of integrins and enhanced adhesion to laminin, fibronectin and vitronectin, which were known binding proteins of

Gal-3[232, 233]. Mucin2, which is also a major ligand of Gal-3, was overexpressed after transfection of a colon cancer carcinoma cell line with Gal-3[234]. Cao et al. [190] showed that the stimulatory effect of exogenous Gal-3 on re-epithelialization of wounds is inhibited by lactose, which gives a hint that intracellular expression of Gal-3 might have a regulatory effect on the glycosylation of proteins, which serve as galectin-ligands. Interaction of Gal-3 with nuclear matrix as well as DNA and RNA was proven and presumably explains how Gal-3 can influence complex biological processes[110, 235]. Unfortunately, we could not verify any dependencies between intrinsic galectin-expression and external galectin reaction in RPE cells (figure 25). Stable knock-down of Gal-1 and Gal-3 was induced by the LentiCRISPR/Cas9 system in ARPE19 cells and could be verified by Western Blot analysis. By FACS analysis we tested binding of Gal-1 and Gal-3 on uninfected, Gal-1 ko and Gal-3 ko cells and couldn't reveal any changes in galectin binding by galectin knockdown. To check for changes in complex-type N-glycosylation on the cell surface induced by galectin, binding of the plant lectin PHAL was also investigated. Neither change in galectin-binding nor in glycosylation structures could be revealed by knockdown of Gal-1 and Gal-3. Concluding, intracellular expression of Gal-1 and Gal-3 may have influences on other cellular processes but not on complex-type N-glycosylation processes in RPE cells.

9.5. Interactors of Gal-1 and Gal-3

A proteome-wide interaction study was designed to identify specific interactors for Gal-1 and Gal-3 on mesenchymal RPE cell surfaces to get deeper insights in the functional effects of galectins on RPE cells in context of PVR. It resulted in a total of 131 significant Gal-3 interacting binding partners while only 15 proteins remained as significant Gal-1 ligands (figure 27). The unequal number of interactors can be explained by structural differences of Gal-1 and Gal-3 in their CRD domains. Gal-3 is the only known chimera type galectin and it cross-links glycoproteins by its C-terminal domain and multimerizes by its N-terminal domain after binding to saccharide ligands[82, 102]. In contrast to that, Gal-1 consists of one CRD and can form homodimers by its N-terminal domain[61, 84, 87, 88]. The rigid dimeric structure of Gal-1 and the flexible pentameric Gal-3 structure can reason the different numbers of glycoprotein ligands. The pentameric form of Gal-3 may facilitate to bind more different glycoprotein receptors on the RPE cell surface. Stillman

et al. [73] showed for instance, that lower concentrations of Gal-3 are required to trigger T cell death than of Gal-1, suggesting that Gal-3 is able to bind more ligands simultaneously.

By coupling of galectins to sepharose beads, physiological multimerization is presumably hindered and this conformation change might influence the ability of the CRD domain to bind glycoproteins. However, the binding activity of Gal-1 and Gal-3 after coupling to the beads was confirmed by incubation with asialofetuin, a known interactor via β-galactoside moieties (figure 26). *In vivo*, ligand binding occurs at the CRD domain while multimerization of galectins and formation of cross-linked lattices is triggered by the N-terminal domain (figure 6)[102, 109]. Consequently, multimerization is *in vivo* not important for recognition of specific ligands and coupling of galectins to beads should not generally hinder identification of galectin interactors. However, we can't exclude a different behavior of Gal-1 and Gal-3 with respect to forced monomerization through bead coupling, but Gal-1 and Gal-3 pull-down experiments were done in parallel under the same conditions with the same RPE cell lysates and multimerization is at least equally important for Gal-3 as compared to Gal-1. Thus, we assume that the lower numbers of Gal-1 interactors are not due to technical limitations, but rather reflect a reduced spectrum of interactors.

Nevertheless, the identified Gal-1 and Gal-3 interactors have many common features. They are distributed in the same cellular components, mainly in membranes, and play a role in multiple binding processes (figure 28). In the analysis of galectin-interactors in whole RPE cell lysates, both intra- and extracellular interactors were revealed. It is known, that Gal-1 and Gal-3 are present both inside and outside the cell, and that Gal-1 and Gal-3 interact also with intracellular proteins. For example, they are involved in processes like pre-mRNA splicing[110, 236], but these processes are assumed to be based on protein-protein interactions rather than carbohydrate-lectin interactions on the cell surface or extracellular matrix (ECM)[66]. In this approach, interacting proteins were eluted with ß-lactose to verify carbohydrate-dependent binding on Galectins. Thus, we are focusing on the Gal-1 and Gal-3 interactors on cell-surface and ECM. Seven Gal-1 interactors and 67 of the 131 identified Gal-3 interactors are localized in plasma membrane or on the cell surface, based on GeneRanker analysis (table 3). Figure 28

shows the distribution of the identified interactors on cellular components. Most of the interactors are localized in membranes, the extracellular space or intraluminal, validating that this approach mainly pulled down the carbohydrate-dependent interacting ligands.

Several galectin interactors in different cell types are known so far[141]. Gal-3 interacts for instance with EGFR and TGF-βR in tumor cells[124, 237]. Both, Gal-1 and Gal-3, bind to β1-integrins[118, 238, 239] and extracellular matrix molecules like fibronectin and laminin[94, 130, 240]. Besides, Gal-1 and Gal-3 can also bind to immune cell glycoproteins and to neural recognition molecules[73, 76, 122, 241-244]. ITGB1 and CD147 (BSG), the two previously identified counter-receptors for Gal-3 in RPE cells were confirmed with this approach[118]. Additionally, known interactors of Gal-1 or Gal-3 like laminin[94, 130], LAMP1 and LAMP2[245] and integrins[118, 238, 246] among others were confirmed. Most of these interactors were identified in distinct cell types, but not in RPE cells. Thus we could on the one hand confirm several of the known interactors in RPE cells, and on the other hand identify many new so far unknown interactors.

9.5.1. LRP1 and PDGFRB as galectin interactors

For validation we focused on two novel identified Gal-1 and Gal-3 interactors: LRP1 and PDGFRB. LRP1 (or CD91) is a 600kDa glycoprotein, consisting of an extracellular and a transmembrane domain[247, 248]. LRP1 recognizes at least 30 different ligands, among others lipoproteins[249], the β-amyloid precursor protein[191], and the protease inhibitor α2-macroglobulin (α2M), which is responsible for the clearance of several growth factors and cytokines like for example TGF-β[250-252]. LRP1 recognizes extracellular ligands and induces endocytosis for degradation by lysosomes[193]. Thus, it is assumed that LRP1 also plays a significant role in the clearance of α2-M-associated growth factors and could potentially be involved in pathologic events during PVR development[194]. Hollborn et al. [194] found that LRP1 mRNA levels are upregulated in human RPE cells, stimulated with TGF-β1, TGF-β2 or VEGF. They hypothesize that protease treatment aiming to induce α2M-mediated clearance of growth factors accompanied by increased LRP1-mediated endocytosis is a potential treatment strategy for PVR[194]. Yet, in PVR RPE and RMG cells are exposed to high amounts of growth factors and cytokines. Though Milenkovic et al.

[253] found that α2M inhibited RMG cell proliferation, it remains unclear, whether it is possible to clear most of these growth factors by α2M activation or by intravitreal addition of α2M. It is also known that several signaling pathways - including ERK/MAPK, Akt and NF-κB - are activated by binding of α2M to LRP1 in distinct cell types including macrophages and RMG cells. Bonacci et al. [254] found that proliferation and MAPK-ERK1/2 activation in a macrophage-derived cell-line is induced by binding of α2M to LRP1. They could verify that α2M promotes expression and secretion of matrix-metalloproteinase MMP-9, which was also mediated by MAPK-ERK1/2 and NF- κB[255]. α2M activates also glial fibrillary acidic protein (GFAP) expression in RMG cells induced by LRP1, which is assumed to be mediated by the JAK/STAT signaling pathway[256]. Barcelona et al. [257] found that α2M - mediated by LRP1 - induces RMG cell migration by regulating MT1-MMP activity. We show here that α2M is a significant Gal-3 interactor with an enrichment factor over 30.9 and a p-value of 0.002 (table 2). Which effect binding of Gal-1 and Gal-3 on LRP1 or α2M has on cellular processes of RPE cells, remains to be solved.

Interestingly, LRP1 can be tyrosine phosphorylated by the growth factor receptor PDGFR, which in turn regulates its activity by endocytosis and intracellular trafficking of LRP1[258-260]. Thus, LRP1 is predicted to interact as a co-receptor that modulates PDGFR initiated signal transduction pathways, like for example the control of cell migration[258-260]. In this study, we identified Galectin-induced cross-linking of Gal-1 or Gal-3 with LRP1 and ITGB1 and of Gal-3 with PDGFRB and ITGB1 (figure 29). PDGF and its receptor PDGFR are expressed in RPE and glial cells and are assumed to contribute to PVR development[17]. PDGF exists as a 30kDa dimer and it is distinguished between PDGF-AA, PDGF-BB, PDGF-AB, PDGF-CC and PDGF-DD. PDGF receptors also exist as α and β forms and can homo- and heterodimerize, resulting in the formation of PDGFR-αα, PDGFR-ββ and PDGFR-αβ[261]. Both PDGF and PDGFRs are present in epiretinal membranes isolated from patients with PVR and PDGF in vitreous is associated with PVR in clinical studies[15, 262, 263]. PDGFs are the most abundant of all growth factors present in the vitreous of PVR patients[22, 264]. Blocking PDGFR reduced PVR associated cellular responses, but neutralizing PDGF failed to prevent PVR *in vitro*, because PDGFR is activated not only by PDGF but also by non-PDGF agents (like Insulin, EGF, FGF, HGF)[14, 196]. This indirect

activation of mainly PDGFRα by non-PDGFs is assumed to also involve reactive oxygen species (ROS) and a Src family kinase (SFK)[14, 264]. Taken together, it is assumed that activation of PDGF receptors and their signaling pathways play an important role in PVR development and thus they are attractive as a potential target to prevent development of PVR, but direct evidence of the influence of PDGFR among other factors for PVR remain to be elucidated[22].

9.6. Galectin multimerization, lattice formation and signal transduction

Galectin-glycoprotein lattices play major roles in regulating cell functions: organizing membrane domains, regulating the signaling threshold at the cell surface and determination of receptor residency time by inhibition or induction of endocytosis[265]. The galectin lattice also regulates the receptor kinase signaling and the functionality of membrane receptors including integrins[72]. Here we identified Galectin-induced cross-linking of Gal-1 or Gal-3 with LRP1 and ITGB1 and of Gal-3 with PDGFRB and ITGB1 (figure 29). The galectin-lattice regulated the distribution of glycoproteins at the cell surface. In cells treated with Gal-1 and Gal-3 large speckle staining patterns of both galectins, LRP1, PDGFRB and ITGB1 were revealed, whereas in untreated cells staining of these glycoproteins was more diffuse (figure 29). Thus, the galectin lattice is characterized by a phase transition from soluble complexes to a dynamic microdomain assembled as a gel-like polymer which orders glycoproteins on the cell surface[102, 266]. Besides, the galectin lattice is an additional layer of membrane organization, because N-glycans on extracellular domains are often flexible and extend hundreds of Ångstroms away from the plasma membrane[72]. Chimera or tandem-repeat galectins are often more potent in lattice-formation and triggering cell responses than prototype galectins[267]. Compared to Gal-1, Gal-3 forms heterogenous, disorganized cross-linking complexes[102]. Yet, it is assumed that different galectin isoforms can compete or cooperate in lattice formation or might form segregated lattices, but about this phenomenon little is known so far[72].

The affinity of glycoproteins to the galectin lattice is dependent on the number and branching of their N-glycans and thus on the activity of Golgi N-acetylglucosaminyltransferase-branching enzymes[72, 268]. Here we could show that

galectin lattice formation was N-glycan dependent. By treatment of cells with Kifunensine no cluster formation occurred any more (figure 31). The number of Asn-x-Ser/Thr (NxS/T) N-glycan sites is proportional to the affinity of transmembrane glycoproteins for the galectin lattice[105, 268], where x can be any amino acid except Proline. Because of the broad heterogeneity of N-glycan-branching pathways and the resulting diverse NxS/T sites in glycoproteins, the number of potential galectin-binding glycoforms can become very large[72]. Lau et al. [268] showed in a computational approach that the number of NxS/T in mammalian receptor kinases varies considerably, but receptor kinases involved in growth, oncogenesis and proliferation (e.g. EGFR) have by trend more NxS/T sites and longer extracellular domains. Receptors that mediate vasculature formation, organogenesis, differentiation and cell cycle arrest (e.g. TGFβ) have in general lower N-glycan multiplicities[268]. Thus, the glycome seems to have functional implications at the cellular level, because receptors with only one or few glycosylation sites are below the threshold for lattice association, whereas receptor kinases with five or more glycosylated sites are largely associated with the galectin lattice[72, 268]. Interestingly, activation of EGFR, which is equipped with eight N-glycans, stimulates for instance UDP-GlcNAc biosynthesis and enhances positive feedback to hexosamine/N-glycan processing[72, 268]. This leads to the recruitment of TGFβR (with two N-glycans) into the galectin lattice and induction of EMT processes[72, 268]. Therefore we assume that glycan structure is primarily important for functional effects of galectins on diverse cells.

Interestingly, Gal-1 also induced clustering of PDGFRB and ITGB1 (data not shown), even though PDGFRB was not identified as Gal-1 interactor by the pull-down experiments, giving a hint that Gal-1 not only forms lattices with specific interactors, but larger interacting protein complexes might be included. The experimental set-up with the galectin pull-down assays results in an initial set of galectin interactors, but does not allow distinguishing between direct and indirect galectin interactors, which is a general problem in interactome studies based on pull-down approaches. The identified galectin interactor LRP1 is an endocytotic receptor and associates with PDGFR in endosomal compartments. Here we wanted to investigate, if Gal-1 and Gal-3 are endocytosed in RPE cells or if the galectin isoforms are retained on the cell surface due to clustering

with cell surface receptors. FACS analysis of Gal-1 and Gal-3 endocytosis studies revealed that Gal-1 and Gal-3 are endocytosed increasingly over time (figure 32). Many different theories of galectin endocytosis have been described and endocytosis processes seem to be different in distinct cell types. It is assumed that endocytic uptake of Gal-3 can be both carbohydrate-dependent and independent in different cell types and Gal-1 endocytosis is mediated with clathrin-coated vesicles but also by raft-dependent endocytosis [269, 270]. Straube et al. [271] showed that Gal-3 enters epithelial MDCK cells at the apical membrane via non-clathrin mediated mechanism and traverses endosomal organelles from where it is recycled back to the cell surface. Here, the analyzed endocytosis processes of Gal-1 and Gal-3 were both carbohydrate- and dynamin-dependent. Yet cellular mechanisms that are involved in galectin-uptake are poorly understood[271]. In the literature, many approaches describe that galectins determine receptor residency time by inhibition or induction of endocytosis. Markowska et al. [123] found that Gal-3 phosphorylates VEGFR2 in endothelial cells and retains the receptor on the plasma membrane, while in Mgat5 and Gal-3 knockout cells VEGFR2 was internalized. Gal-3 also interacts with EGF and TGF receptors by Mgat5-modified N-glycans and delays their endocytic removal, which results in promoting EGF and TGF signaling[124]. In breast carcinoma cells, Gal-3 for example mediates the endocytosis of ITGB1 in a lactose-dependent manner[129, 271].

In depth characterization of downstream signals influenced by Gal-1 and Gal-3 interaction with the identified glycan-dependent interactors will provide more insight how galectins modify RPE cell behavior. By simultaneous screening of changes in phosphorylation profiles of distinct protein kinases, we could show that both ERK/MAPK and Akt signaling pathways are affected by galectin binding (figure 33). ERK phosphorylation was stable up to 30 minute after galectin treatment. Akt, which is also called protein kinase B, is one of the main downstream targets of the phosphatidylinositol (PI) 3-kinase pathway[272, 273]. GSK-3α/β and Pras-40 are substrates of Akt[272-274] and accordingly, both were also phosphorylated after galectin treatment. Since it is known that LRP1 and PDGFRB associate in endosomal compartments and affect MAPK and Akt/PI 3-kinase pathways[195], we assume that galectin induced cluster formation of LRP1, ITGB1 and PDGFRB on the cell surface have an influence on those

signaling pathways in RPE cells. In many biological systems of autoimmune disease, T-cell development and cancer cell biology, it is described that clustering of ordered arrays of galectins and their glycoprotein ligands on the cell surface is required for cellular signaling and adhesion processes[72]. The interplay between the different ligands – direct or indirect – is very important to get deeper insights in the functional effects of galectins on RPE cells.

10. Perspectives

In conclusion, analyzing the EMT process of RPE cells with a focus on glycan structures emphasized the high impact of glycomic fingerprints for the pathogenesis of PVR and for functional effects of galectins. To find the missing link between the transition to a mesenchymal phenotype and an aberrant glycostructure upon PVR pathology, altered expression profiles of glycosyltransferases might be helpful to analyze. Galectins are involved in many cellular but also in many pathological processes. In most galectin-based therapeutic approaches galectins themselves are targeted to prevent pathological disorders. Our strategy in preventing PVR associated cellular events was to use exogenously Gal-1 and Gal-3 as therapeutic agent assuming a specific surface glycosylation pattern as therapeutic target. We identified the functionally relevant oligosaccharide determinants, namely β1,6(GlcNAc)-branched N-glycans, and in a proteome-wide comprehensive Gal-1 and Gal-3 interactome screening approach we identified individual glycoproteins carrying the relevant glycoform for galectin-binding.

Finally, clinical relevance of galectins has to be evaluated. Because of the relative selectivity of Gal-1 and Gal-3 for the myofibroblastic RPE phenotype together with its capability to inhibit early PVR-associated cellular events carbohydrate-dependently, we speculate that from a therapeutic perspective targeting β1,6(GlcNAc)-branched N-glycans by recombinant Gal-1 or Gal-3 or other carbohydrate-based drugs may allow to selectively target transdifferentiated cells present in the vitreous and thus provide a novel concept for prophylaxis of PVR. Therefore, Gal-1 and Gal-3 have to be stabilized or galectin-mimetics have to be designed and tested for cytotoxicity and immunogenicity under *in vivo* conditions in a suitable animal model for PVR.

From a diagnostic perspective, results from these studies may provide a basis for diagnostic glycophenotyping of cells isolated from the vitreous of patients suffering from early PVR. Consequently this can contribute to the development of plant lectin- or galectin-carbohydrate-interaction based prognostic markers to define the individual risk for development of PVR.

11. Abbreviations

α2M: alpha-2-macroglobulin

α-SMA: α -smooth muscle actin

ABC: ammonium bicarbonate

Akt: protein kinase b

Asn: asparagine

BCA: bicinchoninic acid assay

BSG: Basigin

CAD: collision-activated dissociation

cAMP: Cyclic adenosine monophosphate

CBP: Carbohydrate Binding Protein

CD: cluster of differentiation

CMLE: classic maximum likelihood estimation

CNBr: cyanogen bromide

CNX: Calnexin

ConA: Concanavalin A

CRD: carbohydrate recognition domain

DAPI: 4',6-diamidino-2-phenylindole

DB: Database

DDA: data-dependent analysis

DIA: data-independent analysis

DMEM: Dulbecco's modified Eagles medium

DMNJ: deoxymannojirimycin

DNA: Deoxyribonucleic acid

DTT: dithiothreitol

ECM: extracellular matrix

EGF: epidermal growth factor

EMT: epithelial-to-mesenchymal transition

ER: Endoplasmic reticulum

ERK: extracellular signal-regulated kinases

ESI: electrospray ionization

FACS: fluorescence-activated cell scanning

FastAP: Fast Alkaline Phosphatase

FC: fold change

FCS: fetal calf serum

FDR: False Discovery Rate

FGF: fibroblast growth factor

FT: Fourier transformation

Gal-1: Galectin-1

Gal-3: Galectin-3

GalNAc: N-acetylgalactosamine

GAPDH: Glyceraldehyde 3-phosphate dehydrogenase

GCNT1: 2 N-acetylglucosaminyltransferase 1

GFAP: glial fibrillary acidic protein

GFP: green fluorescent protein

GlcNAc: N-acetylglucosamine

GnT5: N-acetylglucosaminyltransferase 5

GO: gene ontology

GSK-3α/β: glycogen synthase kinase

HCD: Higher-energy collisional dissociation

HGF: hepatocyte growth factor

HPLC: high-performance liquid chromatography

HRP: horseradish peroxidase

Ig: immunoglobulin

IL: interleukin

INF: interferon

ITGB1: integrin beta 1

JAK: janus kinase

Kif: Kifunensine

LacNAc: N-acetyllactosamine

LAMP: lysosomal-membrane-associated glycoprotein

LRP1: low-density lipoprotein receptor

LV: lentivirus

Mac-2: macrophage surface antigen

Mal2: Maackia Amurensis Lectin-2

MALDI: matrix-assisted laser desorption/ionization

MAPK: mitogen-activated protein kinase

MEGM: mammary epithelial cell growth medium

MEMα: minimum essential medium

Mes: mesenchymal

MET: mesenchymal-to-epithelial-transition

Mgat5: β-N-acetylglucosaminyltransferase 5

MRM: multiple reaction monitoring

MS: mass spectrometry

MUC1: Mucin 1

Nat: native

NCAM: neural cell adhesion molecule

NFκB: nuclear factor 'kappa-light-chain-enhancer' of activated B-cells

PBS: phosphate-buffered saline

PDGFRB: platelet-derived growth factor receptor beta

PEDF: pigment epithelium-derived growth factor

PHAL: phytohemagglutinin-L

PI3-K: phosphatidyl inositol 3-kinase

PMF: peptide mass fingerprinting

PNA: peanut agglutinin

Pras: proline-rich protein

PVR: proliferative vitreoretinopathy

RBC: red blood cell

RF: radio frequency

RMG: retinal Müller glial cells

RNA: Ribonucleic acid

ROS: reactive oxygen species

RP: reverse phase

RPE: retinal pigment epithelial cells

RT: room temperature

Ser: serine

SFK: Src family kinase

SRM: selected reaction monitoring

SP: signal peptide

STAT: signal transducer and activator of transcription

ST3Gal1: ∝2,3 sialyltransferase 1

ST6Gal1: ∝2,6 sialyltransferase 1

TFA: trifluoroacetic acid

TGF-β: transforming growth factor beta

THT: triiodo-thyronin

Thr: threonine

TMD: transmembrane domain

TNF: tumor necrosis factor

TOF: time-of-flight

TXR: texas red

UA: urea

VEGF: vascular endothelial growth factor

XIC: extracted ion chromatogram

ZO-1: zonula occludens-1

12. References

[1] Cardillo, J. A., Stout, J. T., LaBree, L., Azen, S. P., Omphroy, L., Cui, J. Z., Kimura, H., Hinton, D. R., and Ryan, S. J. (1997) Post-traumatic Proliferative Vitreoretinopathy, *Ophthalmology 104*, 1166-1173.

[2] Machemer, R. (1988) Proliferative vitreoretinopathy (PVR): a personal account of its pathogenesis and treatment, *Investigative ophthalmology & visual science 29*, 1771-1783.

[3] Pastor, J. C. (1998) Proliferative vitreoretinopathy: an overview, *Survey of ophthalmology 43*, 3-18.

[4] Hilton, G., Machemer, R., Michels, R., Okun, E., Schepens, C., Schwartz, A., and Committee, R. S. T. (1983) The classification of retinal detachment with proliferative vitreoretinopathy, *Ophthalmology 90*, 121-125.

[5] Machemer, R. (1978) Pathogenesis and classification of massive periretinal proliferation, *British Journal of Ophthalmology 62*, 737-747.

[6] Pastor, J. C., de la Rúa, E. R. g., and Martín, F. (2002) Proliferative vitreoretinopathy: risk factors and pathobiology, *Progress in Retinal and Eye Research 21*, 127-144.

[7] Machemer, R., m Aaberg, T., Freeman, H. M., Alexander, R. I., John, S. L., and Ronald, M. M. (1991) An updated classification of retinal detachment with proliferative vitreoretinopathy, *American journal of ophthalmology 112*, 159-165.

[8] Sadaka, A., and Giuliari, G. P. (2012) Proliferative vitreoretinopathy: current and emerging treatments, *Clin Ophthalmol 6*, 1325-1333.

[9] Vinores, S., Campochiaro, P. A., and Conway, B. P. (1990) Ultrastructural and electron-immunocytochemical characterization of cells in epiretinal membranes, *Investigative ophthalmology & visual science 31*, 14-28.

[10] Yang, S., Li, H., Li, M., and Wang, F. (2015) Mechanisms of epithelial-mesenchymal transition in proliferative vitreoretinopathy, *Discovery medicine 20*, 207-217.

[11] Hiscott, P., Sheridan, C., Magee, R. M., and Grierson, I. (1999) Matrix and the retinal pigment epithelium in proliferative retinal disease, *Progress in retinal and eye research 18*, 167-190.

[12] Wiedemann, P. (1992) Growth factors in retinal diseases: proliferative vitreoretinopathy, proliferative diabetic retinopathy, and retinal degeneration, *Survey of ophthalmology 36*, 373-384.

[13] Kampik, A., Kenyon, K. R., Michels, R. G., Green, W. R., and Zenaida, C. (1981) Epiretinal and vitreous membranes: comparative study of 56 cases, *Archives of ophthalmology 99*, 1445-1454.

[14] Lei, H., Velez, G., Hovland, P., Hirose, T., Gilbertson, D., and Kazlauskas, A. (2009) Growth factors outside the PDGF family drive experimental PVR, *Investigative ophthalmology & visual science 50*, 3394-3403.

[15] Lei, H., Rheaume, M.-A., and Kazlauskas, A. (2010) Recent developments in our understanding of how platelet-derived growth factor (PDGF) and its receptors contribute to proliferative vitreoretinopathy, *Experimental eye research 90*, 376-381.

[16] Baudouin, C., Fredj-Reygrobellet, D., Brignole, F., Nègre, F., Lapalus, P., and Gastaud, P. (1993) Growth factors in vitreous and subretinal fluid cells from patients with proliferative vitreoretinopathy, *Ophthalmic research 25*, 52-59.

[17] Cui, J., Chiu, A., Maberley, D., Ma, P., Samad, A., and Matsubara, J. (2007) Stage specificity of novel growth factor expression during development of proliferative vitreoretinopathy, *Eye 21*, 200-208.

[18] Choudhury, P., Chen, W., and Hunt, R. C. (1997) Production of platelet-derived growth factor by interleukin-1 beta and transforming growth factor-beta-stimulated retinal pigment epithelial cells leads to contraction of collagen gels, *Investigative ophthalmology & visual science 38*, 824-833.

[19] El-Ghrably, I., Dua, H. S., Orr, G. M., Fischer, D., and Tighe, P. J. (2001) Intravitreal invading cells contribute to vitreal cytokine milieu in proliferative vitreoretinopathy, *British Journal of Ophthalmology 85*, 461-470.

[20] Kon, C. H., Occleston, N. L., Aylward, G. W., and Khaw, P. T. (1999) Expression of vitreous cytokines in proliferative vitreoretinopathy: a prospective study, *Investigative ophthalmology & visual science 40*, 705-712.

[21] Limb, G., Little, B., Meager, A., Ogilvie, J., Wolstencroft, R., Franks, W., Chignell, A., and Dumonde, D. (1991) Cytokines in proliferative vitreoretinopathy, *Eye 5*, 686-693.

[22] Chen, Z., Shao, Y., and Li, X. (2015) The roles of signaling pathways in epithelial-to-mesenchymal transition of PVR, *Molecular Vision 21*, 706-710.

[23] Kuriakose, R. K., Xu, K., Chin, E. K., and Almeida, D. R. (2017) Proliferative Vitreoretinopathy (PVR) Update: Current Surgical Techniques and Emerging Medical Management, *Journal of VitreoRetinal Diseases*, 2474126417697592.

[24] Pennock, S., Rheaume, M.-A., Mukai, S., and Kazlauskas, A. (2011) A novel strategy to develop therapeutic approaches to prevent proliferative vitreoretinopathy, *The American journal of pathology 179*, 2931-2940.

[25] Velez, G., Weingarden, A. R., Lei, H., Kazlauskas, A., and Gao, G. (2013) SU9518 Inhibits Proliferative Vitreoretinopathy in Fibroblast and Genetically Modified Müller Cell–Induced Rabbit Models, *Investigative ophthalmology & visual science 54*, 1392-1397.

[26] Priglinger, C., and Priglinger, S. (2013) [Pharmacological approach to treatment of proliferative vitreoretinopathy], *Der Ophthalmologe: Zeitschrift der Deutschen Ophthalmologischen Gesellschaft 110*, 948-959.

[27] Wiedemann, P., Hilgers, R., Bauer, P., Heimann, K., and Group, D. S. (1998) Adjunctive daunorubicin in the treatment of proliferative vitreoretinopathy: results of a multicenter clinical trial, *American journal of ophthalmology 126*, 550-559.

[28] Charteris, D. G., Aylward, G. W., Wong, D., Groenewald, C., Asaria, R. H. Y., and Bunce, C. (2004) A randomized controlled trial of combined 5-fluorouracil and low-molecular-weight heparin in management of established proliferative vitreoretinopathy, *Ophthalmology 111*, 2240-2245.

[29] Turgut, B., Uyar, F., Ustundag, B., Celiker, U., Akpolat, N., and Demir, T. (2012) The impact of tacrolimus on growth factors in experimental proliferative vitreoretinopathy, *Retina 32*, 232-241.

[30] Kita, T., Hata, Y., Arita, R., Kawahara, S., Miura, M., Nakao, S., Mochizuki, Y., Enaida, H., Goto, Y., Shimokawa, H., Hafezi-Moghadam, A., and Ishibashi, T. (2008) Role of TGF-β in proliferative vitreoretinal diseases and ROCK as a therapeutic target, *Proceedings of the National Academy of Sciences 105*, 17504-17509.

[31] Zheng, Y., Ikuno, Y., Ohj, M., Kusaka, S., Jiang, R., Çekiç, O., Sawa, M., and Tano, Y. (2003) Platelet-derived Growth Factor Receptor Kinase Inhibitor AG1295 and Inhibition of Experimental Proliferative Vitreoretinopathy, *Japanese Journal of Ophthalmology 47*, 158-165.

[32] Fronk, A. H., and Vargis, E. (2016) Methods for culturing retinal pigment epithelial cells: a review of current protocols and future recommendations, *Journal of Tissue Engineering 7*, 2041731416650838.

[33] Bonilha, V. L. (2014) Retinal pigment epithelium (RPE) cytoskeleton in vivo and in vitro, *Experimental eye research 126*, 38-45.

[34] Rizzolo, L. J., Peng, S., Luo, Y., and Xiao, W. (2011) Integration of tight junctions and claudins with the barrier functions of the retinal pigment epithelium, *Progress in retinal and eye research 30*, 296-323.

[35] Kay, P., Yang, Y. C., and Paraoan, L. (2013) Directional protein secretion by the retinal pigment epithelium: roles in retinal health and the development of age-related macular degeneration, *Journal of cellular and molecular medicine 17*, 833-843.

[36] Strauss, O. (2005) The retinal pigment epithelium in visual function, *Physiological reviews 85*, 845-881.

[37] Röhlich, P. (1970) The interphotoreceptor matrix: electron microscopic and histochemical observations on the vertebrate retina, *Experimental eye research 10*, 80-86.

[38] Bok, D. (1993) The retinal pigment epithelium: a versatile partner in vision, *Journal of Cell Science 1993*, 189-195.

[39] Kawazoe, Y., Sugita, S., Keino, H., Yamada, Y., Imai, A., Horie, S., and Mochizuki, M. (2012) Retinoic acid from retinal pigment epithelium induces T regulatory cells, *Experimental eye research 94*, 32-40.

[40] Luo, C., Chen, M., and Xu, H. (2011) Complement gene expression and regulation in mouse retina and retinal pigment epithelium/choroid, *Molecular Vision 17*, 1588-1597.

[41] Thiery, J. P., Acloque, H., Huang, R. Y., and Nieto, M. A. (2009) Epithelial-mesenchymal transitions in development and disease, *cell 139*, 871-890.

[42] Kalluri, R., and Weinberg, R. A. (2009) The basics of epithelial-mesenchymal transition, *The Journal of clinical investigation 119*, 1420-1428.

[43] Tamiya, S., Liu, L., and Kaplan, H. J. (2010) Epithelial-mesenchymal transition and proliferation of retinal pigment epithelial cells initiated upon loss of cell-cell contact, *Investigative ophthalmology & visual science 51*, 2755-2763.

[44] Zeisberg, M., and Neilson, E. G. (2009) Biomarkers for epithelial-mesenchymal transitions, *The Journal of clinical investigation 119*, 1429-1437.

[45] Grisanti, S., and Guidry, C. (1995) Transdifferentiation of retinal pigment epithelial cells from epithelial to mesenchymal phenotype, *Investigative ophthalmology & visual science 36*, 391-405.

[46] Nawshad, A., LaGamba, D., Polad, A., and Hay, E. D. (2005) Transforming growth factor-β signaling during epithelial-mesenchymal transformation: implications for embryogenesis and tumor metastasis, *Cells Tissues Organs 179*, 11-23.

[47] Massagué, J. (1998) TGF-β signal transduction, *Annual review of biochemistry 67*, 753-791.

[48] Saika, S., Kono-Saika, S., Tanaka, T., Yamanaka, O., Ohnishi, Y., Sato, M., Muragaki, Y., Ooshima, A., Yoo, J., Flanders, K. C., and Roberts, A. B. (2004) Smad3 is required for dedifferentiation of retinal pigment epithelium following retinal detachment in mice, *Laboratory investigation 84*, 1245-1258.

[49] Li, M., Li, H., Liu, X., Xu, D., and Wang, F. (2016) MicroRNA-29b regulates TGF-β1-mediated epithelial–mesenchymal transition of retinal pigment epithelial cells by targeting AKT2, *Experimental cell research 345*, 115-124.

[50] Li, H., Li, M., Xu, D., Zhao, C., Liu, G., and Wang, F. (2014) Overexpression of Snail in retinal pigment epithelial triggered epithelial–mesenchymal transition, *Biochemical and biophysical research communications 446*, 347-351.

[51] Barondes, S. H., Castronovo, V., Cooper, D. N. W., Cummings, R. D., Drickamer, K., Felzi, T., Gitt, M. A., Hirabayashi, J., Hughes, C., Kasai, K.-i., Leffler, H., Liu, F.-T., Lotan, R., Mercurio, A. M., Monsigny, M., Pillai, S., Poirer, F., Raz, A., Rigby, P. W. J., Rini, J. M., and Wang, J. L. (1994) Galectins: a family of animal pgalactoside-binding lectins, *Cell 76*, 597-598.

[52] Cooper, D. N. (2002) Galectinomics: finding themes in complexity, *Biochimica et Biophysica Acta (BBA)-General Subjects 1572*, 209-231.

[53] Leffler, H., Carlsson, S., Hedlund, M., Qian, Y., and Poirier, F. (2002) Introduction to galectins, *Glycoconjugate journal 19*, 433-440.

[54] Hirabayashi, J., and Kasai, K.-i. (1993) The family of metazoan metal-independent β-galactoside-binding lectins: structure, function and molecular evolution, *Glycobiology 3*, 297-304.

[55] Varki, A., Cummings, R., Esko, J., Freeze, H., Hart, G., and Marth, J. (1998) Essentials of glycobiology, 1999, *Cold Spring Harber Laboratory Press, New York*, Chapter 22.

[56] Cooper, D. N., and Barondes, S. H. (1999) God must love galectins; he made so many of them, *Glycobiology 9*, 979-984.
[57] Rapoport, E., and Bovin, N. (2015) Specificity of human galectins on cell surfaces, *Biochemistry (Moscow) 80*, 846-856.
[58] Römer, C. E., and Elling, L. (2011) *Galectins: Structures, binding properties and function in cell adhesion*, INTECH Open Access Publisher.
[59] Seetharaman, J., Kanigsberg, A., Slaaby, R., Leffler, H., Barondes, S. H., and Rini, J. M. (1998) X-ray crystal structure of the human galectin-3 carbohydrate recognition domain at 2.1-Å resolution, *Journal of Biological Chemistry 273*, 13047-13052.
[60] Liao, D.-I., Kapadia, G., Ahmed, H., Vasta, G. R., and Herzberg, O. (1994) Structure of S-lectin, a developmentally regulated vertebrate beta-galactoside-binding protein, *Proceedings of the National Academy of Sciences 91*, 1428-1432.
[61] Lobsanov, Y. D., Gitt, M., Leffler, H., Barondes, S., and Rini, J. (1993) X-ray crystal structure of the human dimeric S-Lac lectin, L-14-II, in complex with lactose at 2.9-A resolution, *Journal of Biological Chemistry 268*, 27034-27038.
[62] Rini, J. M. (1995) Lectin structure, *Annual review of biophysics and biomolecular structure 24*, 551-577.
[63] Dumic, J., Dabelic, S., and Flögel, M. (2006) Galectin-3: an open-ended story, *Biochimica et Biophysica Acta (BBA)-General Subjects 1760*, 616-635.
[64] Hughes, R. C. (2001) Galectins as modulators of cell adhesion, *Biochimie 83*, 667-676.
[65] Hughes, R. C. (1999) Secretion of the galectin family of mammalian carbohydrate-binding proteins, *Biochimica et Biophysica Acta (BBA)-General Subjects 1473*, 172-185.
[66] Liu, F.-T., and Rabinovich, G. A. (2005) Galectins as modulators of tumour progression, *Nature Reviews Cancer 5*, 29-41.
[67] Poirier, F. (2002) Roles of galectins in vivo, *Biochemical Society Symposia 69*, 95-103.
[68] Yang, R.-Y., Rabinovich, G. A., and Liu, F.-T. (2008) Galectins: structure, function and therapeutic potential, *Expert reviews in molecular medicine 10*.
[69] Gabius, H.-J. (2011) The sugar code: fundamentals of glycosciences, pp 456-459, John Wiley & Sons.
[70] Elola, M., Wolfenstein-Todel, C., Troncoso, M., Vasta, G., and Rabinovich, G. (2007) Galectins: matricellular glycan-binding proteins linking cell adhesion, migration, and survival, *Cellular and Molecular Life Sciences 64*, 1679-1700.
[71] Rabinovich, G. A., Toscano, M. A., Jackson, S. S., and Vasta, G. R. (2007) Functions of cell surface galectin-glycoprotein lattices, *Current opinion in structural biology 17*, 513-520.
[72] Nabi, I. R., Shankar, J., and Dennis, J. W. (2015) The galectin lattice at a glance, *Journal of cell science 128*, 2213-2219.
[73] Stillman, B. N., Hsu, D. K., Pang, M., Brewer, C. F., Johnson, P., Liu, F.-T., and Baum, L. G. (2006) Galectin-3 and galectin-1 bind distinct cell surface glycoprotein receptors to induce T cell death, *The Journal of Immunology 176*, 778-789.
[74] Kopitz, J., von Reitzenstein, C., André, S., Kaltner, H., Uhl, J., Ehemann, V., Cantz, M., and Gabius, H.-J. (2001) Negative regulation of neuroblastoma cell growth by carbohydrate-dependent surface binding of galectin-1 and functional divergence from galectin-3, *Journal of Biological Chemistry 276*, 35917-35923.
[75] Ahmad, N., Gabius, H.-J., Sabesan, S., Oscarson, S., and Brewer, C. F. (2004) Thermodynamic binding studies of bivalent oligosaccharides to galectin-1, galectin-3, and the carbohydrate recognition domain of galectin-3, *Glycobiology 14*, 817-825.
[76] Pace, K. E., Hahn, H. P., Pang, M., Nguyen, J. T., and Baum, L. G. (2000) Cutting edge: CD7 delivers a pro-apoptotic signal during galectin-1-induced T cell death, *The Journal of Immunology 165*, 2331-2334.
[77] Yang, R.-Y., Hsu, D. K., and LIu, F.-T. (1996) Expression of galectin-3 modulates T-cell growth and apoptosis, *Proceedings of the National Academy of Sciences 93*, 6737-6742.

[78] Almkvist, J., and Karlsson, A. (2002) Galectins as inflammatory mediators, *Glycoconjugate journal 19*, 575-581.

[79] Almkvist, J., Dahlgren, C., Leffler, H., and Karlsson, A. (2002) Activation of the neutrophil nicotinamide adenine dinucleotide phosphate oxidase by galectin-1, *The Journal of Immunology 168*, 4034-4041.

[80] Chiariotti, L., Salvatore, P., Frunzio, R., and Bruni, C. B. (2002) Galectin genes: regulation of expression, *Glycoconjugate journal 19*, 441-449.

[81] Klyosov, A. A., and Traber, P. G. (2012) Galectins in disease and potential therapeutic approaches, In *Galectins and Disease Implications for Targeted Therapeutics*, pp 3-43, ACS Publications.

[82] Gabius, H. J. (1997) Animal lectins, *European Journal of Biochemistry 243*, 543-576.

[83] Camby, I., Le Mercier, M., Lefranc, F., and Kiss, R. (2006) Galectin-1: a small protein with major functions, *Glycobiology 16*, 137R-157R.

[84] Cho, M., and Cummings, R. D. (1997) Galectin-1: oligomeric structure and interactions with polylactosamine, *Trends in Glycoscience and Glycotechnology 9*, 47-56.

[85] Fred Brewer, C. (2002) Binding and cross-linking properties of galectins, *Biochimica et Biophysica Acta (BBA) - General Subjects 1572*, 255-262.

[86] Brewer, C. F. (1997) Cross-linking activities of galectins and other multivalent lectins, *Trends in Glycoscience and Glycotechnology 9*, 155-165.

[87] Bourne, Y., Bolgiano, B., Liao, D.-I., Strecker, G., Cantau, P., Herzberg, O., Feizi, T., and Cambillau, C. (1994) Crosslinking of mammalian lectin (galectin-1) by complex biantennary saccharides, *Nature Structural & Molecular Biology 1*, 863-870.

[88] Gupta, D., and Brewer, C. F. (1994) Homogeneous Aggregation of the 14-kDa. beta.-Galactoside Specific Vertebrate Lectin Complex with Asialofetuin in Mixed Systems, *Biochemistry 33*, 5526-5530.

[89] Leppänen, A., Stowell, S., Blixt, O., and Cummings, R. D. (2005) Dimeric galectin-1 binds with high affinity to α2, 3-sialylated and non-sialylated terminal N-acetyllactosamine units on surface-bound extended glycans, *Journal of Biological Chemistry 280*, 5549-5562.

[90] Cummings, R. L., FT. (2009) Galectins, In *Essentials of Glycobiology* (Varki A, C. R., Esko JD, et al., Ed.) 2nd ed., Cold Spring Harbor Laboratory Press, Chapter 33.

[91] Nishi, N., Abe, A., Iwaki, J., Yoshida, H., Itoh, A., Shoji, H., Kamitori, S., Hirabayashi, J., and Nakamura, T. (2008) Functional and structural bases of a cysteine-less mutant as a long-lasting substitute for galectin-1, *Glycobiology 18*, 1065-1073.

[92] Nickel, W. (2005) Unconventional secretory routes: direct protein export across the plasma membrane of mammalian cells, *Traffic 6*, 607-614.

[93] Vas, V., Fajka-Boja, R., Ion, G., Dudics, V., Monostori, É., and Uher, F. (2005) Biphasic Effect of Recombinant Galectin-1 on the Growth and Death of Early Hematopoietic Cells, *Stem Cells 23*, 279-287.

[94] Moiseeva, E. P., Spring, E. L., Baron, J. H., and de Bono, D. (1999) Galectin 1 modulates attachment, spreading and migration of cultured vascular smooth muscle cells via interactions with cellular receptors and components of extracellular matrix, *Journal of vascular research 36*, 47-58.

[95] Clausse, N., van den Brûle, F., Waltregny, D., Garnier, F., and Castronovo, V. (1999) Galectin-1 expression in prostate tumor-associated capillary endothelial cells is increased by prostate carcinoma cells and modulates heterotypic cell–cell adhesion, *Angiogenesis 3*, 317-325.

[96] Camby, I., Belot, N., Lefranc, F., Sadeghi, N., De Launoit, Y., Kaltner, H., Musette, S., Darro, F., Danguy, A., Salmon, I., Gabius, H.-J., and Kiss, R. (2002) Galectin-1 modulates human glioblastoma cell migration into the brain through modifications to the actin cytoskeleton and levels of expression of small GTPases, *Journal of Neuropathology & Experimental Neurology 61*, 585-596.

[97] Hittelet, A., Legendre, H., Nagy, N., Bronckart, Y., Pector, J. C., Salmon, I., Yeaton, P., Gabius, H. J., Kiss, R., and Camby, I. (2003) Upregulation of galectins-1 and-3 in human colon cancer and their role in regulating cell migration, *International journal of cancer 103*, 370-379.

[98] Andersen, H., Jensen, O. N., Moiseeva, E. P., and Eriksen, E. F. (2003) A Proteome Study of Secreted Prostatic Factors Affecting Osteoblastic Activity: Galectin-1 Is Involved in Differentiation of Human Bone Marrow Stromal Cells, *Journal of Bone and Mineral Research 18*, 195-203.

[99] Puche, A., Poirier, F., Hair, M., Bartlett, P., and Key, B. (1996) Role of galectin-1 in the developing mouse olfactory system, *Developmental biology 179*, 274-287.

[100] Sango, K., Tokashiki, A., Ajiki, K., Horie, M., Kawano, H., Watabe, K., Horie, H., and Kadoya, T. (2004) Synthesis, localization and externalization of galectin-1 in mature dorsal root ganglion neurons and Schwann cells, *European Journal of Neuroscience 19,* 55-64.

[101] Liu, F.-T., Hsu, D. K., Zuberi, R. I., Kuwabara, I., Chi, E. Y., and Henderson Jr, W. R. (1995) Expression and function of galectin-3, a beta-galactoside-binding lectin, in human monocytes and macrophages, *The American journal of pathology 147*, 1016.

[102] Ahmad, N., Gabius, H.-J., André, S., Kaltner, H., Sabesan, S., Roy, R., Liu, B., Macaluso, F., and Brewer, C. F. (2004) Galectin-3 precipitates as a pentamer with synthetic multivalent carbohydrates and forms heterogeneous cross-linked complexes, *Journal of Biological Chemistry 279*, 10841-10847.

[103] Menon, R. P., and Hughes, R. C. (1999) Determinants in the N-terminal domains of galectin-3 for secretion by a novel pathway circumventing the endoplasmic reticulum–Golgi complex, *European journal of biochemistry 264*, 569-576.

[104] Gong, H. C., Honjo, Y., Nangia-Makker, P., Hogan, V., Mazurak, N., Bresalier, R. S., and Raz, A. (1999) The NH2 terminus of galectin-3 governs cellular compartmentalization and functions in cancer cells, *Cancer research 59*, 6239-6245.

[105] Hirabayashi, J., Hashidate, T., Arata, Y., Nishi, N., Nakamura, T., Hirashima, M., Urashima, T., Oka, T., Futai, M., Muller, W. E., Yagi, F., and Fasai, K. (2002) Oligosaccharide specificity of galectins: a search by frontal affinity chromatography, *Biochimica et Biophysica Acta (BBA)-General Subjects 1572*, 232-254.

[106] Newlaczyl, A. U., and Yu, L.-G. (2011) Galectin-3–a jack-of-all-trades in cancer, *Cancer letters 313*, 123-128.

[107] Mazurek, N., Conklin, J., Byrd, J. C., Raz, A., and Bresalier, R. S. (2000) Phosphorylation of the β-galactoside-binding protein galectin-3 modulates binding to its ligands, *Journal of Biological Chemistry 275*, 36311-36315.

[108] Agrwal, N., Sun, Q., Wang, S. Y., and Wang, J. L. (1993) Carbohydrate-binding protein 35. I. Properties of the recombinant polypeptide and the individuality of the domains, *Journal of Biological Chemistry 268*, 14932-14939.

[109] Vijayakumar, S., Peng, H., and Schwartz, G. J. (2013) Galectin-3 mediates oligomerization of secreted hensin using its carbohydrate-recognition domain, *American Journal of Physiology-Renal Physiology 305*, F90-F99.

[110] Dagher, S. F., Wang, J. L., and Patterson, R. J. (1995) Identification of galectin-3 as a factor in pre-mRNA splicing, *Proceedings of the National Academy of Sciences 92*, 1213-1217.

[111] Li, L.-c., Li, J., and Gao, J. (2014) Functions of galectin-3 and its role in fibrotic diseases, *Journal of Pharmacology and Experimental Therapeutics 351*, 336-343.

[112] Agrwal, N., Wang, J., and Voss, P. (1989) Carbohydrate-binding protein 35. Levels of transcription and mRNA accumulation in quiescent and proliferating cells, *Journal of Biological Chemistry 264*, 17236-17242.

[113] Alge, C. S., Suppmann, S., Priglinger, S. G., Neubauer, A. S., May, C. A., Hauck, S., Welge-Lussen, U., Ueffing, M., and Kampik, A. (2003) Comparative proteome analysis of native

differentiated and cultured dedifferentiated human RPE cells, *Investigative ophthalmology & visual science 44*, 3629-3641.

[114] Alge-Priglinger, C. S., André, S., Schoeffl, H., Kampik, A., Strauss, R. W., Kernt, M., Gabius, H.-J., and Priglinger, S. G. (2011) Negative regulation of RPE cell attachment by carbohydrate-dependent cell surface binding of galectin-3 and inhibition of the ERK–MAPK pathway, *Biochimie 93*, 477-488.

[115] Alge, C. S., Priglinger, S. G., Kook, D., Schmid, H., Haritoglou, C., Welge-Lussen, U., and Kampik, A. (2006) Galectin-1 influences migration of retinal pigment epithelial cells, *Investigative ophthalmology & visual science 47*, 415-426.

[116] Priglinger, C. S., Obermann, J., Szober, C. M., Merl-Pham, J., Ohmayer, U., Behler, J., Gruhn, F., Kreutzer, T. C., Wertheimer, C., Geerlof, A., Priglinger, S. G., and Hauck, S. M. (2016) Epithelial-to-Mesenchymal Transition of RPE Cells In Vitro Confers Increased [Beta] 1, 6-N-Glycosylation and Increased Susceptibility to Galectin-3 Binding, *PloS one 11*.

[117] Alge-Priglinger, C. S., André, S., Kreutzer, T. C., Deeg, C. A., Kampik, A., Kernt, M., Schöffl, H., Priglinger, S. G., and Gabius, H.-J. (2009) Inhibition of human retinal pigment epithelial cell attachment, spreading, and migration by the human lectin galectin-1, *Molecular Vision 15*, 2162-2173.

[118] Priglinger, C. S., Szober, C. M., Priglinger, S. G., Merl, J., Euler, K. N., Kernt, M., Gondi, G., Behler, J., Geerlof, A., Kampik, A., Ueffing, M., and Hauck, S. M. (2013) Galectin-3 induces clustering of CD147 and integrin-β1 transmembrane glycoprotein receptors on the RPE cell surface, *PloS one 8*, e70011.

[119] Kadhirvel, S., Håkansson, M., Genheden, S., Diehl, C., Qvist, J., Weininger, U., Nilsson, U., Leffler, H., Ryde, U., Akke, M., and Logan, D. T. (2012) The carbohydrate-binding site in galectin-3 is preorganized to recognize a sugarlike framework of oxygens: ultra-high-resolution structures and water dynamics, *Biochemistry 51*, 296-306.

[120] Patnaik, S. K., Potvin, B., Carlsson, S., Sturm, D., Leffler, H., and Stanley, P. (2006) Complex N-glycans are the major ligands for galectin-1,-3, and-8 on Chinese hamster ovary cells, *Glycobiology 16*, 305-317.

[121] Yu, L.-G., Andrews, N., Zhao, Q., McKean, D., Williams, J. F., Connor, L. J., Gerasimenko, O. V., Hilkens, J., Hirabayashi, J., Kasai, K., and Rhodes, J. M. (2007) Galectin-3 interaction with Thomsen-Friedenreich disaccharide on cancer-associated MUC1 causes increased cancer cell endothelial adhesion, *Journal of Biological Chemistry 282*, 773-781.

[122] Probstmeier, R., Montag, D., and Schachner, M. (1995) Galectin-3, a β-Galactoside-Binding Animal Lectin, Binds to Neural Recognition Molecules, *Journal of neurochemistry 64*, 2465-2472.

[123] Markowska, A. I., Jefferies, K. C., and Panjwani, N. (2011) Galectin-3 protein modulates cell surface expression and activation of vascular endothelial growth factor receptor 2 in human endothelial cells, *Journal of Biological Chemistry 286*, 29913-29921.

[124] Partridge, E. A., Le Roy, C., Di Guglielmo, G. M., Pawling, J., Cheung, P., Granovsky, M., Nabi, I. R., Wrana, J. L., and Dennis, J. W. (2004) Regulation of cytokine receptors by Golgi N-glycan processing and endocytosis, *Science 306*, 120-124.

[125] Rapoport, E., Kurmyshkina, O., and Bovin, N. (2008) Mammalian galectins: structure, carbohydrate specificity, and functions, *Biochemistry (Moscow) 73*, 393-405.

[126] Markowska, A. I., Liu, F.-T., and Panjwani, N. (2010) Galectin-3 is an important mediator of VEGF-and bFGF-mediated angiogenic response, *The Journal of experimental medicine 207*, 1981-1993.

[127] Pace, K. E., Lee, C., Stewart, P. L., and Baum, L. G. (1999) Restricted receptor segregation into membrane microdomains occurs on human T cells during apoptosis induced by galectin-1, *The Journal of Immunology 163*, 3801-3811.

[128] Dong, S., and Hughes, R. C. (1997) Macrophage surface glycoproteins binding to galectin-3 (Mac-2-antigen), *Glycoconjugate journal 14*, 267-274.

[129] Furtak, V., Hatcher, F., and Ochieng, J. (2001) Galectin-3 mediates the endocytosis of β-1 integrins by breast carcinoma cells, *Biochemical and biophysical research communications 289*, 845-850.
[130] Kuwabara, I., and Liu, F.-T. (1996) Galectin-3 promotes adhesion of human neutrophils to laminin, *The Journal of Immunology 156*, 3939-3944.
[131] Ochieng, J., Leite-Browning, M. L., and Warfield, P. (1998) Regulation of cellular adhesion to extracellular matrix proteins by galectin-3, *Biochemical and biophysical research communications 246*, 788-791.
[132] Alberts, B., Johnson, A., Lewis, J., Walter, P., Raff, M., and Roberts, K. (2002) Molecular Biology of the Cell 4th Edition: International Student Edition, Routledge, Chapter 19.
[133] Varki, A., Esko, J. D., and Colley, K. J. (2009) Cellular Organization of Glycosylation, In *Essentials of Glycobiology* (Varki A, C. R., Esko JD, et al., , Ed.), Cold Spring Harbor Laboratory Press, Chapter 3.
[134] Varki, A. (1993) Biological roles of oligosaccharides: all of the theories are correct, *Glycobiology 3*, 97-130.
[135] Ohtsubo, K., and Marth, J. D. (2006) Glycosylation in cellular mechanisms of health and disease, *Cell 126*, 855-867.
[136] Van Kooyk, Y., and Rabinovich, G. A. (2008) Protein-glycan interactions in the control of innate and adaptive immune responses, *Nature immunology 9*, 593-601.
[137] Brockhausen, I. (2006) Mucin-type O-glycans in human colon and breast cancer: glycodynamics and functions, *EMBO reports 7*, 599-604.
[138] Varki, A. (2007) Glycan-based interactions involving vertebrate sialic-acid-recognizing proteins, *Nature 446*, 1023-1029.
[139] Wolfert, M. A., and Boons, G.-J. (2013) Adaptive immune activation: glycosylation does matter, *Nature chemical biology 9*, 776-784.
[140] Buskas, T., Ingale, S., and Boons, G.-J. (2006) Glycopeptides as versatile tools for glycobiology, *Glycobiology 16*, 113R-136R.
[141] Boscher, C., Dennis, J. W., and Nabi, I. R. (2011) Glycosylation, galectins and cellular signaling, *Current opinion in cell biology 23*, 383-392.
[142] Schwarz, F., and Aebi, M. (2011) Mechanisms and principles of N-linked protein glycosylation, *Current opinion in structural biology 21*, 576-582.
[143] Ellgaard, L., and Helenius, A. (2003) Quality control in the endoplasmic reticulum, *Nature reviews Molecular cell biology 4*, 181-191.
[144] Cummings, R. D. (2009) The repertoire of glycan determinants in the human glycome, *Molecular BioSystems 5*, 1087-1104.
[145] Stanley P, S. H., Taniguchi N. (2009) N-Glycans, In *Essentials of Glycobiology.* (Varki A, C. R., Esko JD, et al., , Ed.), Cold Spring Harbor Laboratory Press, Chapter 8.
[146] Rabinovich, G. A., and Toscano, M. A. (2009) Turning'sweet'on immunity: galectin–glycan interactions in immune tolerance and inflammation, *Nature Reviews Immunology 9*, 338-352.
[147] Wilkins, M. R., Pasquali, C., Appel, R. D., Ou, K., Golaz, O., Sanchez, J.-C., Yan, J. X., Gooley, A. A., Hughes, G., Humphery-Smith, I., Williams, K. L., and Hochstrasser, D. F. (1996) From proteins to proteomes: large scale protein identification by two-dimensional electrophoresis and arnino acid analysis, *Nature Biotechnology 14*, 61-65.
[148] Wilkins, M. R., Sanchez, J.-C., Gooley, A. A., Appel, R. D., Humphery-Smith, I., Hochstrasser, D. F., and Williams, K. L. (1996) Progress with proteome projects: why all proteins expressed by a genome should be identified and how to do it, *Biotechnology and genetic engineering reviews 13*, 19-50.
[149] Reinders, J., and Sickmann, A. (2009) *Proteomics: methods and protocols*, Humana Press Dordrecht, Chapter 1.

[150] Domon, B., and Aebersold, R. (2010) Options and considerations when selecting a quantitative proteomics strategy, *Nature biotechnology 28*, 710-721.
[151] Lottspeich, F. (1999) Proteome analysis: a pathway to the functional analysis of proteins, *Angewandte Chemie International Edition 38*, 2476-2492.
[152] Anderson, N. L., and Anderson, N. (2002) The human plasma proteome, *Mol Cell Proteomics 1*, 845-867.
[153] Perry, R. H., Cooks, R. G., and Noll, R. J. (2008) Orbitrap mass spectrometry: instrumentation, ion motion and applications, *Mass spectrometry reviews 27*, 661-699.
[154] Aebersold, R., and Mann, M. (2003) Mass spectrometry-based proteomics, *Nature 422*, 198-207.
[155] Westermeier, R., Naven, T., and Höpker, H.-R. (2008) Proteomics in practice: a guide to successful experimental design, John Wiley & Sons, Chapter 3.
[156] Chait, B. T. (2006) Mass spectrometry: bottom-up or top-down?, *Science 314*, 65-66.
[157] Bogdanov, B., and Smith, R. D. (2005) Proteomics by FTICR mass spectrometry: top down and bottom up, *Mass Spectrometry Reviews 24*, 168-200.
[158] VerBerkmoes, N. C., Bundy, J. L., Hauser, L., Asano, K. G., Razumovskaya, J., Larimer, F., Hettich, R. L., and Stephenson, J. L. (2002) Integrating "top-down" and "bottom-up" mass spectrometric approaches for proteomic analysis of Shewanella oneidensis, *Journal of proteome research 1*, 239-252.
[159] Zhang, Y., Fonslow, B. R., Shan, B., Baek, M.-C., and Yates III, J. R. (2013) Protein analysis by shotgun/bottom-up proteomics, *Chemical reviews 113*, 2343-2394.
[160] Steen, H., and Mann, M. (2004) The ABC's (and XYZ's) of peptide sequencing, *Nature reviews Molecular cell biology 5*, 699-711.
[161] von Hagen, J. (2008) *Proteomics sample preparation*, John Wiley & Sons, Chapter 4.
[162] Fenn, J., Mann, M., Meng, C., Wong, S., and Whitehouse, C. (1989) Electrospray ionization for mass spectrometry of large biomolecules, *Science 246*, 64-71.
[163] Fenn, J. B., Mann, M., Meng, C. K., Wong, S. F., and Whitehouse, C. M. (1990) Electrospray ionization–principles and practice, *Mass Spectrometry Reviews 9*, 37-70.
[164] Hu, Q., Noll, R. J., Li, H., Makarov, A., Hardman, M., and Graham Cooks, R. (2005) The Orbitrap: a new mass spectrometer, *Journal of mass spectrometry 40*, 430-443.
[165] Makarov, A. (2000) Electrostatic axially harmonic orbital trapping: a high-performance technique of mass analysis, *Analytical chemistry 72*, 1156-1162.
[166] Douglas, D. J., Frank, A. J., and Mao, D. (2005) Linear ion traps in mass spectrometry, *Mass spectrometry reviews 24*, 1-29.
[167] Doerr, A. (2015) DIA mass spectrometry: data-independent acquisition (DIA) mass spectrometry may change how proteomic data are generated, *Nature Methods 12*, 35-36.
[168] Smith, J. C. Modern techniques in quantitative proteomics, In *Advanced LC-MS applications for proteomics* (Pennington, S. R., Ed.), Chapter 5.
[169] Studier, F. W. (2005) Protein production by auto-induction in high-density shaking cultures, *Protein expression and purification 41*, 207-234.
[170] Sanjana, N. E., Shalem, O., and Zhang, F. (2014) Improved vectors and genome-wide libraries for CRISPR screening, *Nature methods 11*, 783-784.
[171] Obermann, J., Priglinger, C. S., Merl-Pham, J., Geerlof, A., Priglinger, S., Götz, M., and Hauck, S. M. (2017) Proteome-wide identification of glycosylation-dependent interactors of Galectin-1 and Galectin-3 on mesenchymal retinal pigment epithelial cells, *Molecular & Cellular Proteomics*, mcp. M116. 066381.
[172] Kuznetsova, A. V., Kurinov, A. M., and Aleksandrova, M. A. (2014) Cell models to study regulation of cell transformation in pathologies of retinal pigment epithelium, *Journal of ophthalmology 2014*.

[173] Dunn, K., Aotaki-Keen, A., Putkey, F., and Hjelmeland, L. M. (1996) ARPE-19, a human retinal pigment epithelial cell line with differentiated properties, *Experimental eye research 62*, 155-170.

[174] Maminishkis, A., Chen, S., Jalickee, S., Banzon, T., Shi, G., Wang, F. E., Ehalt, T., Hammer, J. A., and Miller, S. S. (2006) Confluent monolayers of cultured human fetal retinal pigment epithelium exhibit morphology and physiology of native tissue, *Investigative ophthalmology & visual science 47*, 3612-3624.

[175] Nowak, T., Haywood, P., and Barondes, S. (1976) Developmentally regulated lectin in embryonic chick muscle and a myogenic cell line, *Biochemical and biophysical research communications 68*, 650-657.

[176] St-Pierre, C., Ouellet, M., Giguère, D., Ohtake, R., Roy, R., Sato, S., and Tremblay, M. J. (2012) Galectin-1-specific inhibitors as a new class of compounds to treat HIV-1 infection, *Antimicrobial agents and chemotherapy 56*, 154-162.

[177] Riss, T. L., Moravec, R. A., Niles, A. L., Duellman, S., Benink, H. A., Worzella, T. J., and Minor, L. (2013 May 1 [Updated 2016 Jul 1]) Cell viability assays, (Sittampalam GS, C. N., Brimacombe K, et al., Ed.), Assay Guidance Manual [Internet]. Bethesda (MD): Eli Lilly & Company and the National Center for Advancing Translational Sciences.

[178] Hsu, P. D., Scott, D. A., Weinstein, J. A., Ran, F. A., Konermann, S., Agarwala, V., Li, Y., Fine, E. J., Wu, X., Shalem, O., Cradick, T. J., Marraffini, L. A., Bao, G., and Zhang, F. (2013) DNA targeting specificity of RNA-guided Cas9 nucleases, *Nature biotechnology 31*, 827-832.

[179] Shalem, O., Sanjana, N. E., Hartenian, E., Shi, X., Scott, D. A., Mikkelsen, T. S., Heckl, D., Ebert, B. L., Root, D. E., Doench, J. G., and Zhang, F. (2014) Genome-scale CRISPR-Cas9 knockout screening in human cells, *Science 343*, 84-87.

[180] Wisniewski, J. R., Zougman, A., Nagaraj, N., and Mann, M. (2009) Universal sample preparation method for proteome analysis, *Nature methods 6*, 359.

[181] Hauck, S. M., Dietter, J., Kramer, R. L., Hofmaier, F., Zipplies, J. K., Amann, B., Feuchtinger, A., Deeg, C. A., and Ueffing, M. (2010) Deciphering membrane-associated molecular processes in target tissue of autoimmune uveitis by label-free quantitative mass spectrometry, *Molecular & Cellular Proteomics 9*, 2292-2305.

[182] Merl, J., Deeg, C. A., Swadzba, M. E., Ueffing, M., and Hauck, S. M. (2013) Identification of autoantigens in body fluids by combining pull-downs and organic precipitations of intact immune complexes with quantitative label-free mass spectrometry, *Journal of proteome research 12*, 5656-5665.

[183] Ly, A., Merl-Pham, J., Priller, M., Gruhn, F., Senninger, N., Ueffing, M., and Hauck, S. M. (2016) Proteomic profiling suggests central role of STAT signaling during retinal degeneration in the rd10 mouse model, *Journal of proteome research 15*, 1350-1359.

[184] Grosche, A., Hauser, A., Lepper, M. F., Mayo, R., von Toerne, C., Merl-Pham, J., and Hauck, S. M. (2015) The proteome of native adult Muller glial cells from murine retina, *Molecular & Cellular Proteomics*, mcp. M115. 052183.

[185] Tyanova, S., Temu, T., Sinitcyn, P., Carlson, A., Hein, M. Y., Geiger, T., Mann, M., and Cox, J. (2016) The Perseus computational platform for comprehensive analysis of (prote) omics data, *Nature methods 13*, 731-740.

[186] Käll, L., Krogh, A., and Sonnhammer, E. L. (2004) A combined transmembrane topology and signal peptide prediction method, *Journal of molecular biology 338*, 1027-1036.

[187] Pathan, M., Keerthikumar, S., Ang, C. S., Gangoda, L., Quek, C. Y., Williamson, N. A., Mouradov, D., Sieber, O. M., Simpson, R. J., Salim, A., Bacic, A., Hill, A. F., Stroud, D. A., Ryan, M. T., Agbinya, J. I., Mariadason, J. M., Burgess, A. W., and Mathivanan, S. (2015) FunRich: An open access standalone functional enrichment and interaction network analysis tool, *Proteomics 15*, 2597-2601.

[188] Bindea, G., Mlecnik, B., Hackl, H., Charoentong, P., Tosolini, M., Kirilovsky, A., Fridman, W.-H., Pagès, F., Trajanoski, Z., and Galon, J. (2009) ClueGO: a Cytoscape plug-in to decipher

functionally grouped gene ontology and pathway annotation networks, *Bioinformatics 25*, 1091-1093.

[189] Schneider, C. A., Rasband, W. S., and Eliceiri, K. W. (2012) NIH Image to ImageJ: 25 years of image analysis, *Nature methods 9*, 671.

[190] Cao, Z., Said, N., Amin, S., Wu, H. K., Bruce, A., Garate, M., Hsu, D. K., Kuwabara, I., Liu, F.-T., and Panjwani, N. (2002) Galectins-3 and-7, but not galectin-1, play a role in re-epithelialization of wounds, *Journal of Biological Chemistry 277*, 42299-42305.

[191] Kounnas, M. Z., Moir, R. D., Rebeck, G. W., Bush, A. I., Argraves, W. S., Tanzi, R. E., Hyman, B. T., and Strickland, D. K. (1995) LDL receptor-related protein, a multifunctional ApoE receptor, binds secreted β-amyloid precursor protein and mediates its degradation, *Cell 82*, 331-340.

[192] Ulery, P. G., Beers, J., Mikhailenko, I., Tanzi, R. E., Rebeck, G. W., Hyman, B. T., and Strickland, D. K. (2000) Modulation of β-amyloid precursor protein processing by the low density lipoprotein receptor-related protein (LRP) Evidence that LRP contributes to the pathogenesis of Alzheimer's disease, *Journal of Biological Chemistry 275*, 7410-7415.

[193] Li, Y., Lu, W., Marzolo, M. P., and Bu, G. (2001) Differential functions of members of the low density lipoprotein receptor family suggested by their distinct endocytosis rates, *Journal of Biological Chemistry 276*, 18000-18006.

[194] Hollborn, M., Birkenmeier, G., Saalbach, A., Iandiev, I., Reichenbach, A., Wiedemann, P., and Kohen, L. (2004) Expression of LRP1 in retinal pigment epithelial cells and its regulation by growth factors, *Investigative ophthalmology & visual science 45*, 2033-2038.

[195] Muratoglu, S. C., Mikhailenko, I., Newton, C., Migliorini, M., and Strickland, D. K. (2010) Low density lipoprotein receptor-related protein 1 (LRP1) forms a signaling complex with platelet-derived growth factor receptor-β in endosomes and regulates activation of the MAPK pathway, *Journal of Biological Chemistry 285*, 14308-14317.

[196] Cui, J., Lei, H., Samad, A., Basavanthappa, S., Maberley, D., Matsubara, J., and Kazlauskas, A. (2009) PDGF receptors are activated in human epiretinal membranes, *Experimental eye research 88*, 438-444.

[197] Kayakiri, H., Kasahara, C., Oku, T., and Hashimoto, M. (1990) Synthesis of kifunensine, an immunomodulating substance isolated from microbial source, *Tetrahedron letters 31*, 225-226.

[198] Elbein, A. D. (1991) Glycosidase inhibitors: inhibitors of N-linked oligosaccharide processing, *The FASEB Journal 5*, 3055-3063.

[199] Elbein, A. D., Tropea, J. E., Mitchell, M., and Kaushal, G. P. (1990) Kifunensine, a potent inhibitor of the glycoprotein processing mannosidase I, *Journal of Biological Chemistry 265*, 15599-15605.

[200] Macia, E., Ehrlich, M., Massol, R., Boucrot, E., Brunner, C., and Kirchhausen, T. (2006) Dynasore, a cell-permeable inhibitor of dynamin, *Developmental cell 10*, 839-850.

[201] Hjelmeland, L. M., Fujikawa, A., Oltjen, S. L., Smit-McBride, Z., and Braunschweig, D. (2010) Quantification of retinal pigment epithelial phenotypic variation using laser scanning cytometry, *Molecular Vision 16*, 1108-1121.

[202] Grierson, I., Hiscott, P., Hogg, P., Robey, H., Mazure, A., and Larkin, G. (1994) Development, repair and regeneration of the retinal pigment epithelium, *Eye 8*, 255-262.

[203] Hauck, S. M., Suppmann, S., and Ueffing, M. (2003) Proteomic profiling of primary retinal Müller glia cells reveals a shift in expression patterns upon adaptation to in vitro conditions, *Glia 44*, 251-263.

[204] Schmidt, Johanna M., Panzilius, E., Bartsch, Harald S., Irmler, M., Beckers, J., Kari, V., Linnemann, Jelena R., Dragoi, D., Hirschi, B., Kloos, Uwe J., Sass, S., Theis, F., Kahlert, S., Johnsen, Steven A., Sotlar, K., and Scheel, Christina H. (2015) Stem-cell-like properties

and epithelial plasticity arise as stable traits after transient Twist1 activation, *Cell reports 10*, 131-139.

[205] Zheng, X., Baker, H., Hancock, W. S., Fawaz, F., McCaman, M., and Pungor, E. (2006) Proteomic analysis for the assessment of different lots of fetal bovine serum as a raw material for cell culture. Part IV. Application of proteomics to the manufacture of biological drugs, *Biotechnology progress 22*, 1294-1300.

[206] Baker, H., DeAngelis, B., and Frank, O. (1988) Vitamins and other metabolites in various sera commonly used for cell culturing, *Cellular and Molecular Life Sciences 44*, 1007-1010.

[207] Boone, C., Mantel, N., Caruso, T., Kazam, E., and Stevenson, R. (1971) Quality control studies on fetal bovine serum used in tissue culture, *In Vitro Cellular & Developmental Biology-Plant 7*, 174-189.

[208] Inman, G. J., Nicolás, F. J., Callahan, J. F., Harling, J. D., Gaster, L. M., Reith, A. D., Laping, N. J., and Hill, C. S. (2002) SB-431542 is a potent and specific inhibitor of transforming growth factor-β superfamily type I activin receptor-like kinase (ALK) receptors ALK4, ALK5, and ALK7, *Molecular pharmacology 62*, 65-74.

[209] Lamouille, S., Xu, J., and Derynck, R. (2014) Molecular mechanisms of epithelial–mesenchymal transition, *Nature reviews Molecular cell biology 15*, 178-196.

[210] Tojo, M., Hamashima, Y., Hanyu, A., Kajimoto, T., Saitoh, M., Miyazono, K., Node, M., and Imamura, T. (2005) The ALK-5 inhibitor A-83-01 inhibits Smad signaling and epithelial-to-mesenchymal transition by transforming growth factor-β, *Cancer science 96*, 791-800.

[211] Halder, S. K., Beauchamp, R. D., and Datta, P. K. (2005) A specific inhibitor of TGF-β receptor kinase, SB-431542, as a potent antitumor agent for human cancers, *Neoplasia 7*, 509-521.

[212] Connor Jr, T. B., Roberts, A. B., Sporn, M., Danielpour, D., Dart, L. L., Michels, R. G., de Bustros, S., Enger, C., Kato, H., and Lansing, M. (1989) Correlation of fibrosis and transforming growth factor-beta type 2 levels in the eye, *Journal of Clinical Investigation 83*, 1661.

[213] Bochaton-Piallat, M.-L., Kapetanios, A. D., Donati, G., Redard, M., Gabbiani, G., and Pournaras, C. J. (2000) TGF-β1, TGF-β receptor II and ED-A fibronectin expression in myofibroblast of vitreoretinopathy, *Investigative ophthalmology & visual science 41*, 2336-2342.

[214] Xiao, W., Chen, X., Liu, X., Luo, L., Ye, S., and Liu, Y. (2014) Trichostatin A, a histone deacetylase inhibitor, suppresses proliferation and epithelial–mesenchymal transition in retinal pigment epithelium cells, *Journal of cellular and molecular medicine 18*, 646-655.

[215] Bakin, A. V., Rinehart, C., Tomlinson, A. K., and Arteaga, C. L. (2002) p38 mitogen-activated protein kinase is required for TGFβ-mediated fibroblastic transdifferentiation and cell migration, *Journal of cell science 115*, 3193-3206.

[216] Bhowmick, N. A., Ghiassi, M., Bakin, A., Aakre, M., Lundquist, C. A., Engel, M. E., Arteaga, C. L., and Moses, H. L. (2001) Transforming growth factor-β1 mediates epithelial to mesenchymal transdifferentiation through a RhoA-dependent mechanism, *Molecular biology of the cell 12*, 27-36.

[217] Olson, M. F. (2008) Applications for ROCK kinase inhibition, *Current opinion in cell biology 20*, 242-248.

[218] Das, S., Becker, B. N., Hoffmann, F. M., and Mertz, J. E. (2009) Complete reversal of epithelial to mesenchymal transition requires inhibition of both ZEB expression and the Rho pathway, *BMC cell biology 10*, 94.

[219] Zhang, A., Dong, Z., and Yang, T. (2006) Prostaglandin D2 inhibits TGF-β1-induced epithelial-to-mesenchymal transition in MDCK cells, *American Journal of Physiology-Renal Physiology 291*, F1332-F1342.

[220] Pattabiraman, D. R., Bierie, B., Kober, K. I., Thiru, P., Krall, J. A., Zill, C., Reinhardt, F., Tam, W. L., and Weinberg, R. A. (2016) Activation of PKA leads to mesenchymal-to-epithelial transition and loss of tumor-initiating ability, *Science 351*, aad3680.

[221] Seamon, K. B., Padgett, W., and Daly, J. W. (1981) Forskolin: unique diterpene activator of adenylate cyclase in membranes and in intact cells, *Proceedings of the National Academy of Sciences 78*, 3363-3367.

[222] Sapio, L., Gallo, M., Illiano, M., Chiosi, E., Naviglio, D., Spina, A., and Naviglio, S. (2016) The Natural cAMP Elevating Compound Forskolin in Cancer Therapy: Is it Time?, *Journal of Cellular Physiology*, 232: 922–927.

[223] Wagh, V., Patil, P., Surana, S., and Wagh, K. (2012) Forskolin: upcoming antiglaucoma molecule, *Journal of postgraduate medicine 58*, 199.

[224] de Souza Palma, C., Grassi, M. L., Thomé, C. H., Ferreira, G. A., Albuquerque, D., Pinto, M. T., Melo, F. U. F., Kashima, S., Covas, D. T., Pitteri, S. J., and Faça, V. M. (2016) Proteomic Analysis of Epithelial to Mesenchymal Transition (EMT) Reveals Cross-talk between SNAIL and HDAC1 Proteins in Breast Cancer Cells, *Molecular & Cellular Proteomics 15*, 906-917.

[225] Li, X., Wang, X., Tan, Z., Chen, S., and Guan, F. (2016) Role of Glycans in Cancer Cells Undergoing Epithelial–Mesenchymal Transition, *Frontiers in Oncology 6*, 33.

[226] Fernandes, B., Sagman, U., Auger, M., Demetrio, M., and Dennis, J. (1991) β1–6 branched oligosaccharides as a marker of tumor progression in human breast and colon neoplasia, *Cancer research 51*, 718-723.

[227] Granovsky, M., Fata, J., Pawling, J., Muller, W. J., Khokha, R., and Dennis, J. W. (2000) Suppression of tumor growth and metastasis in Mgat5-deficient mice, *Nature medicine 6*, 306-312.

[228] Demetriou, M., Nabi, I. R., Coppolino, M., Dedhar, S., and Dennis, J. W. (1995) Reduced contact-inhibition and substratum adhesion in epithelial cells expressing GlcNAc-transferase V, *Journal of Cell Biology 130*, 383-392.

[229] Seelentag, W. K., Li, W.-P., Schmitz, S.-F. H., Metzger, U., Aeberhard, P., Heitz, P. U., and Roth, J. (1998) Prognostic value of β1, 6-branched oligosaccharides in human colorectal carcinoma, *Cancer Research 58*, 5559-5564.

[230] Li, N., Xu, H., Fan, K., Liu, X., Qi, J., Zhao, C., Yin, P., Wang, L., Li, Z., and Zha, X. (2014) Altered β1, 6-GlcNAc branched N-glycans impair TGF-β-mediated Epithelial-to-Mesenchymal Transition through Smad signalling pathway in human lung cancer, *Journal of cellular and molecular medicine 18*, 1975-1991.

[231] Saravanan, C., Cao, Z., Head, S. R., and Panjwani, N. (2010) Analysis of differential expression of glycosyltransferases in healing corneas by glycogene microarrays, *Glycobiology 20*, 13-23.

[232] Warfield, P., Makker, P., Raz, A., and Ochieng, J. (1996) Adhesion of human breast carcinoma to extracellular matrix proteins is modulated by galectin-3, *Invasion & metastasis 17*, 101-112.

[233] Matarrese, P., Fusco, O., Tinari, N., Natoli, C., Liu, F. T., Semeraro, M. L., Malorni, W., and Iacobelli, S. (2000) Galectin-3 overexpression protects from apoptosis by improving cell adhesion properties, *International journal of cancer 85*, 545-554.

[234] Dudas, S. P., Yunker, C. K., Sternberg, L. R., Byrd, J. C., and Bresalier, R. S. (2002) Expression of human intestinal mucin is modulated by the β-galactoside binding protein galectin-3 in colon cancer, *Gastroenterology 123*, 817-826.

[235] Wang, L., Inohara, H., Pienta, K. J., and Raz, A. (1995) Galectin-3 is a nuclear matrix protein which binds RNA, *Biochemical and biophysical research communications 217*, 292-303.

[236] Vyakarnam, A., Dagher, S. F., Wang, J. L., and Patterson, R. J. (1997) Evidence for a role for galectin-1 in pre-mRNA splicing, *Molecular and cellular biology 17*, 4730-4737.

[237] Lajoie, P., Partridge, E. A., Guay, G., Goetz, J. G., Pawling, J., Lagana, A., Joshi, B., Dennis, J. W., and Nabi, I. R. (2007) Plasma membrane domain organization regulates EGFR signaling in tumor cells, *The Journal of cell biology 179*, 341-356.

[238] Saravanan, C., Liu, F.-T., Gipson, I. K., and Panjwani, N. (2009) Galectin-3 promotes lamellipodia formation in epithelial cells by interacting with complex N-glycans on α3β1 integrin, *Journal of cell science 122*, 3684-3693.

[239] Moiseeva, E. P., Williams, B., Goodall, A. H., and Samani, N. J. (2003) Galectin-1 interacts with β-1 subunit of integrin, *Biochemical and biophysical research communications 310*, 1010-1016.

[240] Kariya, Y., Kawamura, C., Tabei, T., and Gu, J. (2010) Bisecting GlcNAc residues on laminin-332 down-regulate galectin-3-dependent keratinocyte motility, *Journal of Biological Chemistry 285*, 3330-3340.

[241] Perillo, N. L., Pace, K. E., Seilhamer, J. J., and Baum, L. G. (1995) Apoptosis of T cells mediated by galectin-1, *Nature 378*, 736-739.

[242] Hernandez, J. D., Nguyen, J. T., He, J., Wang, W., Ardman, B., Green, J. M., Fukuda, M., and Baum, L. G. (2006) Galectin-1 binds different CD43 glycoforms to cluster CD43 and regulate T cell death, *The Journal of Immunology 177*, 5328-5336.

[243] Walzel, H., Blach, M., Hirabayashi, J., Kasai, K.-I., and Brock, J. (2000) Involvement of CD2 and CD3 in galectin-1 induced signaling in human Jurkat T-cells, *Glycobiology 10*, 131-140.

[244] Fukumori, T., Takenaka, Y., Yoshii, T., Kim, H.-R. C., Hogan, V., Inohara, H., Kagawa, S., and Raz, A. (2003) CD29 and CD7 mediate galectin-3-induced type II T-cell apoptosis, *Cancer research 63*, 8302-8311.

[245] CASTRONOVO, V., WATTIAUX, R., and WATTIAUX-DE CONINCK, S. (1998) Expression of Lamp-1 and Lamp-2 and their interactions with galectin-3 in human tumor cells, *Int. J. Cancer 75*, 105-111.

[246] Gu, M., Wang, W., Song, W. K., Cooper, D., and Kaufman, S. J. (1994) Selective modulation of the interaction of alpha 7 beta 1 integrin with fibronectin and laminin by L-14 lectin during skeletal muscle differentiation, *Journal of cell science 107*, 175-181.

[247] Herz, J., Kowal, R. C., Goldstein, J. L., and Brown, M. S. (1990) Proteolytic processing of the 600 kd low density lipoprotein receptor-related protein (LRP) occurs in a trans-Golgi compartment, *The EMBO journal 9*, 1769.

[248] Herz, J., Hamann, U., Rogne, S., Myklebost, O., Gausepohl, H., and Stanley, K. K. (1988) Surface location and high affinity for calcium of a 500-kd liver membrane protein closely related to the LDL-receptor suggest a physiological role as lipoprotein receptor, *The EMBO journal 7*, 4119.

[249] Beisiegel, U., Weber, W., Ihrke, G., Herz, J., and Stanley, K. K. (1989) The LDL-receptor-related protein, LRP, is an apolipoprotein E-binding protein, *Nature 341*, 162-164.

[250] Kristensen, T., Moestrup, S. K., Gliemann, J., Bendtsen, L., Sand, O., and Sottrup-Jensen, L. (1990) Evidence that the newly cloned low-density-lipoprotein receptor related protein (LRP) is the α2-macroglobulin receptor, *Febs Letters 276*, 151-155.

[251] Strickland, D. K., Ashcom, J., Williams, S., Burgess, W., Migliorini, M., and Argraves, W. S. (1990) Sequence identity between the alpha 2-macroglobulin receptor and low density lipoprotein receptor-related protein suggests that this molecule is a multifunctional receptor, *Journal of Biological Chemistry 265*, 17401-17404.

[252] Herz, J., and Strickland, D. K. (2001) LRP: a multifunctional scavenger and signaling receptor, *The Journal of clinical investigation 108*, 779-784.

[253] Milenkovic, I., Birkenmeier, G., Wiedemann, P., Reichenbach, A., and Bringmann, A. (2005) Effect of α2-macroglobulin on retinal glial cell proliferation, *Graefe's Archive for Clinical and Experimental Ophthalmology 243*, 811-816.

[254] Bonacci, G. R., Cáceres, L. C., Sánchez, M. C., and Chiabrando, G. A. (2007) Activated α 2-macroglobulin induces cell proliferation and mitogen-activated protein kinase activation by LRP-1 in the J774 macrophage-derived cell line, *Archives of biochemistry and biophysics 460*, 100-106.

[255] Cáceres, L. C., Bonacci, G. R., Sánchez, M. C., and Chiabrando, G. A. (2010) Activated α2 macroglobulin induces matrix metalloproteinase 9 expression by low-density lipoprotein receptor-related protein 1 through MAPK-ERK1/2 and NF-κB activation in macrophage-derived cell lines, *Journal of cellular biochemistry 111*, 607-617.

[256] Barcelona, P. F., Ortiz, S. G., Chiabrando, G. A., and Sánchez, M. C. (2011) α2-Macroglobulin induces glial fibrillary acidic protein expression mediated by low-density lipoprotein receptor-related protein 1 in Müller cells, *Investigative ophthalmology & visual science 52*, 778-786.

[257] Barcelona, P. F., Jaldín-Fincati, J. R., Sánchez, M. C., and Chiabrando, G. A. (2013) Activated α2-macroglobulin induces Müller glial cell migration by regulating MT1-MMP activity through LRP1, *The FASEB Journal 27*, 3181-3197.

[258] Boucher, P., Gotthardt, M., Li, W.-P., Anderson, R. G., and Herz, J. (2003) LRP: role in vascular wall integrity and protection from atherosclerosis, *Science 300*, 329-332.

[259] Boucher, P., Liu, P., Gotthardt, M., Hiesberger, T., Anderson, R. G., and Herz, J. (2002) Platelet-derived growth factor mediates tyrosine phosphorylation of the cytoplasmic domain of the low density lipoprotein receptor-related protein in caveolae, *Journal of Biological Chemistry 277*, 15507-15513.

[260] Loukinova, E., Ranganathan, S., Kuznetsov, S., Gorlatova, N., Migliorini, M. M., Loukinov, D., Ulery, P. G., Mikhailenko, I., Lawrence, D. A., and Strickland, D. K. (2002) Platelet-derived growth factor (PDGF)-induced tyrosine phosphorylation of the low density lipoprotein receptor-related protein (LRP) Evidence for integrated co-receptor function between LRP and the PDGF, *Journal of Biological Chemistry 277*, 15499-15506.

[261] Heldin, C.-H., and Westermark, B. (1990) Platelet-derived growth factor: mechanism of action and possible in vivo function, *Cell regulation 1*, 555.

[262] Robbins, S. G., Mixon, R. N., Wilson, D. J., Hart, C. E., Robertson, J. E., Westra, I., Planck, S. R., and Rosenbaum, J. T. (1994) Platelet-derived growth factor ligands and receptors immunolocalized in proliferative retinal diseases, *Investigative ophthalmology & visual science 35*, 3649-3663.

[263] Lei, H., Hovland, P., Velez, G., Haran, A., Gilbertson, D., Hirose, T., and Kazlauskas, A. (2007) A potential role for PDGF-C in experimental and clinical proliferative vitreoretinopathy, *Investigative ophthalmology & visual science 48*, 2335-2342.

[264] Pennock, S., Haddock, L. J., Eliott, D., Mukai, S., and Kazlauskas, A. (2014) Is neutralizing vitreal growth factors a viable strategy to prevent proliferative vitreoretinopathy?, *Progress in retinal and eye research 40*, 16-34.

[265] Garner, O. B., and Baum, L. G. (2008) Galectin–glycan lattices regulate cell-surface glycoprotein organization and signalling, *Biochemical Society transactions 36*, 1472-1477.

[266] Li, P., Banjade, S., Cheng, H.-C., Kim, S., Chen, B., Guo, L., Llaguno, M., Hollingsworth, J. V., King, D. S., Banani, S. F., Russo, P. S., Jiang, Q.-X., Nixon, B. T., and Rosen, M. K. (2012) Phase transitions in the assembly of multivalent signalling proteins, *Nature 483*, 336-340.

[267] Earl, L. A., Bi, S., and Baum, L. G. (2011) Galectin multimerization and lattice formation are regulated by linker region structure, *Glycobiology 21*, 6-12.

[268] Lau, K. S., Partridge, E. A., Grigorian, A., Silvescu, C. I., Reinhold, V. N., Demetriou, M., and Dennis, J. W. (2007) Complex N-glycan number and degree of branching cooperate to regulate cell proliferation and differentiation, *Cell 129*, 123-134.

[269] Lepur, A., Carlsson, M. C., Novak, R., Dumić, J., Nilsson, U. J., and Leffler, H. (2012) Galectin-3 endocytosis by carbohydrate independent and dependent pathways in different macrophage like cell types, *Biochimica et Biophysica Acta (BBA)-General Subjects 1820*, 804-818.

[270] Fajka-Boja, R., Blasko, A., Kovacs-Solyom, F., Szebeni, G., Toth, G., and Monostori, E. (2008) Co-localization of galectin-1 with GM1 ganglioside in the course of its clathrin-and raft-dependent endocytosis, *Cellular and Molecular Life Sciences 65*, 2586-2593.

[271] Straube, T., von Mach, T., Hönig, E., Greb, C., Schneider, D., and Jacob, R. (2013) pH-Dependent Recycling of Galectin-3 at the Apical Membrane of Epithelial Cells, *Traffic 14*, 1014-1027.

[272] Kovacina, K. S., Park, G. Y., Bae, S. S., Guzzetta, A. W., Schaefer, E., Birnbaum, M. J., and Roth, R. A. (2003) Identification of a proline-rich Akt substrate as a 14-3-3 binding partner, *Journal of Biological Chemistry 278*, 10189-10194.

[273] Cantley, L. C. (2002) The phosphoinositide 3-kinase pathway, *Science 296*, 1655-1657.

[274] Wang, H., Zhang, Q., Wen, Q., Zheng, Y., Lazarovici, P., Jiang, H., Lin, J., and Zheng, W. (2012) Proline-rich Akt substrate of 40kDa (PRAS40): a novel downstream target of PI3k/Akt signaling pathway, *Cellular signalling 24*, 17-24.

13. Publications and Presentations

Parts of this work were already published in:

Peer-reviewed publications

Obermann, J., Priglinger, C. S., Merl-Pham, J., Geerlof, A., Priglinger, S., Götz, M., and Hauck, S. M. (2017) Proteome-wide identification of glycosylation-dependent interactors of Galectin-1 and Galectin-3 on mesenchymal retinal pigment epithelial cells, *Molecular & Cellular Proteomics*, mcp. M116. 066381.

Priglinger, C. S., Obermann, J., Szober, C. M., Merl-Pham, J., Ohmayer, U., Behler, J., Gruhn, F., Kreutzer, T. C., Wertheimer, C., Geerlof, A., Priglinger, S. G., and Hauck, S. M. (2016) Epithelial-to-Mesenchymal Transition of RPE Cells In Vitro Confers Increased β-1, 6-N-Glycosylation and Increased Susceptibility to Galectin-3 Binding, *PloS one 11*.

Sirko, S., Irmler, M., Gascón, S., Bek, S., Schneider, S., Dimou, L., Obermann, J., De Souza Paiva, D., Poirier, F., Beckers, J., Hauck, S. M., Barde, Y. A., and Götz, M. (2015) Astrocyte reactivity after brain injury: The role of galectins 1 and 3, *Glia 63*, 2340-2361.

Poster presentations

Proteomic forum 2015, Berlin, Germany: “Identification of galectin-specific glycoprotein ligands on RPE and RMG cells”. March 2015

EMBO workshop, Mandelieu, France: Transducing glycan information into function: Lessons from galectins: “Identification of Galectin-1 and Galectin-3 interactors on the cell surface of mesenchymal retinal pigment epithelial cells”. November 2016

Proteomic forum 2017, Potsdam, Germany: “Proteome-wide identification of glycosylation-dependent interactors of Galectin-1 and Galectin-3 on mesenchymal retinal pigment epithelial cells”. April 2017

14. Danksagung

An dieser Stelle möchte ich mich bei all denjenigen bedanken, die in den letzten drei Jahren mit mir zusammen gearbeitet haben und mich bei der Erstellung dieser Arbeit unterstützt und gefördert haben.

Zunächst gilt mein Dank Frau Prof. Dr. Magdalena Götz. Sie hat es mir überhaupt erst ermöglicht diese Arbeit an der LMU München durchführen zu können. Für ihre wissenschaftlichen Diskussionen und Anleitungen während meiner Arbeit und bei meinen Thesis Advisory Committees möchte ich mich herzlich bedanken.

Mein besonderer Dank geht an Dr. Stefanie Hauck und Dr. Claudia Priglinger für die Vergabe dieses interessanten Themas. Bei Steffi möchte ich mich für die hervorragende Betreuung während der gesamten Doktorarbeit, für die Zeit, die sie meiner Arbeit gewidmet hat, und für die Unterstützung in konzeptionellen, technischen und wissenschaftlichen Fragen ganz herzlich bedanken. Ich bedanke mich, dass sie mir ermöglicht hat meine Ideen in diesem Projekt frei einbringen zu dürfen und dabei viele neue Methoden erlernen und etablieren zu können. An dieser Stelle bedanke ich mich auch noch für den Kauf des neuen Mikroskops, das für mich nicht nur herausfordernd, sondern auch sehr spannend war. Der Freiraum und das Vertrauen, das mir von ihr entgegen gebracht wurde, sind nicht selbstverständlich. Claudia danke ich ebenfalls für ihre wissenschaftliche Betreuung und für die Kooperation mit der Augenklinik der LMU München. Ohne sie wäre der Zugang zu humanen RPE Proben unmöglich gewesen.

Bei Fabian Gruhn, Nicole Senninger und Jennifer Behler möchte ich mich herzlich für die Unterstützung in vielerlei Hinsicht bedanken. In neue Methoden wurde ich von Beginn meiner Doktorarbeit fachsicher eingelernt, meine zahlreichen Fragen wurden immer beantwortet und meine vielen Bestellungen sofort bearbeitet. Falls ich im Labor mal wieder irgendetwas nicht finden konnte, wussten sie immer Rat. Aber nicht nur die fachliche Unterstützung, sondern auch die lustigen und erheiternden Gespräche waren es, die das gemeinsame Arbeiten im Labor sehr angenehm gemacht haben und beispielsweise auch eine Augenpräparation kurzweilig werden ließ. Den TAs der Core Facility – Sandra Helm, Nicole Holthöfer und Michael Bock – danke ich sehr für die Messung meiner Proben und für die Unterstützung in technischen Fragen.

Mein besonderer Dank gilt ebenfalls den Postdocs, die mir immer mit Rat und Tat zur Seite gestanden haben. Ich danke Dr. Juliane Merl-Pham für den unglaublich hilfreichen wissenschaftlichen und konzeptionellen Input zu meiner Arbeit sowie auch für das Korrekturlesen des Papers und meiner Arbeit. Dr. Christine von Törne und Dr. Agnese Petrera danke ich für ihr offenes Ohr und für ihre fachliche Unterstützung. Mein ganz besonderer Dank geht an Dr. Uli Ohmayer für seine Hilfe in proteomischen Fragen, seine aufbauenden Worte, für die lustigen Gespräche im Doktoranden-Büro und dafür, dass er sich immer wieder erkundigt hat, „ob's klappt".

Bedanken möchte ich mich auch bei meinen Doktoranden-Kollegen Marlen Lepper, Marco Rahm, Linda Mühlhäußer und Sandra Sagmeister. Vor allem Marlen und Marco danke ich für die gemeinsame – und trotz allem schöne – Zeit, unsere gegenseitige moralische Unterstützung und für die kollegiale Hilfsbereitschaft.

Weiteren Personen, denen ich noch meinen Dank entgegen bringen möchte sind: Arie Geerlof für die schnelle und zuverlässige Produktion der Galektine; Prisca Chapouton für ihren Input in meinen Thesis Committee Treffen; Saskia Hanf für die Hilfe in allen möglichen organisatorischen und verwaltungstechnischen Fragen; Marcel Blindert für die schnelle Hilfe, wenn mal wieder ein Computer oder ein Programm den Geist aufgegeben hatten; den Mädels aus der Tierphysiologie für die zuverlässige Lieferung von Schweineaugen in den sehr frühen Morgenstunden; Barbara Ammann für die Einweisung in die Welt der Mikroskopie zu Beginn meiner Doktorarbeit; der Arbeitsgruppe Daniel für die Möglichkeit ihr FACS Gerät benutzen zu dürfen; der Arbeitsgruppe Ziegler für die Mitbenutzung des Digital Developer Fusion FX.

Abschließend möchte ich mich bei meinen Freunden und meiner Familie, aber vor allem bei meinen Eltern und Alex bedanken. Ihr seid die gesamte Zeit immer für mich da gewesen, habt mich unterstützt, meine Sorgen und Ärgernisse ertragen, mir zugehört und mich vor allem immer wieder bestärkt, an mich zu glauben und weiter zu machen. Eigentlich kann man es nicht in Worte fassen. Ich bin euch einfach unendlich dankbar!